Master's thesis

NTNU
Norwegian University of Science and Technology
Faculty of Information Technology and Electrical Engineering
Department of Mathematical Sciences

Solvor Sevland

Multivariate Periodic Wavelets on the Pattern

Master's thesis in Mathematics, MLREAL
Supervisor: Ronny Bergmann
June 2023

NTNU
Norwegian University of
Science and Technology

Solvor Sevland

Multivariate Periodic Wavelets on the Pattern

Master's thesis in Mathematics, MLREAL
Supervisor: Ronny Bergmann
June 2023

Norwegian University of Science and Technology
Faculty of Information Technology and Electrical Engineering
Department of Mathematical Sciences

Abstract

In this thesis we analyze images and detect edges using multivariate periodic wavelets and multiresolution analysis. We present the congruence class of the d-variate lattice $\Lambda(\mathbf{M})$ as the pattern $\mathcal{P}(\mathbf{M})$ of $\mathbf{M}$ for a regular integer matrix $\mathbf{M}$, which not necessarily is diagonal. By fixing the ordering of the pattern we find a generating group, $\mathcal{G}(\mathbf{M}^{\mathrm{T}})$ of $\mathbf{M}^{\mathrm{T}}$, and derive a variant of the fast Fourier transform on $\mathcal{P}(\mathbf{M})$. Further, we explore the potential applications of these lattice properties in performing a fast wavelet decomposition. Here, the inclusion of the subpattern $\mathcal{P}(\mathbf{N}) \subseteq \mathcal{P}(\mathbf{M})$, with $\mathbf{M} = \mathbf{J}\mathbf{N}$, for regular integer matrices $\mathbf{J}, \mathbf{N}$, is crucial. We show that a shift invariant space with respect to $\mathbf{M}$ can be subjected to an orthogonal decomposition and decomposed into $|\det \mathbf{J}|$ spaces. The focus is on the case when $|\det \mathbf{J}| = 2$, that is $V_{\mathbf{M}}^{\varphi} = \operatorname{span}\{T(\mathbf{y})\varphi : \mathbf{y} \in \mathcal{P}(\mathbf{M}), \varphi \in L^2(\mathbb{T}^d)\} = V_{\mathbf{N}}^{\xi} \oplus W_{\mathbf{N}}^{\psi}$, where $T(\mathbf{y})\varphi$ is the translation function. Additionally, the choice of $\mathbf{J}$ is discussed in the context of characterizing the direction of the decomposition, and fulfilling the inclusion property in the case where $d = 2$. Lastly, we provide instances that emphasize the theoretical findings by implementing the wavelet transform in the programming language Julia and when the orthonormal Dirichlet kernel is used to generate $V_{\mathbf{M}}^{\varphi}$.

Samandrag

I denne masteren analyserer me bilete og oppdagar kantar ved hjelp av fleirdimensjonale periodiske wavelets og fleirskala-analyse, på engelsk multiresolusion analysis. Me presanterer kongruensklassa til det d-variate gitteret $\Lambda(\mathbf{M})$ som mønsteret $\mathcal{P}(\mathbf{M})$ av $\mathbf{M}$ for ei regulær heiltalsmatrise $\mathbf{M}$, som ikkje nødvendigvis er diagonal. Ved å fastsetja rekkjefølgja til mønsteret finn me ei genererande gruppe, $\mathcal{G}(\mathbf{M}^{\mathrm{T}})$ for $\mathbf{M}$, og presenterer ein variant av den raske Fourier-transformasjonen på $\mathcal{P}(\mathbf{M})$. Vidare utforskar me dei potensielle bruksområda for eigenskapane til gitteret for å utføra ein rask wavlet-transformasjon. Her er inklusjonen av undermønsteret $\mathcal{P}(\mathbf{N}) \subseteq \mathcal{P}(\mathbf{M})$, med $\mathbf{M} = \mathbf{JN}$, for regulære heiltalsmatriser $\mathbf{J}, \mathbf{N}$, avgjerande. Me viser at eit forskyvingsinvariant rom med omsyn til $\mathbf{M}$ kan underleggjast ei orthogonal dekomposisjon og verta dekomponert i $|\det \mathbf{J}|$ rom. I denne oppgåva fokuserast det på tilfellet kor $|\det \mathbf{J}| = 2$, det vil seie $V_{\mathbf{M}}^{\varphi} = \operatorname{span}\{T(\mathbf{y})\varphi : \mathbf{y} \in \mathcal{P}(\mathbf{M}), \varphi \in L^2(\mathbb{T}^d)\} = V_{\mathbf{N}}^{\xi} \oplus W_{\mathbf{N}}^{\psi}$, der $T(\mathbf{y})\varphi$ er forskyvingsfunksjonen. Avslutningsvis vert det gjeve døme som understrekar dei teoretiske funna ved å implementera wavelet-transformasjonen i programmeringsspråket Julia når den ortonormale Dirichlet-kjerna vert brukt til å generera $V_{\mathbf{M}}^{\varphi}$.

Acknowledgements

This master's thesis is the culmination of my specialization of mathematics in the five-year Master's degree programme of Natural Science with Teacher Education at Norwegian University of Science and Technology (NTNU).

The first person I would like to thank is my supervisor, Ronny Bergmann, for his invaluable guidance in the process of writing this thesis. The expertise and dedication of his have been important in shaping the success of this thesis. I am truly grateful for his patience in assisting me with programming challenges and providing valuable insights during our discussions. Furthermore, I would like to thank him for introducing me to the interesting and engaging topic of wavelets.

Secondly, thank you to my study friends for making the days at school enjoyable. The last semester, not to mention the past five years, would not have been the same without you. I would also like to thank my family for their support throughout my years of study. Thank you to my roommate for attentively listening to both my frustrations and moments of great joy regarding the work with this thesis. I am truly grateful for the individuals who have contributed to making my years of study in Trondheim absolutely fantastic, both academically and socially. Thank you for the unforgettable time.

Trondheim, June 2023

Solvor Sevland

Contents

CHAPTER 1

Introduction

The field of image processing plays a crucial role in various applications, ranging from medical imaging to satellite imaging and computer vision. One of the important tasks in image processing is to detect edges in images and determine the location of fine details. This is done by exposing variations in color or intensity, which correspond to borders between objects or regions. A wavelet transform enables the separation of details, the so called wavelets, from the overall structure of the image. Prominent examples of wavelet transforms utilize the Morlet wavelet [15], Daubechies wavelet [10] or the Meyer wavelet [19].

The focus of this thesis is to study the framework of multivariate periodic wavelets, as detailed in [14, 20]. This is previously done in [18, 4, 5] by utilizing the orthonormal Dirichlet kernel defined by a regular integer matrix. An other function to consider in this framework is the de la Vallée Poussin function, as done in [3].

Previously, this specific fast wavelet transform was implemented in MATLAB[1] and Mathematica[2] Our aim is to develop a code that is both efficient and readable in the sense that it aligns with the notation of the theory in this thesis, leveraging both the speed and expressiveness of Julia language [6]. This process started during the work of the specialization project [21], and is continued in this thesis. Further, we aim to elaborate on the theory presented in [18] and [4] by providing visualizations and additional details to some of the proofs. In addition, present some numerical implementation of the fast wavelet transform.

The practical application wavelets have in the field of image processing is valuable asset for a teacher in mathematics. It enables a demonstration of some of the utilities of the subject, which can help motivate students to engage in mathematics and the natural sciences. Moreover, knowledge of image processing serves as a solid foundation for interdisciplinary initiatives involving both physics and computer science.

[1] Code available at: https://github.com/kellertuer/MPAWL-Matlab.git
[2] Code available at: https://github.com/kellertuer/MPAWL.git

Thesis structure

Chapter 2

This chapter includes a brief introduction to the function space $L^2(\mathbb{T}^d)$ and its inner product. Additionally, it covers the concepts of the Fourier series and the fast Fourier transform and some of their properties. The Smith normal form is defined.

Chapter 3

This chapter introduces the pattern and the generating group, establishing their foundational aspects. An ordering of the elements in the pattern and the generating group is presented, and the derivation of the fast Fourier transform on the pattern is shown. Furthermore, the chapter defines a subpattern and expounds upon its properties.

Chapter 4

The shift invariant space is introduced in this chapter, in addition to the function we employ to generate the space in order to exemplify the theory. Along with outlining properties of the basis of the space, we show that the function of choice fulfill these properties. We then establish the existence of an orthogonal decomposition of the shift invariant space, and state a condition to determine if the decomposition indeed is orthogonal. Lastly, a comprehensive description of the fast decomposition algorithm, i.e., the wavelet transform, is provided.

Chapter 5

In this chapter we discuss the interpolation problem arising when sampling a function on the pattern. We also delve into the numerical implementation of the wavelet transform. Subsequently, a thorough exploration of the numerical implementation of the wavelet transform is provided.

Chapter 6

The wavelet transform is first applied to three functions with discontinuities and conduct a comparative analysis among them. Then a multi-level decomposition is performed on one of the aforementioned functions. Lastly, we utilize the multi-level decomposition to determine the direction of an edge within an image.

Chapter 7

This chapter provides a summary of the thesis and a short conclusion, in addition to a brief discussion of possible future work.

CHAPTER 2

Preliminaries

2.1 Function Space and Fourier Series

The considered function space is the space all of square integrable functions on torus, $L^2(\mathbb{T}^d)$, $\mathbb{T}^d = [0, 2\pi)^d$. This space is the Hilbert space of 2π-periodic d-variate functions, with respect to the inner product defined as

$$\langle f, g\rangle_{L^2} := \frac{1}{(2\pi)^d} \int_{\mathbb{T}^d} f(\mathbf{x})\overline{g(\mathbf{x})}\mathrm{d}\mathbf{x}, \quad \text{for } f, g \in L^2(\mathbb{T}^d),$$

where $\overline{z}$ denotes the complex conjugate of $z \in \mathbb{C}$. For any $g \in L^2(\mathbb{T}^d)$, the induced norm is given by $\|g\|_{L^2}^2 = \langle g, g\rangle_{L^2}$, see [16, Definition 5.2.7].

The ordered set $\{\mathrm{e}^{\mathrm{i}\mathbf{k}^{\mathrm{T}}\mathbf{x}} : \mathbf{k} \in \mathbb{Z}^d\}$, where $\mathbf{k}^{\mathrm{T}}\mathbf{x} = (x_1k_1 + \ldots + x_dk_d)$ and $\mathbf{x} \in \mathbb{T}^d$, forms an orthonormal basis of $L^2(\mathbb{T}^d)$. Thus, any function $f \in L^2(\mathbb{T}^d)$ can be written as a linear combination in terms of this orthonormal basis as

$$f(\mathbf{x}) \sim \sum_{\mathbf{k}\in\mathbb{Z}^d} c_{\mathbf{k}}(f)\mathrm{e}^{\mathrm{i}\mathbf{k}^{\mathrm{T}}\mathbf{x}}, \quad \text{for } f \in L^2(\mathbb{T}^d),\ \mathbf{x} \in \mathbb{T}^d, \tag{2.1}$$

where $c_{\mathbf{k}}(f) := \langle f, \mathrm{e}^{\mathrm{i}\mathbf{k}^{\mathrm{T}}\circ}\rangle_{L^2}$ is the $\mathbf{k}$-th Fourier coefficient of f indexed by an integer vector $\mathbf{k} \in \mathbb{Z}^d$, see [20, Section 4.1]. If f possesses a continuous derivative, i.e., $f \in L^1(\mathbb{T}^d)$, an equality in (2.1) holds true, due to the implied pointwise convergence, see [22, Theorem 2.1].

In the case where $d = 1$, we define the n-th partial Fourier sum of f as

$$S_n(f) := \sum_{k=-n}^{n} \hat{f}_k \mathrm{e}^{\mathrm{i}kx} = \sum_{k=-n}^{n} \langle f, \mathrm{e}^{\mathrm{i}kx}\rangle \mathrm{e}^{\mathrm{i}kx}, \quad \text{for } n \in \mathbb{N},\ x \in \mathbb{T}.$$

If f is continuous, the partial sum $S_n(f)$ converges uniformly to f for all x, see [16, Sectoin 5.10]. The uniform convergence does not hold for the cases where f is discontinuous. Instead, the partial sum $S_n(f)$ overshoots or undershoots the function f at the discontinuities by about 9 % for all finite numbers n, see [20, Section 1.4.3]. This phenomenon is called Gibbs' phenomenon and highlights the

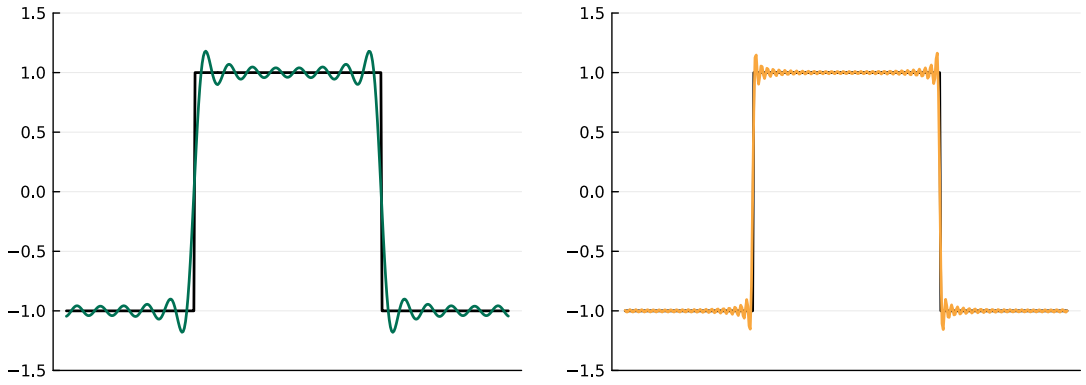

(a) $S_8(f)$ (b) $S_{32}(f)$

Figure 2.1: Gibbs' phenomenon visualized for a square wave and two different partial sums of the Fourier series. The square wave is drawn in black, and the partial sum is drawn in color.

inherent challenge of accurately representing discontinuities or abrupt changes in a function using the partial sum of Fourier series, see [12, Section 1.6] where a formal proof of the phenomenon is provided. The one dimensional partial sum $S_n(f)$ of the Fourier series can be generalized to the d-dimensional case as done in [20, Section 8.1].

Example 2.1. Let $f(x) = \mathbf{1}_{[0,1]}(x)$ be the square wave function, which has discontinuities at $x = 0$ and $x = 1$. We use the partial sum of the Fourier series to approximate f, for $n = 8$ and $n = 32$. $S_8(f)$ and $S_{32}(f)$ along with f are illustrated in Figure 2.1. We approximate f by the partial sum$S_8(f)$ and $S_{32}(f)$, see Figure 2.1. The overshooting and undershooting occur near the discontinuities for both approximations. Further, we observe the there are more In other words, there are high frequent ripples close to the discontinuities as the partial sum $S_n(f)$ tries to represent the discontinuities.

We further introduce $\ell^2(\mathbb{Z}^d)$, the space all of square summable sequences $\mathbf{a} = (a_\mathbf{k})_{\mathbf{k}\in\mathbb{Z}^d}$. With respect to the inner product

$$\langle \mathbf{a}, \mathbf{b}\rangle_{\ell^2} \coloneqq \sum_{\mathbf{k}\in\mathbb{Z}^d} a_\mathbf{k}\overline{b_\mathbf{k}}, \quad \mathbf{a}, \mathbf{b} \in \ell^2(\mathbb{Z}^d),$$

the space $\ell^2(\mathbb{Z}^d)$ forms a Hilbert space. Moreover, the norm $\|\mathbf{a}\|_{\ell^2}^2 = \langle \mathbf{a}, \mathbf{a}\rangle_{\ell^2}$ for all $\mathbf{a} \in \ell^2(\mathbb{Z}^d)$ is induced by the preceding inner product, see [16, Section 5.3].

By [12, Theorem 1.3.3] there exists an isomorphism between $L^2(\mathbb{T}^d)$ and $\ell^2(\mathbb{Z}^d)$, which is stated in the following theorem.

Theorem 2.2 (Parseval's theorem, [20, Theorem 4.5])**.** For any pair of functions $f, g \in L^2(\mathbb{T}^d)$ the following equality holds true:

$$\langle f, g\rangle_{L^2} = \langle \mathbf{c}(f), \mathbf{c}(g)\rangle_{\ell^2} = \sum_{\mathbf{k}\in\mathbb{Z}^d} c_\mathbf{k}(f)\,\overline{c_\mathbf{k}(g)}, \quad \text{for all } f, g \in L^2(\mathbb{T}^d),$$

where $\mathbf{c}(f) = \{c_\mathbf{k}(f)\}_{\mathbf{k}\in\mathbb{Z}^d}$ is the sequence of Fourier coefficients of f.

Given any $\mathbf{y} \in \mathbb{R}^d$ and $f \in L^2(\mathbb{T}^d)$, the translation operator is defined by $T(\mathbf{y})f = f(\circ - 2\pi\mathbf{y})$. Note that

$$\begin{aligned} c_{\mathbf{k}}\left(T(\mathbf{y})f\right) &= \frac{1}{(2\pi)^d}\int_{\mathbb{T}^d} f(\mathbf{x}-2\pi\mathbf{y})\overline{\mathrm{e}^{\mathrm{i}\mathbf{k}^{\mathrm{T}}(\mathbf{x}-2\pi\mathbf{y})}}\mathrm{d}\mathbf{x} \\ &= \frac{1}{(2\pi)^d}\mathrm{e}^{-2\pi\mathrm{i}\mathbf{k}^{\mathrm{T}}\mathbf{y}}\int_{\mathbb{T}^d} f(\mathbf{x})\overline{\mathrm{e}^{\mathrm{i}\mathbf{k}^{\mathrm{T}}\mathbf{x}}}\mathrm{d}\mathbf{x} = \mathrm{e}^{-2\pi\mathrm{i}\mathbf{k}^{\mathrm{T}}\mathbf{y}}c_{\mathbf{k}}\left(f\right). \end{aligned} \tag{2.2}$$

For all $\mathbf{k}, \mathbf{z} \in \mathbb{Z}^d$ we have $\mathrm{e}^{-2\pi\mathrm{i}\mathbf{k}^{\mathrm{T}}\mathbf{z}} = 1$. This justifies the restriction of $\mathbf{y}$ to any shifted unit cube. In this thesis we consider the symmetric unit cube $\left[-\frac{1}{2}, \frac{1}{2}\right)^d$.

2.2 The Fast Fourier Transform

In this sectionm, we provide a description of the fast Fourier transform, FFT. We begin by introducing the discrete Fourier transform, DFT, in one dimension as a motivation for the fast Fourier transform.

Given a vector $\mathbf{b} = (b_j)_{j=0}^{N-1} \in \mathbb{C}^N$, for $N \in \mathbb{N}$, the discrete Fourier transform of $\mathbf{b}$, denoted as $\hat{\mathbf{b}} = (\hat{b}_k)_{k=0}^{N-1} \in \mathbb{C}^N$, is defined by

$$\hat{b}_k = (\mathcal{F}_N(\mathbf{b}))_k \coloneqq \sum_{j=0}^{N-1} b_j e^{-2\pi ikj/N}, \quad \text{for } k \in \mathbb{Z}, \tag{2.3}$$

see [8, Definition 3.1]. Recovering the vector $\mathbf{b}$ from its Fourier transform $\hat{\mathbf{b}}$ is done by the inverse discrete Fourier transform, i.e. $\mathbf{b} = \mathcal{F}_N^{-1}(\hat{\mathbf{b}})$, [8, Theorem 3.3].

Let the function $f \in L^2(\mathbb{T})$ be sampled on a uniform grid $\{\frac{2\pi j}{N} : j = 0, \ldots, N-1\}$, where N is an even natural number. To estimate $c_k(f)$ we employ the trapezoidal rule

$$c_k(f) = \frac{1}{2\pi}\int_0^{2\pi} f(t)\mathrm{e}^{\mathrm{i}kt}\mathrm{d}t \approx \frac{1}{N}\sum_{j=0}^{N-1} f(\tfrac{2\pi j}{N})\mathrm{e}^{\mathrm{i}k\frac{2\pi j}{N}} = \hat{f}_k, \tag{2.4}$$

where $k \in \mathbb{Z}$, see [20, Section 3.1.1]. The function value, or signal value, at each k in the specified uniform lattice is denoted by f_k. A function is said to be N-periodic if $f_{k+N} = f_k$ for any integer k. The Fourier coefficients in Equation (2.4) are N-periodic due to the property $\mathrm{e}^{2\pi\mathrm{i}k} = 1$ for all $k \in \mathbb{Z}$.

When implementing the DFT, we multiply the sequence $\mathbf{b}$ of length N by an $N \times N$ matrix $\mathcal{F}_N$, resulting in a computational complexity of $\mathcal{O}(N^2)$, see [8, Section 3.1.3]. However, this high computational complexity makes the DFT impractical for large datasets. In contrast, the FFT exploits the structure of the DFT to reduce the number of computations required, resulting in a significantly faster algorithm. The complexity of the algorithm is reduced to $\mathcal{O}(N \log N)$, see [8, Section 3.1.3]. We will now provide a brief explanation of how the FFT is derived in one dimension.

Suppose that $N \in \mathbb{Z}$ is even, and let $n \in \mathbb{N}$ represent the number of samplings such that $N = 2n = 2^q$, where $q \in \mathbb{N}\backslash\{1\}$. Additionally, let $\mathbf{b} = (b_j)_{j=0}^{N-1} \in \mathbb{C}^N$ denote a vector which is periodically extended with a period of $N = 2n$. We can

then split the discrete Fourier transform, given in Equation (2.3), into even and odd indices. Each entry looks like

$$\hat{b}_k = \sum_{j=0}^{n-1} b_{2j}\overline{\omega}^{2jk} + \sum_{j=0}^{n-1} b_{2j+1}\overline{\omega}^{(2j+1)k}, \tag{2.5}$$

where $k \in \{0, \dots, N-1\}$ and $\omega = e^{2\pi i/N}$. Furthermore, introducing $W := e^{2\pi i/n} = \omega^2$, allowing us to reformulate the foregoing sums as we reformulate the foregoing sum as

$$\hat{b}_k = \sum_{j=0}^{n-1} b_{2j}\overline{W}^{jk} + \overline{\omega}^k \left(\sum_{j=0}^{n-1} b_{2j+1}\overline{W}^{jk} \right).$$

To simplify the notation, we use $\mathbf{b}_{\text{even}} := (b_0, b_2, \dots, b_{2n-2})$ and $\mathbf{b}_{\text{odd}} := (b_1, b_3, \dots, b_{2n-1})$ to represent the elements with even and odd indices, respectively. Rewriting in terms of the new notation, yields

$$\hat{b}_k = \big(\mathcal{F}_n \cdot \mathbf{b}_{\text{even}}\big)_k + \overline{\omega}^k \big(\mathcal{F}_n \cdot \mathbf{b}_{\text{odd}}\big)_k \quad \text{for } k \in \{0, \dots, n-1\}.$$

Knowing that $\overline{\omega}^{k+n} = \overline{\omega}^k \cdot e^{(-\pi i)} = -\overline{\omega}^k$ and that both $\mathcal{F}_n\mathbf{b}_{\text{even}}$ and $\mathcal{F}_n\mathbf{b}_{\text{odd}}$ are n-periodic, facilitates further reduction of the preceding sum to

$$\hat{b}_k = \big(\mathcal{F}_n\mathbf{b}_{\text{even}}\big)_k + \overline{\omega}^k \big(\mathcal{F}_n\mathbf{b}_{\text{odd}}\big)_k \tag{2.6a}$$

$$\hat{b}_{k+N} = \big(\mathcal{F}_n\mathbf{b}_{\text{even}}\big)_k - \overline{\omega}^k \big(\mathcal{F}_n\mathbf{b}_{\text{odd}}\big)_k, \tag{2.6b}$$

see [8, Section 3.1.3].

Iteratively, we can proceed to divide the two sums in Equation (2.6) in a manner similar to Equation (2.5). In the q-th iteration, we employ a 1×1 Fourier matrix for multiplication. By completing the successive divisions, we obtain the result vector $\hat{\mathbf{b}}$, representing the discrete Fourier transform of $\mathbf{b}$. This particular algorithm has computational complexity $\mathcal{O}(N \log N)$.

2.3 The Smith Normal Form

For a regular matrix $\mathbf{M} \in \mathbb{Z}^{d\times d}$, the Smith normal form of $\mathbf{M}$ is given by the decomposition

$$\mathbf{M} = \mathbf{QER}, \quad \mathbf{Q}, \mathbf{E}, \mathbf{R} \in \mathbb{Z}^{d\times d}, \quad \text{where} \quad \mathbf{E} = \operatorname{diag}\big(\varepsilon_1, \dots, \varepsilon_d\big), \tag{2.7}$$

where $|\det \mathbf{R}| = |\det \mathbf{Q}| = 1$ and $\varepsilon_j \in \mathbb{N}$ are elementary divisors. The matrices $\mathbf{Q}, \mathbf{E}, \mathbf{R}$ are regular matrices which are uniquely determined by the matrix $\mathbf{M}$. The theorem of elementary divisors guarantees the existence of the elementary divisors and, consequently, the existence of the Smith normal decomposition [17, Chapter 10]. The property $\varepsilon_j | \varepsilon_{j+1}$ for $j = 1, \dots, d-1$ holds for every elementary divisor ε_j, see [9, Theorem 4.29]. If $\varepsilon = 1$, we call them trivial elementary divisors. We denote the number of non-trivial elementary divisors of $\mathbf{M}$ by $d_{\mathbf{M}} := \#\{\varepsilon_j > 1\}$.

Example 2.3. For $d = 2$, we compute the Smith normal form for the matrix

$$\mathbf{A} = \begin{bmatrix} 16 & 4 \\ 0 & 16 \end{bmatrix} = \begin{bmatrix} 1 & 0 \\ 4 & 1 \end{bmatrix} \begin{bmatrix} 4 & 0 \\ 0 & 64 \end{bmatrix} \begin{bmatrix} 4 & 1 \\ -1 & 0 \end{bmatrix} = \mathbf{QER}.$$

We see that the elementary divisors of $\mathbf{A}$ are $\varepsilon_1 = 4$ and $\varepsilon_2 = 64$, with ε_1 divides ε_2. Further, no elementary divisors are trivial, leaving $d_{\mathbf{A}} = 2$.

CHAPTER 3

The Pattern and the Generating Group

3.1 Pattern and Generating Group

Let $\mathbf{M}$ be a regular matrix in $\mathbb{Z}^{d\times d}$. Two vectors $\mathbf{h}, \mathbf{k} \in \mathbb{Z}^d$ are called congruent with respect $\mathbf{M}$ if

$$\mathbf{h} \equiv \mathbf{k} \mod \mathbf{M} \quad \Leftrightarrow \quad \exists \mathbf{z} \in \mathbb{Z}^d : \mathbf{k} = \mathbf{h} + \mathbf{M}\mathbf{z}, \tag{3.1}$$

see [4, Section 2.2].

We define the lattice $\Lambda(\mathbf{M})$ of $\mathbf{M}$ as $\Lambda(\mathbf{M}) \coloneqq \mathbf{M}^{-1}\mathbb{Z}^d = \{\mathbf{y} \in \mathbb{R}^d : \mathbf{M}\mathbf{y} \in \mathbb{Z}^d\}$. The lattice describes the equivalence relation with respect to $\mod \mathbf{I}$, where $\mathbf{I}$ is the identity matrix of size $d \times d$ if the size is not specified otherwise. The lattice is 1-periodic [5, Section 2].

The pattern $\mathcal{P}(\mathbf{M})$ of $\mathbf{M}$ is defined as

$$\begin{aligned} \mathcal{P}(\mathbf{M}) :&= \left\{\mathbf{y} \in \left[-\tfrac{1}{2}, \tfrac{1}{2}\right)^d : \mathbf{M}\mathbf{y} \in \mathbb{Z}^d\right\} \\ &= \left(\mathbf{M}^{-1}\mathbb{Z}^d\right) \cap \left[-\tfrac{1}{2}, \tfrac{1}{2}\right)^d = \Lambda\left(\mathbf{M}\right) \cap \left[-\tfrac{1}{2}, \tfrac{1}{2}\right)^d. \end{aligned} \tag{3.2}$$

The pattern is a complete set of congruence classes of integer vectors $\mod \mathbf{I}$ [4, Section 2.2]. Thus, each unit cube of $\mathbb{R}^d$ contains exactly one element of $\mathcal{P}(\mathbf{M})$.

Further, the generating group $\mathcal{G}(\mathbf{M})$ of $\mathbf{M}$ is defined as

$$\mathcal{G}(\mathbf{M}) \coloneqq \mathbf{M}\mathcal{P}(\mathbf{M}) = \left\{\mathbf{h} \in \mathbb{Z}^d : \mathbf{h} = \mathbf{M}\mathbf{y}, \mathbf{y} \in \mathcal{P}(\mathbf{M})\right\}.$$

Every element belonging the set $\mathcal{G}(\mathbf{M})$ is contained within the semi-open parallelepiped $\mathbf{M}\left[-\frac{1}{2}, \frac{1}{2}\right)^d$, see [4, Section 2.2].

For the pattern, the addition operation $+|_{\mathcal{P}(\mathbf{M})}$ is defined as $(\mathbf{y}+\mathbf{z})_{\mathcal{P}(\mathbf{M})} \coloneqq \mathbf{y}+\mathbf{z} \mod \mathbf{I}$. Similarly, $(\mathbf{k}+\mathbf{h})|_{\mathcal{G}(\mathbf{M})} \coloneqq \mathbf{k}+\mathbf{h} \mod \mathbf{M}$, as described in Equation (3.1). The sum of the terms is ensured to be contained within $\mathcal{P}(\mathbf{M})$ and $\mathcal{G}(\mathbf{M})$ due to the addition operations $+|_{\mathcal{P}(\mathbf{M})}$ and $+|_{\mathcal{G}(\mathbf{M})}$, respectively. Additionally, the map $\mathbf{M}\circ : \mathcal{P}(\mathbf{M}) \to \mathcal{G}(\mathbf{M})$ is a group isomorphism between $(\mathcal{P}(\mathbf{M}), +|_{\mathcal{P}(\mathbf{M})})$ and $(\mathcal{G}(\mathbf{M}), +|_{\mathcal{G}(\mathbf{M})})$.

The matrices $\mathbf{Q}$ and $\mathbf{R}$ from Equation (2.7) are coordinate transform matrices of $\mathbb{Z}^d$, that is, bijective maps on $\mathbb{Z}^d$. This results in $\mathcal{G}(\mathbf{M})$ and $\mathcal{G}(\mathbf{E})$ being isomorphic [18, Section 2.2]. The isomorphism gives rise to the generating group $\mathcal{G}(\mathbf{M})$ being a direct product of cyclic groups $\mathcal{C}_{\varepsilon_j}$,

$$\mathcal{G}(\mathbf{M}) \cong \mathcal{G}(\mathbf{E}) \cong \mathcal{C}_{\varepsilon_1} \otimes \cdots \otimes \mathcal{C}_{\varepsilon_d}, \cong \mathcal{C}_{\varepsilon_{d-d_{\mathbf{M}}+1}} \otimes \cdots \otimes \mathcal{C}_{\varepsilon_d}, \tag{3.3}$$

where ε_j is the j-th elementary divisor and $\mathcal{C}_z = \{0, 1, \ldots, z-1\}$ with addition modulo $z \in \mathbb{Z}$ is the cyclic group $\mathbb{Z}/z\mathbb{Z}$, with order $|\mathcal{C}_{\varepsilon_j}| = \varepsilon_j$, see [18, Equation 7]. The right-hand side of (3.3) is a simplification for the cases when $\varepsilon = 1$, that is cycles of length 1.

Note that the transposed matrix $\mathbf{M}^{\mathrm{T}}$ has the same elementary divisors as $\mathbf{M}$, i.e., when decomposing $\mathbf{M}^{\mathrm{T}}$ into $\mathbf{R}^{\mathrm{T}}\mathbf{E}\mathbf{Q}^{\mathrm{T}}$, it has the same diagonal matrix $\mathbf{E}$ as $\mathbf{M}$. Consequently, $\mathcal{G}(\mathbf{M})$ and $\mathcal{G}(\mathbf{M}^{\mathrm{T}})$ are isomorphic, which justifies extending (3.3) to

$$\mathcal{G}(\mathbf{M}) \cong \mathcal{G}(\mathbf{M}^{\mathrm{T}}) \cong \mathcal{G}(\mathbf{E}) \cong \mathcal{P}(\mathbf{E}) \cong \mathcal{P}(\mathbf{M}) \cong \mathcal{P}(\mathbf{M}^{\mathrm{T}}) \cong \mathcal{C}_{\varepsilon_1} \otimes \cdots \otimes \mathcal{C}_{\varepsilon_d}. \tag{3.4}$$

The prior equivalence relation implies that

$$m := |\det \mathbf{M}| = |\mathcal{G}(\mathbf{M})| = |\mathcal{G}(\mathbf{M}^{\mathrm{T}})| = |\mathcal{P}(\mathbf{M}^{\mathrm{T}})| = |\mathcal{P}(\mathbf{M})| = \varepsilon_1 \cdot \cdots \cdot \varepsilon_d, \tag{3.5}$$

and denotes the number of elements in both the pattern and generating group of $\mathbf{M}$ and $\mathbf{M}^{\mathrm{T}}$, see [11, Lemma 2.7].

Example 3.1. For $d = 2$, we consider the following regular integer matrices

$$\mathbf{A}_1 = \begin{bmatrix} 16 & 0 \\ 0 & 16 \end{bmatrix}, \qquad \mathbf{A}_2 = \begin{bmatrix} 8 & 0 \\ 0 & 32 \end{bmatrix}, \qquad \mathbf{A}_3 = \begin{bmatrix} 16 & 4 \\ 0 & 16 \end{bmatrix} \qquad \mathbf{A}_4 = \begin{bmatrix} 16 & 0 \\ -4 & 16 \end{bmatrix}.$$

The patterns and the generating groups of the matrices are plotted in Figure 3.1a, 3.1b, 3.1c and 3.1d, respectively.

Recall from Example 2.3 that the Smith normal form of $\mathbf{A} = \mathbf{A}_3$ is given by

$$\mathbf{A}_3 = \begin{bmatrix} 16 & 4 \\ 0 & 16 \end{bmatrix} = \begin{bmatrix} 1 & 0 \\ 4 & 1 \end{bmatrix} \begin{bmatrix} 4 & 0 \\ 0 & 64 \end{bmatrix} \begin{bmatrix} 4 & 1 \\ -1 & 0 \end{bmatrix} = \mathbf{QER}.$$

By (3.5), both $\mathcal{P}(\mathbf{A}_3)$ and $\mathcal{G}(\mathbf{A}_3)$ have $|\det \mathbf{A}_3| = |\det \mathbf{E}| = 4 \cdot 64 = 256$ elements. This can be observed in Figure 3.1c. With $\mathbf{E} = \mathrm{diag}(4, 64)$, we know that both $\mathcal{P}(\mathbf{A}_3)$ and $\mathcal{G}(\mathbf{A}_3)$ are isomorphic to the direct product of the cyclic groups $\mathcal{C}_4 \otimes \mathcal{C}_{64}$, i.e., consisting of four cycles of length 64.

Note that the diagonal matrices $\mathbf{A}_1$ and $\mathbf{A}_2$ generate squared and rectangular generating groups, respectively, while $\mathbf{A}_3$ and $\mathbf{A}_4$ produce generating groups with a shear in the second and first coordinate, respectively. The shear arises from the fact that one of the off-diagonal entries is non-zero.

3.2 Basis of the Pattern and the Generating Group

The set $\{0, 1/N, \ldots, (N-1)/N\}$ for $N \in \mathbb{N}$, i.e., the one-dimensional pattern $\mathcal{P}(N)$, is equipped with a natural ordering. However, the elements of $\mathcal{P}(\mathbf{M})$ are not ordered naturally. Therefore, we want to define a basis to establish an ordering

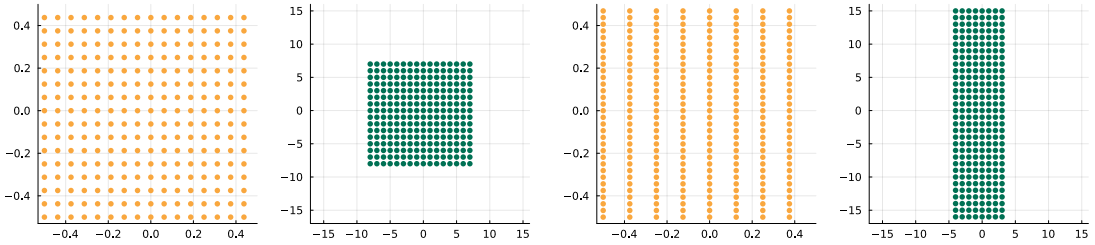

(a) Plot of $\mathcal{P}(\mathbf{A}_1)$ and $\mathcal{G}(\mathbf{A}_1)$, respectively. (b) Plot of $\mathcal{P}(\mathbf{A}_2)$ and $\mathcal{G}(\mathbf{A}_2)$, respectively.

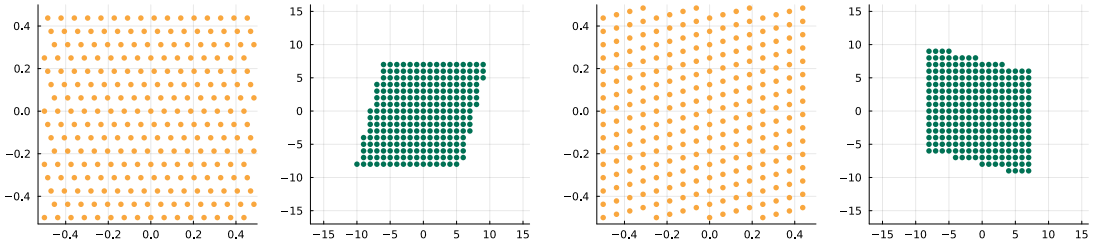

(c) Plot of $\mathcal{P}(\mathbf{A}_3)$ and $\mathcal{G}(\mathbf{A}_3)$, respectively. (d) Plot of $\mathcal{P}(\mathbf{A}_4)$ and $\mathcal{G}(\mathbf{A}_4)$, respectively.

Figure 3.1: Plots of the pattern and the generating group of the four example matrices. Each matrix has a determinant of 256, but different looking patterns and generating groups.

of its elements. Finding a basis for $\mathcal{P}(\mathbf{M})$ that is similar to the tensor product in (3.4), allows us to fix an ordering of the elements of $\mathcal{P}(\mathbf{M})$, and analogous for $\mathcal{G}(\mathbf{M}^{\mathrm{T}})$. First we need to show a lemma that is used to prove the main objectives of this section.

If the two matrices generate the identical pattern $\mathcal{P}(\mathbf{M}) = \mathcal{P}(\mathbf{N})$, for $\mathbf{M}, \mathbf{N} \in \mathbb{Z}^{d\times d}$, we call the matrices equivalent. We denote equivalent matrices by $\mathbf{M} \cong \mathbf{N}$.

Lemma 3.2. Let $\mathbf{M}, \mathbf{N} \in \mathbb{Z}^{d\times d}$. The matrices $\mathbf{M} \cong \mathbf{N}$ are equivalent if and only if there exists a matrix $\mathbf{U} \in \mathbb{Z}^{d\times d}$ with $|\det \mathbf{U}| = 1$ and $\mathbf{N} = \mathbf{U}\mathbf{M}$, see [18, Lemma 2.4].

Proof. First, assume $\mathbf{M}, \mathbf{N} \in \mathbb{Z}^{d\times d}$ are equivalent matrices, i.e., $\mathcal{P}(\mathbf{M}) = \mathcal{P}(\mathbf{N})$. Then given any element $\mathbf{y} \in \mathcal{P}(\mathbf{M})$, we have that $\mathbf{y} \in \mathcal{P}(\mathbf{N})$. By the definition of the pattern, (3.2), we can write $\mathbf{y} = \mathbf{M}^{-1}\mathbf{z}$ for some $\mathbf{z} \in \mathbb{Z}^d$. Further, the equivalence of the matrices premits us to state $\mathbf{y}$ as $\mathbf{y} = \mathbf{N}\mathbf{M}^{-1}\mathbf{z}$. When setting $\mathbf{U} = \mathbf{N}\mathbf{M}^{-1}$ it follows that $\mathbf{U}$ is regular, as both $\mathbf{N}$ and $\mathbf{M}^{-1}$ are regular, [2, Theorem 1.4.6]. By Equation (3.5), we have that $|\det \mathbf{M}| = |\det \mathbf{N}|$, which again implies that $|\det \mathbf{U}| = |\det \mathbf{N}\mathbf{M}^{-1}| = 1$.

Conversely, if there exists a regular matrix $\mathbf{U} \in \mathbb{Z}^{d\times d}$ such that $\mathbf{N} = \mathbf{U}\mathbf{M}$, we have

$$\mathcal{P}(\mathbf{N}) = \mathcal{P}(\mathbf{U}\mathbf{M}) = \{\mathbf{y} : \mathbf{U}\mathbf{M}\mathbf{y} \in \mathbb{Z}^d\} = \{\mathbf{y} : \mathbf{M}\mathbf{y} \in \mathbf{U}^{-1}\mathbb{Z}^d = \mathbb{Z}^d\} = \mathcal{P}(\mathbf{M}). \quad \square$$

Now, fix a regular matrix $\mathbf{M} \in \mathbb{Z}^{d\times d}$. We define the set of vectors

$$\mathbf{y}_{\mathbf{e}_j} \coloneqq \mathbf{R}^{-1}\frac{1}{\varepsilon_{d-d_{\mathbf{M}}+j}}\mathbf{e}_{d-d_{\mathbf{M}}+j}, \quad j = 1, \ldots, d_{\mathbf{M}}, \tag{3.6}$$

where $\mathbf{R}$ is from the Smith normal form being $\mathbf{M} = \mathbf{Q}\mathbf{E}\mathbf{R}$, ε_j denotes the elementary divisors, as shown in Equation (2.7), and $\mathbf{e}_j$ is the j-th unit vector [4,

Equation 8]. The vectors $\mathbf{y}_{\mathbf{e}_j}$ are linearly independent since $\mathbf{R}$ is invertible by construction.

By using $\mathbf{Q}$ with its property $|\det \mathbf{Q}| = 1$, from Equation (2.7), as a change of basis combined with Lemma 3.2, the equality $\Lambda(\mathbf{M}) = \Lambda(\mathbf{ER})$ is justified. The map $f : \Lambda(\mathbf{ER}) \to \Lambda(\mathbf{E})$ given by $f(\mathbf{y}) = \mathbf{Ry}$ is an isomorphism $\Lambda(\mathbf{ER})$ and $\Lambda(\mathbf{E})$. This can be written as

$$\Lambda(\mathbf{M}) = \Lambda(\mathbf{ER}) = \{\mathbf{y} : \mathbf{ERy} \in \mathbb{Z}^d\} \cong \{\mathbf{x} : \mathbf{Ex} \in \mathbb{Z}^d\} = \Lambda(\mathbf{E}).$$

The set $\{\mathbf{Ry}_{\mathbf{e}_j}\}_{j=1}^{d_\mathbf{M}}$ forms a basis for $\mathcal{P}(\mathbf{E})$, which consists of scaled unit vectors. This further implies that every element $\mathbf{x} \in \mathcal{P}(\mathbf{M})$ can be uniquely represented as

$$\mathbf{x} = \sum_{j=1}^{d_\mathbf{M}} \lambda_j \mathbf{y}_{\mathbf{e}_j}\Big|_{\mathcal{P}(\mathbf{E})} = \sum_{j=1}^{d_\mathbf{M}} \lambda_j \frac{1}{\varepsilon_{d-d_\mathbf{M}+j}} \mathbf{e}_{d-d_\mathbf{M}+j}\Big|_{\mathcal{P}(\mathbf{E})}, \quad 0 \le \lambda_j < \varepsilon_{d-d_\mathbf{M}+j}. \tag{3.7}$$

The remaining ε_j excluded in the equation above have the indices $j \le d - d_\mathbf{M}$. These indices corresponds to the trivial elementary divisors, and when subjected to the modular reduction $+|_{\mathcal{P}(\mathbf{M})}$, the vectors vanish, and is therefore omitted in the expression.

We define the set of indices $\mathbb{E}_\mathbf{M}$ as

$$\mathbb{E}_\mathbf{M} = \{0, 1, \ldots, \varepsilon_{d-d_\mathbf{M}+1} - 1\} \times \cdots \times \{0, 1, \ldots, \varepsilon_d - 1\}, \tag{3.8}$$

where ε_j are the elementary divisors of $\mathbf{M}$ and $d_\mathbf{M} = \#\{\varepsilon_j > 1\}$.

By utilizing the lexicographical ordering on the set of indices $\mathbb{E}_\mathbf{M}$, we derive an ordering of the elements of $\mathcal{P}(\mathbf{M})$ based on the chosen basis in Equation (3.6), resulting in

$$\mathcal{P}(\mathbf{M}) = \Big(\sum_{j=1}^{d_\mathbf{M}} \lambda_j \mathbf{y}_{\mathbf{e}_j}\Big|_{\mathcal{P}(\mathbf{M})} \Big)_{(\lambda_1,\ldots,\lambda_{d_\mathbf{M}})=\mathbf{0}}^{\varepsilon_{d-d_\mathbf{M}+1}-1,\ldots,\varepsilon_d-1}, \tag{3.9}$$

see [4, Sec 3].

Similarly, a basis for $\mathcal{G}(\mathbf{M})$ can be generated by left-multiplying each basis vector $\mathbf{y}_{\mathbf{e}_j}$ from Equation (3.6) with the matrix $\mathbf{M}$. Starting with $\mathcal{P}(\mathbf{M}^\mathrm{T})$, we create a basis for $\mathcal{G}(\mathbf{M}^\mathrm{T})$, which is expressed as

$$\mathbf{h}_{\mathbf{e}_j} \coloneqq \mathbf{R}^\mathrm{T} \mathbf{e}_{d-d_\mathbf{M}+j}, \quad j = 1, \ldots, d_\mathbf{M}. \tag{3.10}$$

This gives the expression

$$\mathcal{G}(\mathbf{M}^\mathrm{T}) = \Big(\sum_{j=1}^{d_\mathbf{M}} \mu_j \mathbf{h}_{\mathbf{e}_j}\Big|_{\mathcal{G}(\mathbf{M}^\mathrm{T})} \Big)_{(\mu_1,\ldots,\mu_{d_\mathbf{M}})=\mathbf{0}}^{\varepsilon_{d-d_\mathbf{M}+1}-1,\ldots,\varepsilon_d-1}. \tag{3.11}$$

Each basis vector $\mathbf{x}_{\mathbf{e}_j}$ for both the pattern and the generating group must span a cycle of length $\varepsilon_{d-d_\mathbf{M}+j}$. This is why the ordering of the set of basis vectors is pivotal, see [4, Remark 1]. Furthermore, this implies that the dimension of both $\mathcal{P}(\mathbf{M})$ and $\mathcal{G}(\mathbf{M})$ is $d_\mathbf{M}$ as they are spanned by exacly $d_\mathbf{M}$ basis vectors. By the isomorphism in Equation (3.4), we can address $\mathcal{G}(\mathbf{M})$ and $\mathcal{G}(\mathbf{M}^\mathrm{T})$ by the same set of indices.

Lemma 3.3 ([4, Lemma 1])**.** Let the matrix $\mathbf{M} \in \mathbb{Z}^{d\times d}$ be regular, $\mathbf{y}_{\mathbf{e}_i}$ be the basis of $\mathcal{P}(\mathbf{M})$ and $\mathbf{h}_{\mathbf{e}_j}$ be the basis of $\mathcal{G}(\mathbf{M}^{\mathrm{T}})$, defined in Equation (3.6) and (3.10), respectively. Then $\mathbf{y}_{\mathbf{e}_i}$ and $\mathbf{h}_{\mathbf{e}_j}$ are biorthogonal, i.e.,

$$\langle \mathbf{h}_{\mathbf{e}_j}, \mathbf{y}_{\mathbf{e}_i} \rangle_{\ell^2} = \begin{cases} \frac{1}{\varepsilon_{d-d_{\mathbf{M}}+i}}, & i = j \\ 0, & i \neq j \end{cases}, \qquad \text{for all } i, j = \{1, \dots, d_{\mathbf{M}}\}.$$

Proof. Using the definitions of the bases, we compute the inner product as follows

$$\begin{aligned} \langle \mathbf{h}_{\mathbf{e}_j}, \mathbf{y}_{\mathbf{e}_i} \rangle_{\ell^2} &= \Big\langle \mathbf{R}^{\mathrm{T}} \mathbf{e}_{d-d_{\mathbf{M}}+j}, \mathbf{R}^{-1} \frac{1}{\varepsilon_{d-d_{\mathbf{M}}+i}} \mathbf{e}_{d-d_{\mathbf{M}}+i} \Big\rangle_{\ell^2} \\ &= \frac{1}{\varepsilon_{d-d_{\mathbf{M}}+i}} \mathbf{e}_{d-d_{\mathbf{M}}+j}^{\mathrm{T}} \mathbf{e}_{d-d_{\mathbf{M}}+i} = \begin{cases} \frac{1}{\varepsilon_{d-d_{\mathbf{M}}+i}}, & i = j \\ 0, & i \neq j \end{cases}. \end{aligned}$$

□

Example 3.4. We continue to study the matrix $\mathbf{A}_3$ from Example 3.1 and aim to determine the basis of $\mathcal{P}(\mathbf{A}_3)$ and $\mathcal{G}(\mathbf{A}_3^{\mathrm{T}})$. Referring to the Smith normal form of $\mathbf{A}_3$, we recall having

$$\mathbf{E} = \begin{bmatrix} 4 & 0 \\ 0 & 64 \end{bmatrix}, \qquad \mathbf{R} = \begin{bmatrix} 4 & 1 \\ -1 & 0 \end{bmatrix},$$

i.e., the elementary divisors are $\varepsilon_1 = 4$ and $\varepsilon_2 = 64$. By utilizing the formulas in Equation (3.6) and (3.10) we compute the basis for the pattern and the generating group, respectively, we get the vectors

$$\begin{aligned} \mathbf{y}_{\mathbf{e}_1} &= \big(0, \tfrac{1}{4}\big)^{\mathrm{T}} & \mathbf{h}_{\mathbf{e}_1} &= \big(4, 1\big)^{\mathrm{T}} \\ \mathbf{y}_{\mathbf{e}_2} &= \big(-\tfrac{1}{64}, \tfrac{1}{16}\big)^{\mathrm{T}} & \mathbf{h}_{\mathbf{e}_2} &= \big(-1, 0\big)^{\mathrm{T}}. \end{aligned}$$

These basis vectors are visualized alongside the elements of $\mathcal{P}(\mathbf{A}_3)$ and $\mathcal{G}(\mathbf{A}_3^{\mathrm{T}})$ in Figure 3.2. It is worth noting that the matrix $\mathbf{R}$ influences the step direction of the basis vectors for both the pattern and the generating group, while the elementary divisors determine the step length.

3.3 The Fourier Transform on the Pattern

Based on the previous section, we have establishd an ordering of the elements of $\mathcal{P}(\mathbf{M})$ and $\mathcal{G}(\mathbf{M}^{\mathrm{T}})$, which are known to be biorthogonal. This allows us to define the Fourier transform on the pattern, using $\mathcal{P}(\mathbf{M})$ as time domain and $\mathcal{G}(\mathbf{M}^{\mathrm{T}})$ as the frequency domain. Before doing so, we aim to generalize the Fourier transform from Section 2.2 to the d-variate case.

Consider the function $f \in L^2(\mathbb{T}^d)$, sampled on the uniform grid $\{\frac{2\pi}{N}\mathbf{n} : \mathbf{n} \in \mathbb{Z}^d\}$, where $N \in \mathbb{N}$ is even. Here, we define $I_N = \{0, \dots, N-1\}$ and $I_N^d = \{\mathbf{n} = (n_j)_{j=1}^d : n_j \in I_N\}$. By employing the multivariate trapezoidal rule, we can compute the discrete Fourier coefficients of f, denoted $(c_{\mathbf{k}}(f))_{\mathbf{k}\in\mathbb{Z}^d}$, which are given by

$$c_{\mathbf{k}}(f) = \frac{1}{(2\pi)^d} \int_{\mathbb{T}^d} f(\mathbf{x})\, \mathrm{e}^{-\mathrm{i}\mathbf{k}^{\mathrm{T}}\mathbf{x}} d\mathbf{x} \approx \frac{1}{N^d} \sum_{\mathbf{n}\in I_N^d} f\left(\frac{2\pi}{N}\mathbf{n}\right) \mathrm{e}^{-2\pi\mathrm{i}(\mathbf{k}^{\mathrm{T}}\mathbf{n})/N} = \hat{f}_{\mathbf{k}},$$

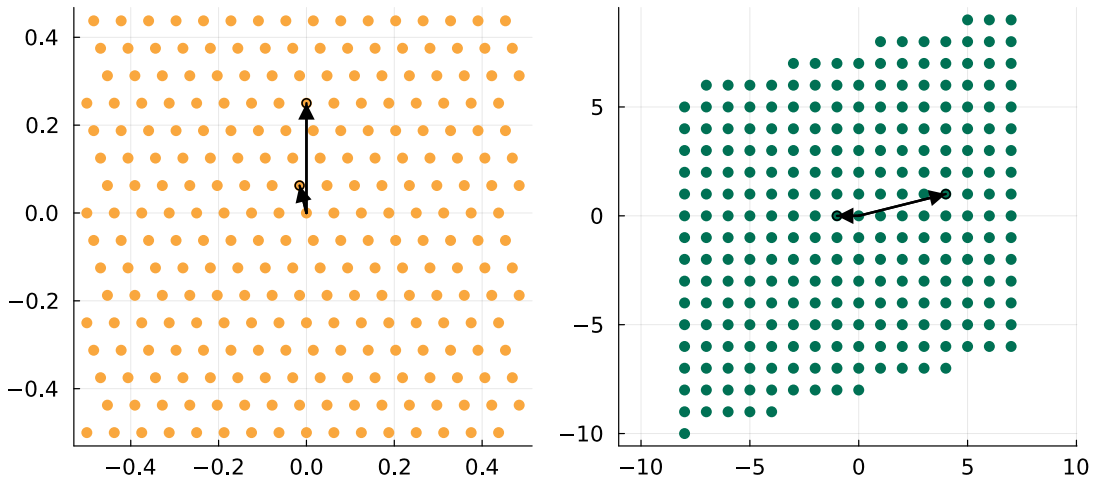

Figure 3.2: Plots of $\mathcal{P}(\mathbf{A}_3)$ and $\mathcal{G}(\mathbf{A}_3^{\mathrm{T}})$, respectively, including their basis vectors.

see [20, Section 4.4.1]. In the 1D case, discussed in Section 2.2, a step corresponds to a segment of length $\frac{1}{N}$, while in the d-variate case, a segment corresponds to a hypercube with side lengths $\frac{1}{N}$. By representing the vector $\mathbf{n} \in \mathbb{Z}^d$ in the uniform grid as a diagonal matrix $\mathbf{D} = \operatorname{diag}(N, \dots, N) \in \mathbb{Z}^{d \times d}$, we obtain an equivalent matrix representation and can utilize the pattern $\mathcal{P}(\mathbf{D})$ as our grid.

To provide a connection to the 1D discrete Fourier transform and introduce the use of the fast Fourier transform on the pattern, we focus on the case $d = 2$. The discrete Fourier coefficients are then given by

$$\begin{aligned} \hat{f}_{\mathbf{k}} &= \frac{1}{N^2} \sum_{n_1=0}^{N-1} \sum_{n_2=0}^{N-1} f\left(\frac{2\pi}{N}\mathbf{n}\right) \mathrm{e}^{-2\pi \mathrm{i} \mathbf{k}^{\mathrm{T}} \mathbf{n}/N} \\ &= \frac{1}{N^2} \sum_{n_1=0}^{N-1} \sum_{n_2=0}^{N-1} f\left(\frac{2\pi}{N}(n_1, n_2)^{\mathrm{T}}\right) \mathrm{e}^{-2\pi \mathrm{i}(k_1 n_1 + k_2 n_2)/N}. \end{aligned} \tag{3.12}$$

Rewriting the last expression yields

$$\hat{f}_{\mathbf{k}} = \frac{1}{N^2} \sum_{n_1=0}^{N-1} \mathrm{e}^{-2\pi \mathrm{i} k_1 n_1/N} \sum_{n_2=0}^{N-1} f\left(\frac{2\pi}{N}(n_1, n_2)^{\mathrm{T}}\right) \mathrm{e}^{-2\pi \mathrm{i} k_2 n_2/N}.$$

By fixing n_1 and performing a 1D Fourier transform iteratively through n_2, we obtain a sequence of values of f expressed as a function of the corresponding values of $\frac{2\pi}{N}(n_1, k)^{\mathrm{T}}$ for $k = 0, \dots, N-1$. Subsequently, applying a 1D Fourier transform to each fixed n_1 of the obtained results yields the Fourier transform of the elements n_2 for a fixed n_1. This approach allows for individual treatment of dimensions by fixing $n_1, \dots, n_{d-1}$ followed by fixing $n_2, \dots, n_{d-2}, n_d$, and so on. As the 2D case breaks down to 1D Fourier transforms, the fast Fourier transform can be employed for efficient computations. This behavious also applies when extending to the d-variate case.

Furthermore, the uniform grid can be generalized to possibly be non-uniform or anisotropic. Consider $N_1, N_2 \in \mathbb{N} \backslash \{1\}$. We construct a grid similarly to before, but now using the index set $I_{N_j} := \{0, \dots, N_j - 1\}$ for $j = \{1, 2\}$. The case when $N_1 \neq N_2$ makes the grid non-uniform. Moreover, the preceding procedure can be

rephrased in terms of matrix multiplication. A matrix representation can be used to express the general d-dimensional Fourier transform case [20, Section 4.4.3], but here, we explicitly write it for $d = 2$. The 2D discrete Fourier transform of a matrix $\mathbf{A} = (a_{k_1,k_2})_{k_1,k_2=\mathbf{0}}^{N_1-1,N_2-1} \in \mathbb{Z}^{N_1\times N_2}$ is given as

$$\hat{\mathbf{A}} = (\hat{a}_{n_1,n_2})_{n_1,n_2=\mathbf{0}}^{N_1-1,N_2-1} := \mathcal{F}_{N_1}\mathbf{A}\mathcal{F}_{N_2}^{\mathrm{T}},$$

where $\mathcal{F}_N$ is the Fourier matrix given in (2.3). The entries of the transformed matrix $\hat{\mathbf{A}}$ are described in Equation (3.12). If we now represent the matrix $\mathbf{A}$ by the vectors $\mathbf{r} = (r_{k_1})_{k_1\in I_{N_1}} \in \mathbb{Z}^{N_1}$ and $\mathbf{c} = (c_{k_2})_{k_2\in I_{N_2}} \in \mathbb{Z}^{N_2}$ such that $\mathbf{A} = \mathbf{r}\mathbf{c}^{\mathrm{T}}$, then the Fourier transform of $\mathbf{A}$ can be expressed as

$$\hat{\mathbf{A}} = \mathcal{F}_{N_1}\mathbf{r}\mathbf{c}^{\mathrm{T}}\mathcal{F}_{N_2}^{\mathrm{T}} = (\hat{r}_{n_1}\cdot\hat{c}_{n_2})_{n_1\in I_{N_1},n_2\in I_{N_2}}.$$

This formulation illustrates the separability of the Fourier transform in matrix representation, [20, Equation 4.53]. The separability allows for the Fourier transform to be performed on the rows and columns of the matrix $\mathbf{A}$ separately, as previously discussed.

The non-uniform 2D discrete Fourier transform is said to be $(N_1, N_2)^{\mathrm{T}}$-periodic, which is shown by the fact that for all $\mathbf{k}, \mathbf{z} \in \mathbb{Z}^2$, we have

$$\hat{a}_{\mathbf{n}} = \hat{a}_{n_1+z_1N_1,n_2+z_2N_2}, \quad n_j \in I_{N_j}, \quad j = \{1, 2\},$$

see [20, Section 4.4.2].

To perform the Fourier transform on the pattern $\mathcal{P}(\mathbf{M})$, we follow a similar approach as in previous cases. The Fourier transform on the pattern $\mathcal{P}(\mathbf{M})$ is approximated by

$$c_{\mathbf{k}}(f) \approx \frac{1}{|\det\mathbf{M}|}\sum_{\mathbf{y}\in\mathcal{P}(\mathbf{M})} f(2\pi\mathbf{y})\mathrm{e}^{-2\pi\mathrm{i}\mathbf{k}^{\mathrm{T}}\mathbf{y}} = \hat{f}_{\mathbf{k}}, \quad \mathbf{k}\in\mathbb{Z}^d. \tag{3.13}$$

By writing out the summands and expressing the elements $\mathbf{y} \in \mathcal{P}(\mathbf{M})$ in terms of the basis vectors $\mathbf{y}_{\mathbf{e}_j}$ known by (3.6), we obtain

$$\begin{aligned}\hat{f}_{\mathbf{k}} &= \frac{1}{m}\sum_{\lambda_1=0}^{\varepsilon_{d-d_{\mathbf{M}}}-1}\cdots\sum_{\lambda_{d_{\mathbf{M}}}=0}^{\varepsilon_d-1} f(2\pi\mathbf{y})\mathrm{e}^{-2\pi\mathrm{i}\mathbf{k}^{\mathrm{T}}(\lambda_1\mathbf{y}_{\mathbf{e}_1}+\ldots+\lambda_{d_{\mathbf{M}}}\mathbf{y}_{\mathbf{e}_{d_{\mathbf{M}}}})} \\ &= \frac{1}{m}\sum_{\lambda_1=0}^{\varepsilon_{d-d_{\mathbf{M}}}-1}\cdots\sum_{\lambda_{d_{\mathbf{M}}-1}=0}^{\varepsilon_{d-1}-1}\mathrm{e}^{-2\pi\mathrm{i}\mathbf{k}^{\mathrm{T}}(\lambda_1\mathbf{y}_{\mathbf{e}_1}+\ldots+\lambda_{d_{\mathbf{M}}-1}\mathbf{y}_{\mathbf{e}_{d_{\mathbf{M}}-1}})}\sum_{\lambda_{d_{\mathbf{M}}}=0}^{\varepsilon_d-1} f(2\pi\mathbf{y})\mathrm{e}^{2\pi\mathrm{i}\mathbf{k}^{\mathrm{T}}(\lambda_{d_{\mathbf{M}}}\mathbf{y}_{\mathbf{e}_{d_{\mathbf{M}}}})},\end{aligned} \tag{3.14}$$

where $\boldsymbol{\lambda} \in \mathbb{E}_{\mathbf{M}}$ and $\mathbf{k} \in \mathbb{Z}^d$.

In a similar manner as for the 2D case, we now fix λ_1 to $\lambda_{d_{\mathbf{M}}-1}$ in Equation (3.14) and perform a 1D fast Fourier transform in $\lambda_{d_{\mathbf{M}}}$. We then fix λ_1 to $\lambda_{d_{\mathbf{M}}-2}$ and $\lambda_{d_{\mathbf{M}}}$ and perform a 1D fast Fourier transform in $\lambda_{d_{\mathbf{M}}-1}$, and so on. In other words, we can compute the fast Fourier transform on the pattern by iterating through one cycle at a time.

The multivariate Fourier matrix is defined as

$$\begin{aligned}\mathcal{F}(\mathbf{M}) :=& \frac{1}{\sqrt{m}}\left(\mathrm{e}^{-2\pi\mathrm{i}\mathbf{h}^{\mathrm{T}}\mathbf{M}^{-1}\mathbf{g}}\right)_{\mathbf{h}\in\mathcal{G}(\mathbf{M}^{\mathrm{T}}),\ \mathbf{g}\in\mathcal{G}(\mathbf{M})} \in \mathbb{C}^{m\times m}\\ =& \frac{1}{\sqrt{m}}\left(\mathrm{e}^{-2\pi\mathrm{i}\mathbf{h}^{\mathrm{T}}\mathbf{y}}\right)_{\mathbf{h}\in\mathcal{G}(\mathbf{M}^{\mathrm{T}}),\ \mathbf{y}\in\mathcal{P}(\mathbf{M})},\end{aligned}$$

where $\mathbf{h} \in \mathcal{G}(\mathbf{M}^{\mathrm{T}})$ adresses the rows, while $\mathbf{g} \in \mathcal{G}(\mathbf{M})$ and $\mathbf{y} \in \mathcal{P}(\mathbf{M})$ adress the columns. The last equality holds true only in the case where the elements of $\mathcal{G}(\mathbf{M})$ and $\mathcal{P}(\mathbf{M})$ are ordered identically with respect to the bijection $\mathbf{M}\circ$, as shown in [4, Equation 6]. Moreover, the multivariate Fourier transform is $\mathbf{M}^{\mathrm{T}}$-periodic. To show this, take any $\mathbf{z} \in \mathbb{Z}^d$, then

$$\begin{aligned}\hat{f}_{\mathbf{h}+\mathbf{M}^{\mathrm{T}}\mathbf{z}} &= \frac{1}{\sqrt{m}}\sum_{\mathbf{y}\in\mathcal{P}(\mathbf{M})}\left(\mathrm{e}^{-2\pi\mathrm{i}(\mathbf{h}+\mathbf{M}^{\mathrm{T}}\mathbf{z})^{\mathrm{T}}\mathbf{y}}\right)\\ &= \frac{1}{\sqrt{m}}\sum_{\mathbf{y}\in\mathcal{P}(\mathbf{M})}\left(\mathrm{e}^{-2\pi\mathrm{i}\mathbf{h}^{\mathrm{T}}\mathbf{y}}\right)\left(\mathrm{e}^{-2\pi\mathrm{i}(\mathbf{M}^{\mathrm{T}}\mathbf{z})^{\mathrm{T}}\mathbf{y}}\right) = \hat{f}_{\mathbf{h}},\end{aligned} \tag{3.15}$$

where $\mathbf{h} \in \mathcal{G}(\mathbf{M}^{\mathrm{T}})$, [3, Lemma 1.17].

Let $\mathbf{a} = (a_{\mathbf{y}})_{\mathbf{y}\in\mathcal{P}(\mathbf{M})} \in \mathbb{C}^m$ be a vector sorted the same way as the columns of the Fourier matrix. Then the Fourier transform of $\mathbf{a}$ is given by

$$\hat{\mathbf{a}} = (\hat{a}_{\mathbf{h}})_{\mathbf{h}\in\mathcal{G}(\mathbf{M}^{\mathrm{T}})} = \Big(\sum_{\mathbf{y}\in\mathcal{P}(\mathbf{M})} a_{\mathbf{y}}\mathrm{e}^{-2\pi\mathrm{i}\mathbf{h}^{\mathrm{T}}\mathbf{y}}\Big)_{\mathbf{h}\in\mathcal{G}(\mathbf{M}^{\mathrm{T}})} = \sqrt{m}\mathcal{F}(\mathbf{M})\mathbf{a} \in \mathbb{C}^m, \tag{3.16}$$

as defined in [18, Equation 10]. Then $\hat{\mathbf{a}}$ has the same ordering as the columns of the Fourier matrix.

So far in this section, we have justified performing the Fourier transform along the cycles of the pattern instead of the traditional rows and columns. This computation can be expressed in a convenient matrix form, as shown in the following lemma from [18, Lemma 2.1] where also a proof can be found.

Lemma 3.5. Let $\mathbf{M} \in \mathbb{Z}^{d\times d}$ be a regular matrix. Then there exists permutation matrices $\mathbf{P}_{\mathbf{h}}$, $\mathbf{P}_{\mathbf{y}}$ on $\mathcal{G}(\mathbf{M}^{\mathrm{T}})$ and $\mathcal{P}(\mathbf{M})$, respectively, so that

$$\mathcal{F}(\mathbf{M}) = \mathbf{P}_{\mathbf{h}}\big(\mathcal{F}_{\varepsilon_1} \otimes \mathcal{F}_{\varepsilon_2} \otimes \cdots \otimes \mathcal{F}_{\varepsilon_d}\big)\mathbf{P}_{\mathbf{y}}, \tag{3.17}$$

where $\otimes$ denotes the Kronecker product, and

$$\mathcal{F}_{\varepsilon} = \frac{1}{\sqrt{\varepsilon}}\left(\mathrm{e}^{-2\pi\mathrm{i}h\varepsilon^{-1}g}\right)_{h,g=0}^{\varepsilon-1},$$

are the standard Fourier matrices indexed by the elementary divisors of the Smith normal form of $\mathbf{M}$ as defined in Equation (2.7).

When using the ordering from (3.9) and (3.11) to construct the Fourier matrix $\mathcal{F}(\mathbf{M})$, Theorem 1 in [4] proofs that the expression in (3.17) simplifies to

$$\mathcal{F}(\mathbf{M}) = \mathcal{F}_{\varepsilon_{d-d_{\mathbf{M}}+1}} \otimes \mathcal{F}_{\varepsilon_{d-d_{\mathbf{M}}+2}} \otimes \cdots \otimes \mathcal{F}_{\varepsilon_d},$$

as the sets of basis vectors are biorthogonal, [3, Theorem 3.9].

The computational complexity of the Fourier transform on $\mathcal{P}(\mathbf{M})$ is $\mathcal{O}(m \log m)$ [4, Theorem 2].

3.4 Properties of Subpatterns

The following section deals with some of the properties of the pattern of $\mathbf{M}$ when the matrix can be expressed as $\mathbf{M} = \mathbf{JN}$ for $\mathbf{J}, \mathbf{N} \in \mathbb{Z}^{d\times d}$. The main results for the section is the inclusion theorem for the subpattern of a decomposed matrix, stated in the first theorem.

Theorem 3.6 ([18, Lemma 2.7])**.** Let $\mathbf{M}, \mathbf{N} \in \mathbb{Z}^{d\times d}$ be regular matrices. Then $\mathcal{P}(\mathbf{N}) \subseteq \mathcal{P}(\mathbf{M})$ if and only if there exists a regular matrix $\mathbf{J} \in \mathbb{Z}^{d\times d}$ such that $\mathbf{M} = \mathbf{JN}$.

Proof. First, assume $\mathcal{P}(\mathbf{N}) \subseteq \mathcal{P}(\mathbf{M})$. Then, by definition of the pattern, we have that $\mathbf{y} = \mathbf{N}^{-1}\mathbf{z} \in \mathcal{P}(\mathbf{N})$ for some $\mathbf{z} \in \mathbb{Z}^d$. Additionally, $\mathbf{y}$ is an element of $\mathcal{P}(\mathbf{M})$ by assumption, implying that $\mathbf{y} = \mathbf{M}^{-1}\mathbf{x}$ for some $\mathbf{x} \in \mathbb{Z}^d$. Combinting the two expressions yields $\mathbf{y} = \mathbf{MN}^{-1}\mathbf{z} \in \mathbb{Z}^d$ for some $\mathbf{z}$. By setting $\mathbf{J} = \mathbf{MN}^{-1}$, we obtain a regular matrix $\mathbf{J} \in \mathbb{Z}^{d\times d}$ since both $\mathbf{M}$ and $\mathbf{N}^{-1}$ are regular.

Conversely, suppose there exists a regular matrix $\mathbf{J} \in \mathbb{Z}^{d\times d}$ such that $\mathbf{M} = \mathbf{JN}$. If $\mathbf{y} \in \mathcal{P}(\mathbf{N})$, it implies $\mathbf{Ny} \in \mathbb{Z}^d$, which further implies $\mathbf{JNy} \in \mathbb{Z}^d$. Hence, if $\mathbf{y} \in \mathcal{P}(\mathbf{N})$, then $\mathbf{y} \in \mathcal{P}(\mathbf{M})$, i.e., $\mathcal{P}(\mathbf{N}) \subseteq \mathcal{P}(\mathbf{M})$, which concludes the proof. □

Note that in general $\mathcal{P}(\mathbf{J}) \nsubseteq \mathcal{P}(\mathbf{M})$, due to the non-commutativity of matrix multiplication.

Lemma 3.7 ([3, Lemma 1.5])**.** Let $\mathbf{M}$ and $\mathbf{N}$ be regular matrices in $\mathbb{Z}^{d\times d}$ related by $\mathbf{M} = \mathbf{JN}$, with $\mathbf{J} \in \mathbb{Z}^{d\times d}$. Then every element $\mathbf{x} \in \mathcal{P}(\mathbf{M})$ can be uniquely expressed in terms of elements of the patterns $\mathcal{P}(\mathbf{N})$ and $\mathcal{P}(\mathbf{J})$ as follows

$$\mathbf{x} = \left(\mathbf{y} + \mathbf{N}^{-1}\mathbf{z}\right)\Big|_{\mathcal{P}(\mathbf{M})}, \quad \mathbf{y} \in \mathcal{P}(\mathbf{N}),\ \mathbf{z} \in \mathcal{P}(\mathbf{J}).$$

Proof. By the definition of a lattice we have

$$\Lambda(\mathbf{M}) = \mathbf{M}^{-1}\mathbb{Z}^d = (\mathbf{JN})^{-1}\mathbb{Z}^d = \mathbf{N}^{-1}\mathbf{J}^{-1}\mathbb{Z}^d = \mathbf{N}^{-1}\Lambda(\mathbf{J}). \tag{3.18}$$

Using the 1-periodicity of any lattice with $\Lambda(\mathbf{I}) = \mathbb{Z}^d$, we obtain

$$\Lambda(\mathbf{J}) = \bigcup_{\mathbf{z}\in\mathcal{P}(\mathbf{J})} \Lambda(\mathbf{I}) + \mathbf{z}.$$

Inserting this into the expression on the right-hand side of (3.18), we get

$$\Lambda(\mathbf{M}) = \bigcup_{\mathbf{z}\in\mathcal{P}(\mathbf{J})} \mathbf{N}^{-1}\Lambda(\mathbf{I}) + \mathbf{N}^{-1}\mathbf{z} = \bigcup_{\mathbf{z}\in\mathcal{P}(\mathbf{J})} \Lambda(\mathbf{N}) + \mathbf{N}^{-1}\mathbf{z}.$$

Intersecting with a unit cube, we arrive at a decomposed expression of the elements $\mathbf{x} \in \mathcal{P}(\mathbf{M})$.

The uniqueness is achieved by the disjointness of the sets in the union. The sets are disjoint because for an element $\mathbf{z} \in \mathcal{P}(\mathbf{J})$, the condition $\mathbf{N}^{-1}\mathbf{z} \in \mathcal{P}(\mathbf{N})$ is true if and only if $\mathbf{z} = \mathbf{0}|_{\mathcal{P}(\mathbf{N})}$. □

Expressing an element $\mathbf{h} \in \mathcal{G}(\mathbf{M}^{\mathrm{T}})$ in terms of $\mathcal{G}(\mathbf{N}^{\mathrm{T}})$ and $\mathcal{G}(\mathbf{J}^{\mathrm{T}})$ requires similar steps as in the preceding lemma. By following the procedure outlined in the proof, we can express an element $\mathbf{y} \in \mathcal{P}(\mathbf{M}^{\mathrm{T}})$ as $\mathbf{y} = \big(\mathbf{x} + \mathbf{J}^{-\mathrm{T}}\mathbf{z}\big)\Big|_{\mathcal{P}(\mathbf{M}^{\mathrm{T}})}$ for $\mathbf{x} \in \mathcal{P}(\mathbf{J}^{\mathrm{T}})$ and $\mathbf{z} \in \mathcal{P}(\mathbf{N}^{\mathrm{T}})$. When now left-multiplying with $\mathbf{M}^{\mathrm{T}}$, we get $\mathbf{h} \in \mathcal{G}(\mathbf{M}^{\mathrm{T}})$, and the decomposition is given by

$$\mathbf{h} = \big(\mathbf{N}^{\mathrm{T}}\mathbf{g} + \mathbf{k}\big)\Big|_{\mathcal{G}(\mathbf{M}^{\mathrm{T}})}, \quad \text{for } \mathbf{g} \in \mathcal{G}(\mathbf{J}^{\mathrm{T}}),\ \mathbf{k} \in \mathcal{G}(\mathbf{N}^{\mathrm{T}}). \tag{3.19}$$

Example 3.8. We proceed with the investigation of $\mathbf{A}_3$, its pattern $\mathcal{P}(\mathbf{A}_3)$ and generating group $\mathcal{G}(\mathbf{A}_3^{\mathrm{T}})$ from Example 3.1. In order to visualize the inclusion $\mathcal{P}(\mathbf{N}) \subseteq \mathcal{P}(\mathbf{A}_3)$ stated in Theorem 3.6, we consider various matrices $\mathbf{J}$ with $|\det \mathbf{J}| = 2$, such that $\mathbf{A}_3 = \mathbf{J}\mathbf{N}$. We study the matrices

$$\mathbf{J}_1 = \begin{bmatrix} 2 & 0 \\ 0 & 1 \end{bmatrix},\ \mathbf{J}_2 = \begin{bmatrix} 1 & 0 \\ 0 & 2 \end{bmatrix},\ \mathbf{J}_3 = \begin{bmatrix} 1 & -1 \\ 1 & 1 \end{bmatrix}, \tag{3.20a}$$

$$\mathbf{J}_4 = \begin{bmatrix} 2 & 0 \\ -1 & 1 \end{bmatrix},\ \mathbf{J}_5 = \begin{bmatrix} 2 & 0 \\ 1 & 1 \end{bmatrix},\ \mathbf{J}_6 = \begin{bmatrix} 1 & -1 \\ 0 & 2 \end{bmatrix},\ \mathbf{J}_7 = \begin{bmatrix} 1 & 1 \\ 0 & 2 \end{bmatrix}, \tag{3.20b}$$

and collect them in the set $\mathcal{J}$, as described in [3, Equation 4.3]. To avoid confusion with the index of the matrix $\mathbf{A}_3$, we use the same index to relate the matrices $\mathbf{J}_i$ and $\mathbf{N}_i$ in the context of $\mathbf{A}_3 = \mathbf{J}_i\mathbf{N}_i$. As an example, when examining the matrix $\mathbf{J}_3$, the corresponding matrix $\mathbf{N}_3$ can be explicitly expressed as follows

$$\mathbf{N}_3 = \mathbf{J}_3^{-1}\mathbf{A}_3 = \begin{bmatrix} \frac{1}{2} & \frac{1}{2} \\ -\frac{1}{2} & \frac{1}{2} \end{bmatrix} \begin{bmatrix} 16 & 4 \\ 0 & 16 \end{bmatrix} = \begin{bmatrix} 8 & 10 \\ -8 & 6 \end{bmatrix}.$$

The figures presented in Figure 3.3 demonstrate the relationship between the matrices $\mathbf{A}_3$, $\mathbf{N}_i$ and the associated directions of the matrices $\mathbf{J}_i$. Specifically, the matrices $\mathbf{J}_1$ and $\mathbf{J}_2$ correspond to scaling along the x- and y-direction, respectively, while $\mathbf{J}_3$ represents a scaling of $2^{-1/2}$ and rotation of 45°. On the other hand, $\mathbf{J}_4$ and $\mathbf{J}_5$ give sheared matrices $\mathbf{N}$ scaled in x-direction clockwise and counterclockwise, respectively. Similarly, $\mathbf{J}_6$ and $\mathbf{J}_7$ shear the corresopnding matrices $\mathbf{N}$ scaled in y-direction counterclockwise and clockwise, respectively.

Remark 3.9. Apart from the matrices discussed in Example 3.8, there are several other matrices $\mathbf{J}$ with a determinant of 2 that could have been considered. For instance, we could investigate the matrices

$$\tilde{\mathbf{J}}_1^{\pm} = \begin{bmatrix} 2 & \pm 1 \\ 0 & 1 \end{bmatrix} \quad \text{or} \quad \tilde{\mathbf{J}}_2^{\pm} = \begin{bmatrix} 1 & 0 \\ \pm 1 & 2 \end{bmatrix},$$

which in fact are the transposed of the matrices in (3.20b).

Theorem 3.6 yields $\mathcal{P}(\mathbf{N}) \subseteq \mathcal{P}(\mathbf{M})$, and thus $\mathcal{G}(\mathbf{J}^{\mathrm{T}}) \subseteq \mathcal{G}(\mathbf{M}^{\mathrm{T}})$. By the non-commutativity of the matrix multiplication and the ordering of $\mathbf{J}\mathbf{N}$ reversing when transposing $\mathbf{M}$, the inclusion $\mathcal{G}(\mathbf{N}^{\mathrm{T}}) \subseteq \mathcal{G}(\mathbf{M}^{\mathrm{T}})$ does not hold true in general. The inclusion property can be rephrased to

$$\mathbf{J}^{-\mathrm{T}}\Big[-\frac{1}{2}, \frac{1}{2}\Big)^d \subseteq \Big[-\frac{1}{2}, \frac{1}{2}\Big)^d. \tag{3.21}$$

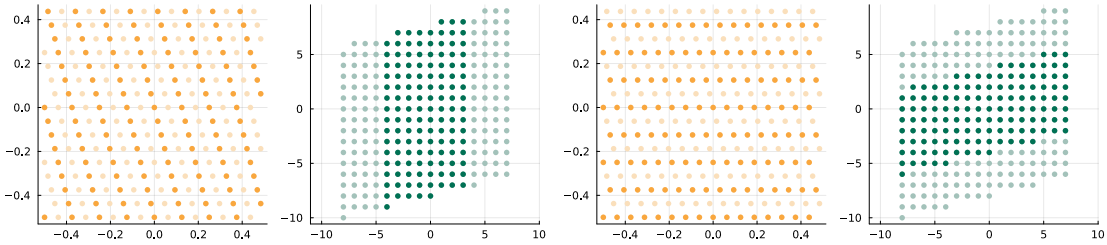

(a) $\mathcal{P}(\mathbf{N}_1) \subset \mathcal{P}(\mathbf{A}_3)$ and $\mathcal{G}(\mathbf{N}_1^{\mathrm{T}}) \subset \mathcal{G}(\mathbf{A}_3^{\mathrm{T}})$. (b) $\mathcal{P}(\mathbf{N}_2) \subset \mathcal{P}(\mathbf{A}_3)$ and $\mathcal{G}(\mathbf{N}_2^{\mathrm{T}}) \subset \mathcal{G}(\mathbf{A}_3^{\mathrm{T}})$.

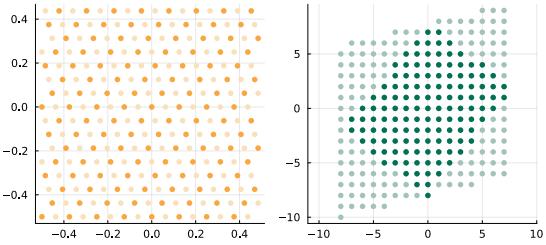

(c) $\mathcal{P}(\mathbf{N}_3) \subset \mathcal{P}(\mathbf{A}_3)$ and $\mathcal{G}(\mathbf{N}_3^{\mathrm{T}}) \subset \mathcal{G}(\mathbf{A}_3^{\mathrm{T}})$.

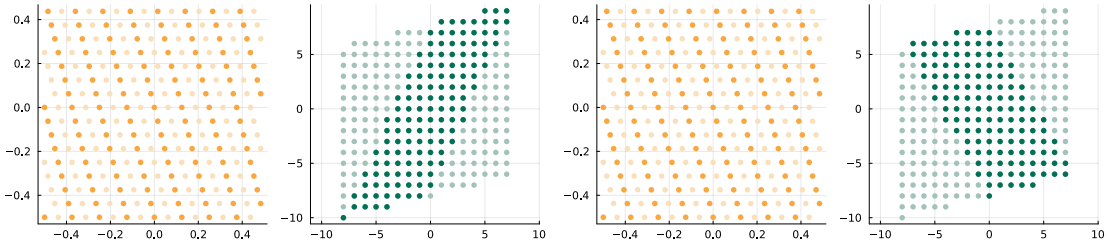

(d) $\mathcal{P}(\mathbf{N}_4) \subset \mathcal{P}(\mathbf{A}_3)$ and $\mathcal{G}(\mathbf{N}_4^{\mathrm{T}}) \subset \mathcal{G}(\mathbf{A}_3^{\mathrm{T}})$. (e) $\mathcal{P}(\mathbf{N}_5) \subset \mathcal{P}(\mathbf{A}_3)$ and $\mathcal{G}(\mathbf{N}_5^{\mathrm{T}}) \subset \mathcal{G}(\mathbf{A}_3^{\mathrm{T}})$.

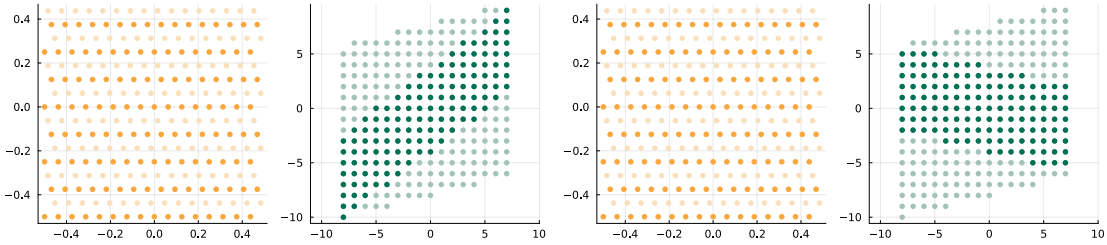

(f) $\mathcal{P}(\mathbf{N}_6) \subset \mathcal{P}(\mathbf{A}_3)$ and $\mathcal{G}(\mathbf{N}_6^{\mathrm{T}}) \subset \mathcal{G}(\mathbf{A}_3^{\mathrm{T}})$. (g) $\mathcal{P}(\mathbf{N}_7) \subset \mathcal{P}(\mathbf{A}_3)$ and $\mathcal{G}(\mathbf{N}_7^{\mathrm{T}}) \subset \mathcal{G}(\mathbf{A}_3^{\mathrm{T}})$.

Figure 3.3: $\mathcal{P}(\mathbf{N})$ is given in dark yellow, $\mathcal{P}(\mathbf{A}_3)$ in light yellow. $\mathcal{G}(\mathbf{N})$ is given in dark green, $\mathcal{G}(\mathbf{A}_3^{\mathrm{T}})$ in light green.

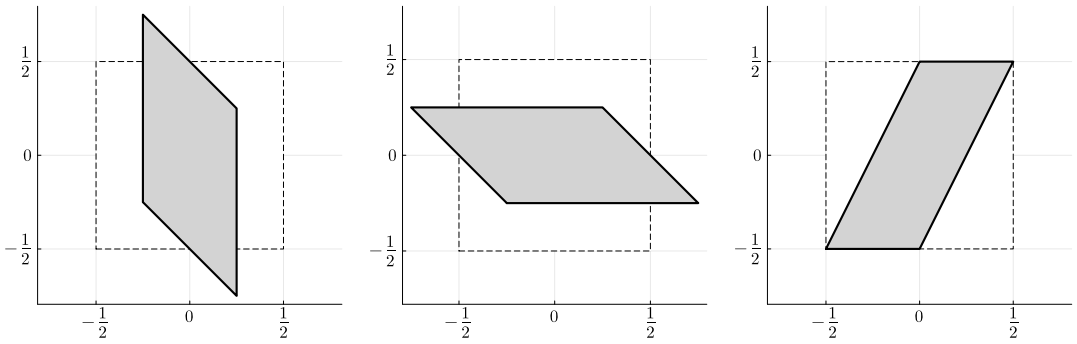

(a) $(\tilde{\mathbf{J}}_1^+)^{-\mathrm{T}}\Big[-\frac{1}{2},\frac{1}{2}\Big)^d$. (b) $(\tilde{\mathbf{J}}_2^+)^{-\mathrm{T}}\Big[-\frac{1}{2},\frac{1}{2}\Big)^d$. (c) $\mathbf{J}_4^{-\mathrm{T}}\Big[-\frac{1}{2},\frac{1}{2}\Big)^d$.

Figure 3.4: Dashed square is $[-\frac{1}{2},\frac{1}{2})^2$, while the grey rectangle is $\mathbf{J}^{-\mathrm{T}}[-\frac{1}{2},\frac{1}{2})^2$.

In contrast to the matrices $\mathbf{J} \in \mathcal{J}$, $\tilde{\mathbf{J}}_1^{\pm}$ and $\tilde{\mathbf{J}}_2^{\pm}$ do not possess the property in Equation (3.21). Figure 3.4 portrayes this consept for the matrices $\tilde{\mathbf{J}}_1^+$, $\tilde{\mathbf{J}}_2^+$ and the matrix $\mathbf{J}_4 \in \mathcal{J}$. We observe that the first two matrices shears too much for the inclusion to be satisfied, whereas $\mathbf{J}_4$ yields a decomposition where (3.21) is fulfilled.

Since we are interested in decomposing the frequency domain $\mathcal{G}(\mathbf{M}^{\mathrm{T}})$, we require $\mathcal{G}(\mathbf{N}^{\mathrm{T}}) \subseteq \mathcal{G}(\mathbf{M}^{\mathrm{T}})$. Therefore, we are only interested in matrices $\mathbf{J}$ satisfying this condition. In particular, the matrices $\mathbf{J} \in \mathcal{J}$ are the only matrices with a determinant of 2 upholding the incusion property $\mathcal{G}(\mathbf{N}^{\mathrm{T}}) \subseteq \mathcal{G}(\mathbf{M}^{\mathrm{T}})$. Wherefore, these matrices are the only matrices of interest for this application.

CHAPTER 4

The Wavelet Transform

4.1 Shift Invariant Spaces

Let $\mathbf{M} \in \mathbb{Z}^{d\times d}$ be a regular matrix. A subspace $V \subseteq L^2(\mathbb{T}^d)$ is called shift invariant with respect to $\mathbf{M}$, or $\mathbf{M}$-shift invariant, if it is spanned by the translates of a function $\varphi \in L^2(\mathbb{T}^d)$, i.e.,

$$T(\mathbf{y})\varphi \coloneqq \varphi(\circ - 2\pi\mathbf{y}) \in V, \qquad \text{for all } \mathbf{y} \in \mathcal{P}(\mathbf{M}), \varphi \in V.$$

see [5, Section 2]. The space of translates with respect to $\mathbf{M}$ of φ is denoted by

$$V_{\mathbf{M}}^{\varphi} \coloneqq \operatorname{span}\{T(\mathbf{y})\varphi : \mathbf{y} \in \mathcal{P}(\mathbf{M})\}. \tag{4.1}$$

The name of the space is due to the fact that the space is invariant under shift on $\mathcal{P}(\mathbf{M})$ of the function φ. It is also referred to as a translation invariant space.

Theorem 4.1 ([18, Theorem 3.1])**.** Let $\mathbf{M} \in \mathbb{Z}^{d\times d}$ be regular. Then the vector of translates of $\varphi \in L^2(\mathbb{T}^d)$ and the vectors of orthogonal splines, i.e.,

$$s_{\mathbf{h}}^{\varphi}(\mathbf{x}) \coloneqq \sum_{\mathbf{z}\in\mathbb{Z}^d} c_{\mathbf{h}+\mathbf{M}^{\mathrm{T}}\mathbf{z}}(\varphi)\mathrm{e}^{\mathrm{i}(\mathbf{h}+\mathbf{M}^{\mathrm{T}}\mathbf{z})^{\mathrm{T}}\mathbf{x}}, \qquad \text{for } \mathbf{h} \in \mathcal{G}(\mathbf{M}^{\mathrm{T}}),$$

fulfill the equation

$$\big(T(\mathbf{y})\varphi\big)_{\mathbf{y}\in\mathcal{P}(\mathbf{M})} = \sqrt{m}\mathcal{F}(\mathbf{M})^{\mathrm{T}}\big(s_{\mathbf{h}}^{\varphi}\big)_{\mathbf{h}\in\mathcal{G}(\mathbf{M}^{\mathrm{T}})}. \tag{4.2}$$

Proof. By the definition of the Fourier series and a property of the translation function, given in (2.1) and (2.2) respectively, we have

$$T(\mathbf{y})\varphi = \sum_{\mathbf{k}\in\mathbb{Z}^d} c_{\mathbf{k}}\big(T(\mathbf{y})\varphi\big)\mathrm{e}^{\mathrm{i}\mathbf{k}^{\mathrm{T}}\mathbf{x}} = \sum_{\mathbf{k}\in\mathbb{Z}^d} \mathrm{e}^{-2\pi\mathrm{i}\mathbf{k}^{\mathrm{T}}\mathbf{y}} c_{\mathbf{k}}(\varphi)\mathrm{e}^{\mathrm{i}\mathbf{k}^{\mathrm{T}}\mathbf{y}}.$$

Inserting $\mathbf{k} = \mathbf{h} + \mathbf{M}^{\mathrm{T}}\mathbf{z}$, where $\mathbf{h} \in \mathcal{G}(\mathbf{M}^{\mathrm{T}})$ and $\mathbf{z} \in \mathbb{Z}^d$ are unique for each $\mathbf{k}$ and further utilizing the fact that $\mathbf{k}^{\mathrm{T}}\mathbf{M}\mathbf{y} \in \mathbb{Z}^d$ for $\mathbf{y} \in \mathcal{P}(\mathbf{M})$ yields

$$T(\mathbf{y})\varphi(\mathbf{x}) = \sum_{\mathbf{h}\in\mathcal{G}(\mathbf{M}^{\mathrm{T}})} \mathrm{e}^{2\pi\mathrm{i}\mathbf{h}^{\mathrm{T}}\mathbf{y}} s_{\mathbf{h}}^{\varphi}(\mathbf{x}).$$

The proof is then completed, since the equation above is an arbitrary row of Equation (4.2). □

Corollary 4.2 ([3, Lemma 1.23c])**.** Let $\mathbf{M} \in \mathbb{Z}^{d\times d}$ be regular and $\varphi \in L^2(\mathbb{T}^d)$. Then the $\mathbf{M}$-invariant subspace $V_{\mathbf{M}}^{\varphi}$ is spanned by the orthogonal splines $\left(s_{\mathbf{h}}^{\varphi}\right)_{\mathbf{h}\in\mathcal{G}(\mathbf{M}^{\mathrm{T}})}$, i.e.,

$$V_{\mathbf{M}}^{\varphi} = \operatorname{span}\{s_{\mathbf{h}}^{\varphi} : \mathbf{h} \in \mathcal{G}(\mathbf{M}^{\mathrm{T}})\}.$$

Proof. Let $\mathbf{y} \in \mathcal{P}(\mathbf{M})$. Writing the function $T(\mathbf{y})\varphi$ as a Fourier series (2.1) combined with the property of the translation function (2.2) yields

$$T(\mathbf{y})\varphi = \sum_{\mathbf{k}\in\mathbb{Z}^d} \mathrm{e}^{-2\pi\mathrm{i}\mathbf{k}^{\mathrm{T}}\mathbf{y}} c_{\mathbf{k}}(\varphi)\mathrm{e}^{\mathrm{i}\mathbf{k}^{\mathrm{T}}\circ}.$$

For every $\mathbf{k} \in \mathbb{Z}^d$ there exists a unique $\mathbf{h} \in \mathcal{G}(\mathbf{M}^{\mathrm{T}})$ and $\mathbf{z} \in \mathbb{Z}^d$ such that $\mathbf{k} = \mathbf{h} + \mathbf{M}^{\mathrm{T}}\mathbf{z}$. We apply this decomposition to each summand in the Fourier series of $T(\mathbf{y})\varphi$. Further, the theorem of Fubini [23, Theorem 1.7.21] justifies the interchange of the sums as the terms are absolutely summable, which then gives

$$T(\mathbf{y})\varphi = \sum_{\mathbf{h}\in\mathcal{G}(\mathbf{M}^{\mathrm{T}})} \mathrm{e}^{-2\pi\mathrm{i}\mathbf{h}^{\mathrm{T}}\mathbf{y}} \sum_{\mathbf{z}\in\mathbb{Z}^d} c_{\mathbf{h}+\mathbf{M}^{\mathrm{T}}\mathbf{z}}(\varphi)\mathrm{e}^{\mathrm{i}(\mathbf{h}+\mathbf{M}^{\mathrm{T}}\mathbf{z})^{\mathrm{T}}\circ} = \sum_{\mathbf{h}\in\mathcal{G}(\mathbf{M}^{\mathrm{T}})} \mathrm{e}^{-2\pi\mathrm{i}\mathbf{h}^{\mathrm{T}}\mathbf{y}} s_{\mathbf{h}}^{\varphi},$$

as $\mathrm{e}^{2\pi\mathrm{i}(\mathbf{M}^{\mathrm{T}}\mathbf{z})^{\mathrm{T}}\mathbf{y}} = 1$ for all $\mathbf{z} \in \mathbb{Z}^d$. Thus, for every $\mathbf{y} \in \mathcal{P}(\mathbf{M})$ the function $T(\mathbf{y})\varphi \in V_{\mathbf{M}}^{s_{\mathbf{h}}^{\varphi}}$ and therefore $V_{\mathbf{M}}^{\varphi} \subseteq V_{\mathbf{M}}^{s_{\mathbf{h}}^{\varphi}}$.

Conversely, for an arbitrary $\mathbf{h} \in \mathcal{G}(\mathbf{M}^{\mathrm{T}})$, we have

$$\begin{aligned}\sum_{\mathbf{y}\in\mathcal{P}(\mathbf{M})} \mathrm{e}^{-2\pi\mathrm{i}\mathbf{h}^{\mathrm{T}}\mathbf{y}} T(\mathbf{y})\varphi &= \sum_{\mathbf{k}\in\mathcal{G}(\mathbf{M}^{\mathrm{T}})} \sum_{\mathbf{y}\in\mathcal{P}(\mathbf{M})} \mathrm{e}^{-2\pi\mathrm{i}(\mathbf{h}-\mathbf{k})^{\mathrm{T}}\mathbf{y}} \sum_{\mathbf{z}\in\mathbb{Z}^d} c_{\mathbf{k}+\mathbf{M}^{\mathrm{T}}\mathbf{z}}(\varphi)\mathrm{e}^{\mathrm{i}(\mathbf{k}+\mathbf{M}^{\mathrm{T}}\mathbf{z})^{\mathrm{T}}\circ} \\ &= m \sum_{\mathbf{z}\in\mathbb{Z}^d} c_{\mathbf{k}+\mathbf{M}^{\mathrm{T}}\mathbf{z}}(\varphi)\mathrm{e}^{\mathrm{i}(\mathbf{k}+\mathbf{M}^{\mathrm{T}}\mathbf{z})^{\mathrm{T}}\circ} \\ &= m s_{\mathbf{h}}^{\varphi},\end{aligned}$$

where the second step is satisfied follows from Equation 1.18 in [3]. Hence $s_{\mathbf{h}}^{\varphi} \in V_{\mathbf{M}}^{\varphi}$ for any $\mathbf{h} \in \mathcal{G}(\mathbf{M}^{\mathrm{T}})$ and the proof is completed. □

Before we study the properties of the translation invariant space $V_{\mathbf{M}}^{\varphi}$, we introduce the function we will use as φ throughout this thesis. We start by defining a general kernel function as

$$D_{\mathbf{M}}(\mathbf{x}) = \sum_{\mathbf{k}\in\mathcal{G}(\mathbf{M}^{\mathrm{T}})} \alpha_{\mathbf{k}}\mathrm{e}^{\mathrm{i}\mathbf{k}^{\mathrm{T}}\mathbf{x}},$$

which in general is complex valued. By extending the sum over $\mathcal{G}(\mathbf{M}^{\mathrm{T}})$ to a frequency domain which is symmetric, we can ensure that the kernel is real valued, as all the imaginary parts will cancel out. Additionally, we require symmetry of the Fourier coefficients of the kernel. The symmetric frequency domain is defined as

$$\mathcal{K}(\mathbf{M}^{\mathrm{T}}) = \mathbb{Z}^d \cap \mathbf{M}^{\mathrm{T}}\bar{Q} = \mathbf{M}^{\mathrm{T}}(\Lambda(\mathbf{M}^{\mathrm{T}}) \cap \bar{Q}) \quad \text{where } \bar{Q} = \left[-\tfrac{1}{2}, \tfrac{1}{2}\right]^d \subset \mathbb{R}^d.$$

The symmetric frequency domain includes all boundary points of the parallelepiped $\mathbf{M}^{\mathrm{T}}\bar{Q}$. Note that $\mathcal{G}(\mathbf{M}^{\mathrm{T}}) \subseteq \mathcal{K}(\mathbf{M}^{\mathrm{T}})$ by construction. Moreover, we want the function to describe details in both time and frequency domain in addition to have a certain localization in the time domain [3, Section 4].

We define the number of surficial planes of the parallelepiped $\mathbf{M}^{\mathrm{T}}\bar{Q}$ that an element $\mathbf{k} \in \mathcal{K}(\mathbf{M}^{\mathrm{T}})$ lies on as

$$r(\mathbf{k}) = \#\Big\{ j : \big|\mathbf{h}^{\mathrm{T}}\mathbf{M}^{-1}\mathbf{e}_j\big| = \frac{1}{2}, \quad \mathbf{h} \equiv \mathbf{k} \mod \mathbf{M}^{\mathrm{T}} \Big\}, \tag{4.3}$$

where $\mathbf{e}_j$ is the j-th unit vector, see [18, Equation 36].

Lemma 4.3 ([18, Lemma 6.3])**.** Let $\mathbf{k} \in \mathcal{K}(\mathbf{M}^{\mathrm{T}})$. Then there are $2^{r(\mathbf{k})}$ points of the form $\mathbf{k} + \mathbf{M}^{\mathrm{T}}\mathbf{z} \in \mathcal{K}(\mathbf{M}^{\mathrm{T}})$, $\mathbf{z} \in \mathbb{Z}^d$ and we have that $r(\mathbf{k} + \mathbf{M}^{\mathrm{T}}\mathbf{z}) = r(\mathbf{k})$.

Proof. Let j be given such that $\mathbf{k}^{\mathrm{T}}\mathbf{M}^{-1}\mathbf{e}_j = \pm\frac{1}{2}$. Hence,

$$(\mathbf{k} \mp \mathbf{M}^{\mathrm{T}}\mathbf{e}_j)^{\mathrm{T}}\mathbf{M}^{-1}\mathbf{e}_j = \mathbf{k}^{\mathrm{T}}\mathbf{M}^{-1}\mathbf{e}_j \mp \mathbf{e}_j^{\mathrm{T}}\mathbf{M}\mathbf{M}^{-1}\mathbf{e}_j = \mathbf{k}^{\mathrm{T}}\mathbf{M}^{-1}\mathbf{e}_j \mp 1 = \mp\frac{1}{2}.$$

For $j \neq i$, the remaining components of $(\mathbf{k} \pm \mathbf{M}^{\mathrm{T}}\mathbf{e}_j)^{\mathrm{T}}\mathbf{M}^{-1}\mathbf{e}_i = \mathbf{k}^{\mathrm{T}}\mathbf{M}^{-1}\mathbf{e}_i$ are unchanged. If we have j and i such that $r(\mathbf{k}) = 1$, we have 2 possibilities for $\mathbf{k} \pm \mathbf{M}^{\mathrm{T}}\mathbf{e}_j$. Further, if we have j and i such that $r(\mathbf{k}) = 2$, we have 4 possibilities. Then, by induction, we have $2^{r(\mathbf{k})}$ elements on the form $\mathbf{k} + \mathbf{M}^{\mathrm{T}}\mathbf{z} \in \mathcal{K}(\mathbf{M}^{\mathrm{T}})$, $\mathbf{z} \in \mathbb{Z}^d$. □

Utilizing the symmetry of $r(\mathbf{k}) = r(-\mathbf{k})$ we define the orthonormal Dirichlet kernel, $D_{\mathbf{M}}^{\perp} : \mathbb{T}^d \to \mathbb{R}$, as

$$D_{\mathbf{M}}^{\perp}(\mathbf{x}) = \frac{1}{\sqrt{m}} \sum_{\mathbf{k} \in \mathcal{K}(\mathbf{M}^{\mathrm{T}})} 2^{-r(\mathbf{k})/2} \mathrm{e}^{\mathrm{i}\mathbf{k}^{\mathrm{T}}\mathbf{x}}, \tag{4.4}$$

where $m = |\det \mathbf{M}|$, see [18, Equation 37]. Figure 4.1 visualizes the Dirichlet kernel in 2D and 3D for the diagonal matrix $\mathbf{M} = \mathbf{A}_1$.

Furthermore, the Fourier coefficients of the orthonormal Dirichlet kernel are given by

$$c_{\mathbf{k}}(D_{\mathbf{M}}^{\perp}) = \begin{cases} \frac{1}{\sqrt{m}} 2^{-r(\mathbf{k})/2} & \text{for } \mathbf{k} \in \mathcal{K}(\mathbf{M}^{\mathrm{T}}), \\ 0 & \text{otherwise}, \end{cases} \tag{4.5}$$

where $r(\mathbf{k})$ is from (4.3), see [4, Section 6.2].

Example 4.4. We study at the scaled $\sqrt{m}c_{\mathbf{k}}(D_{\mathbf{M}}^{\perp})$ to see the powers of 2. For $d = 2$ we have four different scenarios.

- $\mathbf{k}$ is an inner point of $\mathcal{K}(\mathbf{M}^{\mathrm{T}})$, leading to $r(\mathbf{k}) = 0$ and $\sqrt{m}c_{\mathbf{k}}(D_{\mathbf{M}}^{\perp}) = 1$.
- $\mathbf{k}$ is on one of the edges of $\mathcal{K}(\mathbf{M}^{\mathrm{T}})$, making $r(\mathbf{k}) = 1$ and $\sqrt{m}c_{\mathbf{k}}(D_{\mathbf{M}}^{\perp}) = \frac{1}{\sqrt{2}}$.
- $\mathbf{k}$ is a corner point of $\mathcal{K}(\mathbf{M}^{\mathrm{T}})$, resulting in $r(\mathbf{k}) = 2$ and $\sqrt{m}c_{\mathbf{k}}(D_{\mathbf{M}}^{\perp}) = \frac{1}{2}$.
- $\mathbf{k} \notin \mathcal{K}(\mathbf{M}^{\mathrm{T}})$, which means $\sqrt{m}c_{\mathbf{k}}(D_{\mathbf{M}}^{\perp}) = 0$.

The Fourier coefficients are illustrated in Figure 4.2 for $\mathbf{M} = \mathbf{A}_1$ and $\mathbf{M} = \mathbf{A}_3$.

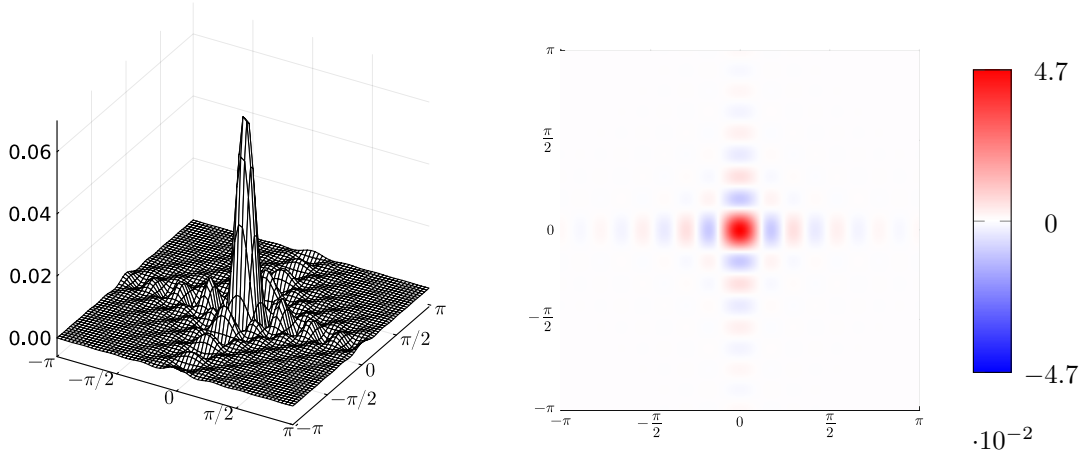

(a) Surface plot of $D^{\perp}_{\mathbf{A}_1}(\mathbf{x})$. (b) 2D plot of $D^{\perp}_{\mathbf{A}_1}(\mathbf{x})$.

Figure 4.1: Plots of the orthonormal Dirichlet kernel $D^{\perp}_{\mathbf{M}}$ for $\mathbf{M} = \mathbf{A}_1$.

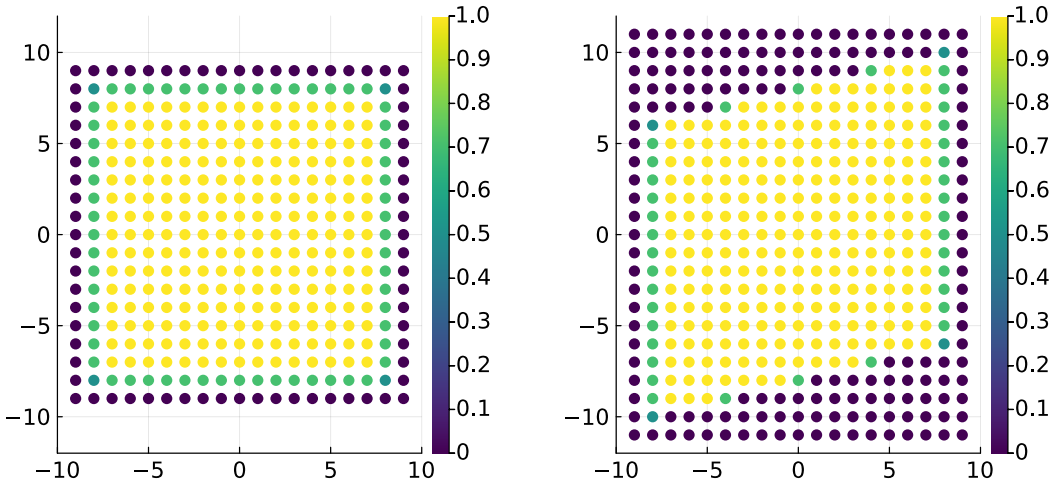

(a) $\sqrt{m}c_{\mathbf{k}}(D^{\perp}_{\mathbf{A}_1})$. (b) $\sqrt{m}c_{\mathbf{k}}(D^{\perp}_{\mathbf{A}_3})$.

Figure 4.2: Plot of the Dirichlet kernel $\sqrt{m}c_{\mathbf{k}}(D^{\perp}_{\mathbf{M}})$ for $\mathbf{M} = \mathbf{A}_1$ and $\mathbf{M} = \mathbf{A}_3$.

Theorem 4.5 ([18, Theorem 3.3])**.** A function $f \in V_{\mathbf{M}}^{\varphi}$ if and only if there exists a vector $\mathbf{a} = (a_{\mathbf{y}})_{\mathbf{y}\in\mathcal{P}(\mathbf{M})}$ where its discrete Fourier transform $\hat{\mathbf{a}} = (\hat{a}_{\mathbf{h}})_{\mathbf{h}\in\mathcal{G}(\mathbf{M}^{\mathrm{T}})}$ fulfills

$$c_{\mathbf{h}+\mathbf{M}^{\mathrm{T}}\mathbf{k}}(f) = \hat{a}_{\mathbf{h}} c_{\mathbf{h}+\mathbf{M}^{\mathrm{T}}\mathbf{k}}(\varphi) \quad \text{for all } \mathbf{h} \in \mathcal{G}(\mathbf{M}^{\mathrm{T}}),\ \mathbf{k} \in \mathbb{Z}^d.$$

Then the function f can be expressed in terms of the basis of $V_{\mathbf{M}}^{\varphi}$ as

$$f = \sum_{\mathbf{y}\in\mathcal{P}(\mathbf{M})} a_{\mathbf{y}} T(\mathbf{y})\varphi.$$

Proof. Assume $f \in V_{\mathbf{M}}^{\varphi}$, then by definition of $V_{\mathbf{M}}^{\varphi}$ in (4.1), there exists a vector $\mathbf{a} = (a_{\mathbf{y}})_{\mathbf{y}\in\mathcal{P}(\mathbf{M})}$ such that

$$f = \sum_{\mathbf{y}\in\mathcal{P}(\mathbf{M})} a_{\mathbf{y}} T(\mathbf{y})\varphi,$$

which in Fourier domain is expressed as

$$c_{\mathbf{k}}(f) = \sum_{\mathbf{y}\in\mathcal{P}(\mathbf{M})} a_{\mathbf{y}} \mathrm{e}^{-2\pi \mathrm{i}\mathbf{k}^{\mathrm{T}}\mathbf{y}} c_{\mathbf{k}}(\varphi),$$

by Equation (2.2). Then for a fixed but arbitrary $\mathbf{k} \in \mathbb{Z}^d$ with a $\mathbf{h} = \mathbf{k}|_{\mathcal{G}(\mathbf{M}^{\mathrm{T}})}$, which is uniquely determined together with $\mathbf{z} \in \mathbb{Z}^d$ such that $\mathbf{k} = \mathbf{h} + \mathbf{M}^{\mathrm{T}}\mathbf{z}$, yields

$$\begin{aligned} c_{\mathbf{h}+\mathbf{M}^{\mathrm{T}}\mathbf{z}}(f) &= \sum_{\mathbf{y}\in\mathcal{P}(\mathbf{M})} a_{\mathbf{y}} \mathrm{e}^{2\pi \mathrm{i}(\mathbf{h}+\mathbf{M}^{\mathrm{T}}\mathbf{z})^{\mathrm{T}}\mathbf{y}} c_{\mathbf{h}+\mathbf{M}^{\mathrm{T}}\mathbf{z}}(\varphi) \\ &= \sum_{\mathbf{y}\in\mathcal{P}(\mathbf{M})} a_{\mathbf{y}} \mathrm{e}^{-2\pi \mathrm{i}\mathbf{h}^{\mathrm{T}}\mathbf{y}} c_{\mathbf{h}+\mathbf{M}^{\mathrm{T}}\mathbf{z}}(\varphi) \\ &= \hat{a}_{\mathbf{h}} c_{\mathbf{h}+\mathbf{M}^{\mathrm{T}}\mathbf{z}}(\varphi), \end{aligned}$$

where the last equality holds by (3.16).

For the opposite case, assume that there exists a vector $\hat{\mathbf{a}} = (\hat{a}_{\mathbf{h}})_{\mathbf{h}\in\mathcal{G}(\mathbf{M}^{\mathrm{T}})}$ satisfying equation

$$c_{\mathbf{h}+\mathbf{M}^{\mathrm{T}}\mathbf{k}}(f) = \hat{a}_{\mathbf{h}} c_{\mathbf{h}+\mathbf{M}^{\mathrm{T}}\mathbf{k}}(\varphi), \quad \text{for all } \mathbf{k} \in \mathbb{Z}^d.$$

Then the vector $\mathbf{a} = (a_{\mathbf{y}})_{\mathbf{y}\in\mathcal{P}(\mathbf{M})}$ is uniquely determined by the inverse discrete Fourier transform of $\hat{\mathbf{a}}$, making the coefficients the weights of the translates of φ in the representation of f, which finishes the proof. □

By the coefficients $\hat{\mathbf{a}} = (\hat{a}_{\mathbf{h}})_{\mathbf{h}\in\mathcal{G}(\mathbf{M}^{\mathrm{T}})}$ we can uniquely determine the function f with respect to the basis of $V_{\mathbf{M}}^{\varphi}$. When knowing the translates, the foregoing theorem allows us to store the coefficients, and not the function itself, in order to determine the function. This is beneficial as the size of $\hat{\mathbf{a}}$ is given by m, while the size of $c_{\mathbf{h}+\mathbf{M}^{\mathrm{T}}\mathbf{z}}(\varphi)$, $\mathbf{h} \in \mathcal{G}(\mathbf{M}^{\mathrm{T}})$, $\mathbf{z} \in \mathbb{Z}^d$ might be bigger.

Theorem 4.6 ([18, Theorem 3.4])**.** Let $\varphi, \psi \in L^2(\mathbb{T}^d)$ be two given functions. Then the Gram matrix $\mathbf{G} = \left(\langle T(\mathbf{x})\varphi, T(\mathbf{y})\psi\rangle\right)_{\mathbf{x},\mathbf{y}\in\mathcal{P}(\mathbf{M})}$ is circulant, and it holds that

$$\mathbf{G} = \mathcal{F}(\mathbf{M})^{\mathrm{T}} \operatorname{diag}\left(m \sum_{\mathbf{k}\in\mathbb{Z}^d} c_{\mathbf{h}+\mathbf{M}^{\mathrm{T}}\mathbf{k}}(\varphi)\overline{c_{\mathbf{h}+\mathbf{M}^{\mathrm{T}}\mathbf{k}}(\psi)}\right)_{\mathbf{h}\in\mathcal{G}(\mathbf{M}^{\mathrm{T}})} \overline{\mathcal{F}(\mathbf{M})}.$$

Proof. The Gram matrix is given as

$$\mathbf{G} = \big(\langle T(\mathbf{x})\varphi, T(\mathbf{y})\psi\rangle\big)_{\mathbf{x},\mathbf{y}\in\mathcal{P}(\mathbf{M})} = \big(\langle \varphi, T(\mathbf{y}-\mathbf{x})\psi\rangle\big)_{\mathbf{x},\mathbf{y}\in\mathcal{P}(\mathbf{M})},$$

where the last equality shows the property of $\mathbf{G}$ being circular. Thus, $\mathbf{G} = \operatorname{circ}\mathbf{a}$, where $\mathbf{a} = (a_{\mathbf{y}})_{\mathbf{y}\in\mathcal{P}(\mathbf{M})} = \big(\langle \varphi, T(\mathbf{y})\psi\rangle\big)_{\mathbf{y}\in\mathcal{P}(\mathbf{M})}$. From [18, Lemma 2.3] we have the assertion that $\operatorname{circ}\mathbf{a} = \mathcal{F}(\mathbf{M})^{\mathrm{T}}\operatorname{diag}(\hat{\mathbf{a}})\,\overline{\mathcal{F}(\mathbf{M})}$ for $\mathbf{a} = (a_{\mathbf{g}})_{\mathbf{g}\in\mathcal{G}(\mathbf{M})}$. Combining the equality with Parseval's identity from Theorem 2.2, yields that for every for $\mathbf{h}\in\mathcal{G}(\mathbf{M}^{\mathrm{T}})$ we have that

$$\begin{aligned}\hat{a}_{\mathbf{h}} &= \sum_{\mathbf{y}\in\mathcal{P}(\mathbf{M})} \langle \varphi, T(\mathbf{y})\psi\rangle \mathrm{e}^{-2\pi\mathrm{i}\mathbf{h}^{\mathrm{T}}\mathbf{y}} = \sum_{\mathbf{y}\in\mathcal{P}(\mathbf{M})} \mathrm{e}^{-2\pi\mathrm{i}\mathbf{h}^{\mathrm{T}}\mathbf{y}} \sum_{\mathbf{k}\in\mathbb{Z}^d} c_{\mathbf{k}}(\varphi)\overline{c_{\mathbf{k}}(T(\mathbf{y})\psi)} \\ &= \sum_{\mathbf{k}\in\mathbb{Z}^d} c_{\mathbf{k}}(\varphi)\overline{c_{\mathbf{k}}(\psi)} \sum_{\mathbf{y}\in\mathcal{P}(\mathbf{M})} \mathrm{e}^{-2\pi\mathrm{i}(\mathbf{h}-\mathbf{k})^{\mathrm{T}}\mathbf{y}}.\end{aligned}$$

Knowing that

$$\sum_{\mathbf{y}\in\mathcal{P}(\mathbf{M})} \mathrm{e}^{-2\pi\mathrm{i}(\mathbf{h}-\mathbf{k})^{\mathrm{T}}\mathbf{y}} = \begin{cases} m & \text{if } \mathbf{h}\equiv\mathbf{k} \mod \mathbf{M}^{\mathrm{T}}, \\ 0 & \text{otherwise,}\end{cases}$$

simplifies the expression to

$$\hat{a}_{\mathbf{h}} = m\sum_{\mathbf{z}\in\mathbb{Z}^d} c_{\mathbf{h}+\mathbf{M}^{\mathrm{T}}\mathbf{z}}(\varphi)\overline{c_{\mathbf{h}+\mathbf{M}^{\mathrm{T}}\mathbf{z}}(\psi)}.$$

and the assertion of the theorem shown, [3, Lemma 1.23f]. □

Theorem 4.7 (Linear independence of translates, [18, Corollary 3.5])**.** The set of translates $\{T(\mathbf{y})\varphi : \mathbf{y}\in\mathcal{P}(\mathbf{M})\}$ is linearly independent if and only if

$$\sum_{\mathbf{k}\in\mathbb{Z}^d} \big|c_{\mathbf{h}+\mathbf{M}^{\mathrm{T}}\mathbf{k}}(\varphi)\big|^2 > 0, \qquad \text{for all } \mathbf{h}\in\mathcal{G}(\mathbf{M}^{\mathrm{T}}). \tag{4.6}$$

Proof. By Theorem 4.6 the Gram matrix $\mathbf{G}$ can be formulated as

$$\mathbf{G} = \mathcal{F}(\mathbf{M})^{\mathrm{T}}\operatorname{diag}\Big(m\sum_{\mathbf{k}\in\mathbb{Z}^d}\big|c_{\mathbf{h}+\mathbf{M}^{\mathrm{T}}\mathbf{k}}(\varphi)\big|^2\Big)_{\mathbf{h}\in\mathcal{G}(\mathbf{M}^{\mathrm{T}})}\overline{\mathcal{F}(\mathbf{M})}.$$

Since both $\mathcal{F}(\mathbf{M})$ and $\overline{\mathcal{F}(\mathbf{M})}$ are regular, we only need to consider the diagonal is the matrix to ensure invertibility of $\mathbf{G}$. The diagonal is matrix is invertible if and only if Equation (4.6) holds true. The invertibility of $\mathbf{G}$ is equivalent to the set of translates being linearly independent. □

Note that the preceding theorem says that $V_{\mathbf{M}}^{\varphi}$ is spanned by $|\mathcal{P}(\mathbf{M})| = m$ translates of φ, which implies that $\dim V_{\mathbf{M}}^{\varphi} = m$, see [18, Section 3] and [1, Section 1].

Proposition 4.8 ([18, Lemma 6.1])**.** The set of translates $\{T(\mathbf{y})D_{\mathbf{M}}^{\perp} : \mathbf{y}\in\mathcal{P}(\mathbf{M})\}$ spans an m-dimensional space $V_{\mathbf{M}}^{D_{\mathbf{M}}^{\perp}}$.

Proof. The Fourier coefficients of $D_{\mathbf{M}}^{\perp}$ in (4.5) are strictly positive for all $\mathbf{h} \in \mathcal{G}(\mathbf{M}^{\mathrm{T}})$ by definition because $\mathcal{G}(\mathbf{M}^{\mathrm{T}}) \subseteq \mathcal{K}(\mathbf{M}^{\mathrm{T}})$. By Theorem 4.7, we obtain the linear independence of the translates of $D_{\mathbf{M}}^{\perp}$, consequently leading to the spanning of an m-dimensional space $V_{\mathbf{M}}^{D_{\mathbf{M}}^{\perp}}$. □

Theorem 4.9 ([18, Corollary 3.6])**.** The set of translates $\{T(\mathbf{y})\varphi : \mathbf{y} \in \mathcal{P}(\mathbf{M})\}$ are orthonormal if and only if

$$\sum_{\mathbf{k}\in\mathbb{Z}^d} \left|c_{\mathbf{h}+\mathbf{M}^{\mathrm{T}}\mathbf{k}}(\varphi)\right|^2 = \frac{1}{m}, \quad \text{for all } \mathbf{h} \in \mathcal{G}(\mathbf{M}^{\mathrm{T}}).$$

Proof. By the definition of the matrix inner product, the Gram matrix can be written as

$$\mathbf{G} = \langle T(\mathbf{x})\varphi, T(\mathbf{y})\varphi\rangle_{\mathbf{x},\mathbf{y}\in\mathcal{P}(\mathbf{M})} = \big(T(\mathbf{x})\varphi\big)^{\mathrm{T}}_{\mathbf{x}\in\mathcal{P}(\mathbf{M})}\big(T(\mathbf{y})\varphi\big)_{\mathbf{y}\in\mathcal{P}(\mathbf{M})}.$$

Furthermore, the definition of an orthonormal matrix [2, Section 7.1] states that the matrices $\big(T(\mathbf{x})\varphi\big)^{\mathrm{T}}_{\mathbf{x}\in\mathcal{P}(\mathbf{M})}$ and $\big(T(\mathbf{y})\varphi\big)_{\mathbf{y}\in\mathcal{P}(\mathbf{M})}$ are orthonormal if and only if it equals the identity matrix, who's eigenvalues are 1. From the assertion of Theorem 4.6, the eigenvalues of the Gram matrix are determined by

$$m\sum_{\mathbf{k}\in\mathbb{Z}^d} \left|c_{\mathbf{h}+\mathbf{M}^{\mathrm{T}}\mathbf{k}}(\varphi)\right|^2, \quad \mathbf{h} \in \mathcal{G}(\mathbf{M}^{\mathrm{T}}),$$

which are equal to 1 if and only if the assertion holds. □

Proposition 4.10 ([18, Theorem 6.4])**.** The translates of $D_{\mathbf{M}}^{\perp}$ are orthonormal to each other.

Proof. Using the Fourier coefficients in Equation (4.5) and Lemma 4.3 we have

$$\begin{aligned}\sum_{\mathbf{z}\in\mathbb{Z}^d} |c_{\mathbf{h}+\mathbf{M}^{\mathrm{T}}\mathbf{z}}(D_{\mathbf{M}}^{\perp})|^2 &= \sum_{\mathbf{z}\in\mathbb{Z}^d} \left|\frac{1}{\sqrt{m}} 2^{-\frac{r(\mathbf{h}+\mathbf{M}^{\mathrm{T}}\mathbf{z})}{2}}\right|^2 \\ &= \sum_{\mathbf{z}\in\mathbb{Z}^d} \left|\frac{1}{\sqrt{m}} 2^{-\frac{r(\mathbf{h})}{2}}\right|^2 \\ &= 2^{r(\mathbf{h})} c_{\mathbf{h}}(D_{\mathbf{M}}^{\perp})^2 = \frac{1}{m}\end{aligned}$$

for all $\mathbf{h} \in \mathcal{G}(\mathbf{M}^{\mathrm{T}}) \subseteq \mathcal{K}(\mathbf{M}^{\mathrm{T}})$. The equality on the first line holds for all $\mathbf{h} \in \mathcal{G}(\mathbf{M}^{\mathrm{T}})$, and since $\mathcal{G}(\mathbf{M}^{\mathrm{T}}) \subseteq \mathcal{K}(\mathbf{M}^{\mathrm{T}})$ the simplification on the second line is valid. By Theorem 4.9, this is equivalent to the translates of $D_{\mathbf{M}}^{\perp}$ being orthonormal. □

4.2 Orthogonal Decomposition on Fixed Patterns

In the following section we look into the decomposition of $V_{\mathbf{M}}^{\varphi}$. Firstly, we establish the existence of an orthogonal decomposition, followed by the formulation of a condition for verifying that such a decomposition is orthogonal. Subsequently, we demonstrate the orthogonal decomposition of the space into n-dimensional subspaces, where $n = |\det \mathbf{N}|$, and discuss the requisite condition for achieving this type of decomposition. Lastly, we analyze the properties of the decomposed subspaces and provide a detailed description of the algorithm for implementing this orthogonal decomposition.

Theorem 4.11 (Existence of orthogonal decomposition, [18, Theorem 4.1])**.** Let $\mathbf{M} = \mathbf{JN} \in \mathbb{Z}^{d\times d}$ with $\mathbf{J}, \mathbf{N} \in \mathbb{Z}^{d\times d}$ and $|\det \mathbf{M}| = m$. Further, let the function $\varphi \in L^2(\mathbb{T}^d)$ generate the m-dimensional $\mathbf{M}$-invariant space $V_{\mathbf{M}}^{\varphi}$. Then there are functions $\xi_{\mathbf{g}} \in L^2(\mathbb{T}^d)$, for $\mathbf{g} \in \mathcal{G}(\mathbf{J}^{\mathrm{T}})$ such that

$$\sum_{\mathbf{k}\in\mathbb{Z}^d} |c_{\mathbf{h}+\mathbf{N}^{\mathrm{T}}\mathbf{k}}(\xi_{\mathbf{g}})|^2 > 0, \qquad \text{for all } \mathbf{h} \in \mathcal{G}(\mathbf{N}^{\mathrm{T}}),$$

which gives rise to the orthogonal decomposition

$$V_{\mathbf{M}}^{\varphi} = \bigoplus_{\mathbf{g}\in\mathcal{G}(\mathbf{J}^{\mathrm{T}})} V_{\mathbf{N}}^{\xi_{\mathbf{g}}}.$$

Proof. By assumption, the $\mathbf{M}$-invariant space $V_{\mathbf{M}}^{\varphi}$ is generated by the linearly independent translates of φ. Additionally, the linear independence of the translates is equivalent to Equation (4.6) from Theorem 4.7. For simplicity we denote the sequence $\mathbf{a}^{\mathbf{h}} = (a_{\mathbf{k}}^{\mathbf{h}})_{\mathbf{k}\in\mathbb{Z}^d}$ for $\mathbf{h} \in \mathcal{G}(\mathbf{M}^{\mathrm{T}})$, where

$$a_{\mathbf{k}}^{\mathbf{h}} = \begin{cases} c_{\mathbf{k}}(\varphi) & \text{if } \mathbf{k} \equiv \mathbf{h} \mod \mathbf{M}^{\mathrm{T}} \in \mathbb{Z}^d, \\ 0 & \text{otherwise.} \end{cases}$$

We can then express a basis of $V_{\mathbf{M}}^{\varphi}$ in terms of $\mathbf{a}^{\mathbf{h}}$ as

$$\Big\{ \sum_{\mathbf{k}\in\mathbb{Z}^d} a_{\mathbf{k}}^{\mathbf{h}} \mathrm{e}^{\mathrm{i}\mathbf{k}^{\mathrm{T}}\circ} : \mathbf{h} \in \mathcal{G}(\mathbf{M}^{\mathrm{T}}) \Big\}$$

by using the notation from Corollary 4.2. Having $\langle \mathrm{e}^{\mathrm{i}\mathbf{k}_1^{\mathrm{T}}\circ}, \mathrm{e}^{\mathrm{i}\mathbf{k}_2^{\mathrm{T}}\circ} \rangle = 0$ when $\mathbf{k}_1 \neq \mathbf{k}_2$, and $a_{\mathbf{k}}^{\mathbf{h}_1} \overline{a}_{\mathbf{k}}^{\mathbf{h}_2} = 0$ for $\mathbf{h}_1 \neq \mathbf{h}_2$, implies that the basis is orthogonal. Utilizing the unique decomposition $\mathbf{h} = \mathbf{N}^{\mathrm{T}}\mathbf{g} + \tilde{\mathbf{h}}$, for $\mathbf{g} \in \mathcal{G}(\mathbf{J}^{\mathrm{T}})$, $\tilde{\mathbf{h}} \in \mathcal{G}(\mathbf{N}^{\mathrm{T}})$ from Equation (3.19), leads to

$$\begin{aligned} V_{\mathbf{M}}^{\varphi} &= \operatorname{span} \Big\{ \sum_{\mathbf{k}\in\mathbb{Z}^d} a_{\mathbf{k}}^{\mathbf{h}} \mathrm{e}^{\mathrm{i}\mathbf{k}^{\mathrm{T}}\circ} : \mathbf{h} \in \mathcal{G}(\mathbf{M}^{\mathrm{T}}) \Big\} \\ &= \bigoplus_{\mathbf{g}\in\mathcal{G}(\mathbf{J}^{\mathrm{T}})} \operatorname{span} \Big\{ \sum_{\mathbf{k}\in\mathbb{Z}^d} a_{\mathbf{k}}^{\tilde{\mathbf{h}}} \mathrm{e}^{\mathrm{i}\mathbf{k}^{\mathrm{T}}\circ} : \tilde{\mathbf{h}} \in \mathcal{G}(\mathbf{N}^{\mathrm{T}}) + \mathbf{N}^{\mathrm{T}}\mathbf{g} \Big\}. \\ &= \bigoplus_{\mathbf{g}\in\mathcal{G}(\mathbf{J}^{\mathrm{T}})} \operatorname{span} \Big\{ \sum_{\mathbf{k}\in\mathbb{Z}^d} c_{\tilde{\mathbf{h}}+\mathbf{N}^{\mathrm{T}}\mathbf{g}+\mathbf{M}^{\mathrm{T}}\mathbf{k}}(\varphi) \mathrm{e}^{\mathrm{i}(\tilde{\mathbf{h}}+\mathbf{N}^{\mathrm{T}}\mathbf{g}+\mathbf{M}^{\mathrm{T}}\mathbf{k})^{\mathrm{T}}\circ} : \tilde{\mathbf{h}} \in \mathcal{G}(\mathbf{N}^{\mathrm{T}}) \Big\}. \end{aligned}$$

Now, for $\tilde{\mathbf{h}} \in \mathcal{G}(\mathbf{N}^{\mathrm{T}})$, $\mathbf{k} \in \mathbb{Z}^d$ and $\mathbf{g}_1, \mathbf{g}_2 \in \mathcal{G}(\mathbf{J}^{\mathrm{T}})$, we define the coefficients

$$c_{\tilde{\mathbf{h}}+\mathbf{N}^{\mathrm{T}}\mathbf{g}_1+\mathbf{M}^{\mathrm{T}}\mathbf{k}}(\xi_{\mathbf{g}_2}) := \begin{cases} c_{\tilde{\mathbf{h}}+\mathbf{N}^{\mathrm{T}}\mathbf{g}_1+\mathbf{M}^{\mathrm{T}}\mathbf{k}}(\varphi) & , \mathbf{g}_1 = \mathbf{g}_2 \\ 0 & , \mathbf{g}_1 \neq \mathbf{g}_2 \end{cases}$$

This definition of $\xi_{\mathbf{g}}$ ensures the simplification of the expression of the basis of $V_{\mathbf{M}}^{\varphi}$, which now can be written as

$$\begin{aligned} V_{\mathbf{M}}^{\varphi} &= \bigoplus_{\mathbf{g}\in\mathcal{G}(\mathbf{J}^{\mathrm{T}})} \operatorname{span} \Big\{ \sum_{\mathbf{k}\in\mathbb{Z}^d} c_{\tilde{\mathbf{h}}+\mathbf{N}^{\mathrm{T}}\mathbf{k}}(\xi_{\mathbf{g}}) \mathrm{e}^{\mathrm{i}(\tilde{\mathbf{h}}+\mathbf{N}^{\mathrm{T}}\mathbf{k})^{\mathrm{T}}\circ} : \tilde{\mathbf{h}} \in \mathcal{G}(\mathbf{N}^{\mathrm{T}}) \Big\} \\ V_{\mathbf{M}}^{\varphi} &= \bigoplus_{\mathbf{g}\in\mathcal{G}(\mathbf{J}^{\mathrm{T}})} V_{\mathbf{N}}^{\xi_{\mathbf{g}}}, \end{aligned}$$

which finishes the proof. □

Note that $|\det \mathbf{J}|$ determines the number of spaces into which $V_{\mathbf{M}}^{\varphi}$ is decomposed, while $|\det \mathbf{N}|$ determines the dimension of each of the decomposed spaces $V_{\mathbf{N}}^{\xi_{\mathbf{g}}}$.

Lemma 4.12 ([3, Lemma 1.30])**.** Let $\mathbf{M}, \mathbf{N} \in \mathbb{Z}^{d\times d}$ be regular with $\mathbf{M} = \mathbf{J}\mathbf{N}$ and $|\det \mathbf{M}| = m$. Let $\varphi \in L^2(\mathbb{T}^d)$ generate the m-dimensional $\mathbf{M}$-invariant space $V_{\mathbf{M}}^{\varphi}$. Moreover, let the functions

$$\xi_j = \sum_{\mathbf{y}\in\mathcal{P}(\mathbf{M})} b_{j,\mathbf{y}} T(\mathbf{y})\varphi \in V_{\mathbf{M}}^{\varphi} \tag{4.7}$$

for $j = 1, \dots, |\det \mathbf{J}|$ be given. Then the following statements hold true:

(i) Let $j \in \{1, \dots, |\det \mathbf{J}|\}$ be fixed. Then the set of translates $\{T(\mathbf{y})\xi_j : \mathbf{y} \in \mathcal{P}(\mathbf{N})\}$ is linearly independent if and only if

$$\sum_{\mathbf{g}\in\mathcal{G}(\mathbf{J}^{\mathrm{T}})} |\hat{b}_{j,\mathbf{h}+\mathbf{N}^{\mathrm{T}}\mathbf{g}}|^2 > 0, \quad \text{for all } \mathbf{h} \in \mathcal{G}(\mathbf{N}^{\mathrm{T}}).$$

(ii) For arbitrary, but fixed $j_1 \neq j_2$, the translates of ξ_{j_1} and ξ_{j_2} are orthogonal, i.e., $\langle T(\mathbf{x})\xi_{j_1}, T(\mathbf{y})\xi_{j_2}\rangle = 0$ for all $\mathbf{x}, \mathbf{y} \in \mathcal{P}(\mathbf{N})$, if and only if

$$\sum_{\mathbf{g}\in\mathcal{G}(\mathbf{J}^{\mathrm{T}})} \hat{b}_{j_1,\mathbf{h}+\mathbf{N}^{\mathrm{T}}\mathbf{g}} \overline{\hat{b}}_{j_2,\mathbf{h}+\mathbf{N}^{\mathrm{T}}\mathbf{g}} \sum_{\mathbf{k}\in\mathbb{Z}^d} |c_{\mathbf{h}+\mathbf{N}^{\mathrm{T}}\mathbf{g}+\mathbf{M}^{\mathrm{T}}\mathbf{k}}(\varphi)|^2 = 0, \quad \text{for all } \mathbf{h} \in \mathcal{G}(\mathbf{N}^{\mathrm{T}}).$$

(iii) Fix $j \in \{1, \dots, |\det \mathbf{J}|\}$. If the translates $\{T(\mathbf{y})\varphi,\ \mathbf{y} \in \mathcal{P}(\mathbf{M})\}$ form an orthonormal basis for $V_{\mathbf{M}}^{\varphi}$, then the translates $\{T(\mathbf{x})\xi_j : \mathbf{x} \in \mathcal{P}(\mathbf{N})\}$, are orthonormal if and only if

$$\sum_{\mathbf{g}\in\mathcal{G}(\mathbf{J}^{\mathrm{T}})} |\hat{b}_{j,\mathbf{h}+\mathbf{N}^{\mathrm{T}}\mathbf{g}}|^2 = |\det \mathbf{J}|, \quad \text{for all } \mathbf{h} \in \mathcal{G}(\mathbf{N}^{\mathrm{T}}).$$

(iv) For a fixed $j \in \{1, \dots, |\det \mathbf{J}|\}$ the vector of translates of ξ_j can be expressed by

$$\overline{\mathcal{F}(\mathbf{N})}\big(T(\mathbf{y})\xi_j\big)_{\mathbf{y}\in\mathcal{P}(\mathbf{N})} = \sqrt{\frac{n}{m}}\mathbf{B}_j \overline{\mathcal{F}(\mathbf{M})}\big(T(\mathbf{y})\varphi\big)_{\mathbf{y}\in\mathcal{P}(\mathbf{M})},$$

where $n = |\det \mathbf{N}|$ and

$$\mathbf{B}_j \coloneqq \Big(\operatorname{diag}\big(\hat{b}_{j,\mathbf{h}+\mathbf{N}^{\mathrm{T}}\mathbf{g}_0}\big)_{\mathbf{k}\in\mathcal{G}(\mathbf{N}^{\mathrm{T}})} \dots \operatorname{diag}\big(\hat{b}_{j,\mathbf{h}+\mathbf{N}^{\mathrm{T}}\mathbf{g}_{|\det \mathbf{J}|-1}}\big)_{\mathbf{k}\in\mathcal{G}(\mathbf{N}^{\mathrm{T}})}\Big) \in \mathbb{C}^{n\times m}. \tag{4.8}$$

Proof.

(i) Equation (4.7) implies by Theorem 4.5, that the Fourier coefficients of ξ_j can be written as $c_{\mathbf{h}+\mathbf{M}^{\mathrm{T}}\mathbf{k}}(\xi_j) = \hat{b}_{j,\mathbf{h}} c_{\mathbf{h}+\mathbf{M}^{\mathrm{T}}\mathbf{k}}(\varphi)$ for all $\mathbf{h} \in \mathcal{G}(\mathbf{M}^{\mathrm{T}})$, $\mathbf{k} \in \mathbb{Z}^d$ and a fixed $j \in \{1, \dots, |\det \mathbf{J}|\}$. Inserting this expression into the assertion of Theorem 4.7, we obtain

$$\sum_{\mathbf{k}\in\mathbb{Z}^d} |\hat{b}_{j,\mathbf{h}+\mathbf{M}^{\mathrm{T}}\mathbf{k}}\ c_{\mathbf{h}+\mathbf{M}^{\mathrm{T}}\mathbf{k}}(\varphi)\ \overline{c_{\mathbf{h}+\mathbf{M}^{\mathrm{T}}\mathbf{k}}(\varphi)}|^2 > 0, \quad \text{for all } \mathbf{h} \in \mathcal{G}(\mathbf{M}^{\mathrm{T}}).$$

Writing $\mathbf{h} \in \mathcal{G}(\mathbf{M}^{\mathrm{T}})$ in terms of elements form $\mathcal{G}(\mathbf{J}^{\mathrm{T}})$ and $\mathcal{G}(\mathbf{N}^{\mathrm{T}})$, expressed in (3.19), simplifies the above expression to

$$\sum_{\mathbf{g}\in\mathcal{G}(\mathbf{J}^{\mathrm{T}})} |\hat{b}_{j,\mathbf{h}+\mathbf{N}^{\mathrm{T}}\mathbf{g}}\, c_{\mathbf{h}+\mathbf{N}^{\mathrm{T}}\mathbf{g}}(\varphi)\, \overline{c_{\mathbf{h}+\mathbf{N}^{\mathrm{T}}\mathbf{g}}(\varphi)}|^2 > 0, \qquad \text{for all } \mathbf{h} \in \mathcal{G}(\mathbf{N}^{\mathrm{T}}).$$

The linear independence of the translates of φ, yields that

$$\sum_{\mathbf{g}\in\mathcal{G}(\mathbf{J}^{\mathrm{T}})} |\hat{b}_{j,\mathbf{h}+\mathbf{N}^{\mathrm{T}}\mathbf{g}}|^2 > 0, \qquad \text{for all } \mathbf{h} \in \mathcal{G}(\mathbf{N}^{\mathrm{T}}).$$

(ii) The verification of orthogonality between the translates of ξ_{j_1} and ξ_{j_2} is equivalent to examining whether their Gram matrix is equal to the zero matrix. By employing Theorem 4.6 and expressing ξ_{j_1} and ξ_{j_2} using Equation (4.7), we establish the validity of the assertion.

(iii) By Theorem 4.9 we know the characteristics of orthonormal translates in terms of Fourier coefficients. Utilizing this knowledge in conjunction with (i), we deduce that for all $\mathbf{h} \in \mathcal{G}(\mathbf{M}^{\mathrm{T}})$ the following equality holds

$$\begin{aligned} |\det \mathbf{J}| = \frac{m}{n} &= m \sum_{\mathbf{l}\in\mathbb{Z}^d} |c_{\mathbf{h}+\mathbf{N}^{\mathrm{T}}\mathbf{l}}(\xi_j)|^2 \\ &= m \sum_{\mathbf{g}\in\mathcal{G}(\mathbf{J}^{\mathrm{T}})} |\hat{b}_{j,\mathbf{h}+\mathbf{N}^{\mathrm{T}}\mathbf{g}}|^2 \sum_{\mathbf{z}\in\mathbb{Z}^d} |c_{\mathbf{h}+\mathbf{N}^{\mathrm{T}}\mathbf{g}+\mathbf{M}^{\mathrm{T}}\mathbf{z}}(\varphi)|^2 \\ &= \sum_{\mathbf{g}\in\mathcal{G}(\mathbf{J}^{\mathrm{T}})} |\hat{b}_{j,\mathbf{h}+\mathbf{N}^{\mathrm{T}}\mathbf{g}}|^2. \end{aligned}$$

(iv) The assertion follows by Theorem 4.1 and ξ_j being a linear combination of translates of φ. Starting with the translates of φ,

$$\overline{\mathcal{F}(\mathbf{M})}\big(T(\mathbf{y})\varphi\big)_{\mathbf{y}\in\mathcal{P}(\mathbf{M})} = \sqrt{m}\Big(\sum_{\mathbf{z}\in\mathbb{Z}^d} c_{\mathbf{h}+\mathbf{M}^{\mathrm{T}}\mathbf{z}}(\varphi)\mathrm{e}^{\mathrm{i}(\mathbf{h}+\mathbf{N}^{\mathrm{T}}\mathbf{z})^{\mathrm{T}}\circ}\Big), \qquad \text{for all } \mathbf{h} \in \mathcal{G}(\mathbf{M}^{\mathrm{T}}).$$

Similarly, the translates of ξ_j can, be written as

$$\begin{aligned} \overline{\mathcal{F}(\mathbf{N})}\big(T(\mathbf{y})\xi_j\big)_{\mathbf{y}\in\mathcal{P}(\mathbf{N})} &= \sqrt{n}\Big(\sum_{\mathbf{z}\in\mathbb{Z}^d} c_{\mathbf{h}+\mathbf{N}^{\mathrm{T}}\mathbf{z}}(\xi_j)\mathrm{e}^{\mathrm{i}(\mathbf{h}+\mathbf{N}^{\mathrm{T}}\mathbf{z})^{\mathrm{T}}\circ}\Big) \\ &= \sqrt{n}\Big(\sum_{\mathbf{g}\in\mathcal{G}(\mathbf{J}^{\mathrm{T}})} \hat{b}_{j,\mathbf{h}+\mathbf{N}^{\mathrm{T}}\mathbf{g}} \sum_{\mathbf{z}\in\mathbb{Z}^d} c_{\mathbf{h}+\mathbf{N}^{\mathrm{T}}\mathbf{g}+\mathbf{M}^{\mathrm{T}}\mathbf{z}}(\varphi)\mathrm{e}^{\mathrm{i}(\mathbf{h}+\mathbf{N}^{\mathrm{T}}\mathbf{g}+\mathbf{M}^{\mathrm{T}}\mathbf{z})^{\mathrm{T}}\circ}\Big) \\ &= \sqrt{\frac{n}{m}}\Big(\sum_{\mathbf{g}\in\mathcal{G}(\mathbf{J}^{\mathrm{T}})} \hat{b}_{j,\mathbf{h}+\mathbf{N}^{\mathrm{T}}\mathbf{g}}\Big)\overline{\mathcal{F}(\mathbf{M})}\big(T(\mathbf{y})\varphi\big)_{\mathbf{y}\in\mathcal{P}(\mathbf{M})} \end{aligned}$$

for all $\mathbf{h} \in \mathcal{G}(\mathbf{N}^{\mathrm{T}})$. The second equality holds by Theorem 4.5. Setting

$$\mathbf{B}_j = \sum_{\mathbf{g}\in\mathcal{G}(\mathbf{J}^{\mathrm{T}})} \hat{b}_{j,\mathbf{h}+\mathbf{N}^{\mathrm{T}}\mathbf{g}},$$

with $\mathbf{B}_j$ as in (4.8), the proof is finished. □

Proposition 4.13 ([18, Lemma 6.5])**.** Let $\mathbf{M} = \mathbf{JN} \in \mathbb{Z}^{d\times d}$ be regular matrices. If $d = 2$ and $\mathbf{J} \in \{\mathbf{J}_1, \mathbf{J}_2, \mathbf{J}_3\}$ from (3.20a), then $D_{\mathbf{N}}^{\perp} \in V_{\mathbf{M}}^{D_{\mathbf{M}}^{\perp}}$.

Proof. By (4.5) we have the Fourier coefficients of both $D_{\mathbf{M}}^{\perp}$ and $D_{\mathbf{N}}^{\perp}$. If $D_{\mathbf{N}}^{\perp} \in V_{\mathbf{M}}^{D_{\mathbf{M}}^{\perp}}$, then it holds that there exists $(\hat{a}_{\mathbf{h}})_{\mathbf{h}\in\mathcal{G}(\mathbf{M}^{\mathrm{T}})}$ such that

$$c_{\mathbf{h}+\mathbf{M}^{\mathrm{T}}\mathbf{z}}(D_{\mathbf{N}}^{\perp}) = \hat{a}_{\mathbf{h}} c_{\mathbf{h}+\mathbf{M}^{\mathrm{T}}\mathbf{z}}(D_{\mathbf{M}}^{\perp}),$$

from Theorem 4.5. Thus, our goal is to show that the coefficients $\hat{a}_{\mathbf{h}}$ exist for all $\mathbf{h} \in \mathcal{G}(\mathbf{M}^{\mathrm{T}})$. By Lemma 4.3 we know that $c_{\mathbf{h}}(D_{\mathbf{M}}^{\perp}) = c_{\mathbf{h}+\mathbf{M}^{\mathrm{T}}\mathbf{z}}(D_{\mathbf{M}}^{\perp})$ for $\mathbf{h}, \mathbf{h}+\mathbf{M}^{\mathrm{T}}\mathbf{z} \in \mathcal{K}(\mathbf{M}^{\mathrm{T}})$ and $\mathbf{z} \in \mathbb{Z}^d$. Additionally, since $\mathbf{h}, \mathbf{h}+\mathbf{M}^{\mathrm{T}}\mathbf{z} \in \mathcal{K}(\mathbf{M}^{\mathrm{T}})$, we have that $r_{\mathbf{M}}(\mathbf{h}) > 0$ due to the construction. We choose to work with $\overline{Q} = \mathbf{M}^{-\mathrm{T}}\mathcal{K}(\mathbf{M}^{\mathrm{T}})$ instead of $\mathcal{K}(\mathbf{M}^{\mathrm{T}})$, where one step $\mathbf{M}^{\mathrm{T}}\mathbf{h}_{\mathbf{e}_j}$ corresponds to one unit step $\mathbf{e}_j$ for $j = \{1, 2\}$ independent of $\mathbf{M}$, where $\mathbf{h}_{\mathbf{e}_j}$ is the basis vector of $\mathcal{G}(\mathbf{M}^{\mathrm{T}})$ in (3.10). Then consider an element $\mathbf{v} = \mathbf{M}^{-\mathrm{T}}\mathbf{h} \in \overline{Q}$ with $\mathbf{h} \in \mathcal{K}(\mathbf{M}^{\mathrm{T}})$, that has at least one component modulus $\frac{1}{2}$, i.e., $\mathbf{v}$ lies on at least one border of $\overline{Q}$. Further, the problem of showing that $c_{\mathbf{h}}(D_{\mathbf{N}}^{\perp}) = c_{\mathbf{h}+\mathbf{M}^{\mathrm{T}}\mathbf{z}}(D_{\mathbf{N}}^{\perp})$ is reduced to showing that $r_{\mathbf{N}}(\mathbf{h}) = r_{\mathbf{N}}(\mathbf{h}+\mathbf{M}^{\mathrm{T}}\mathbf{z})$. This will be done separately for each of the three matrices by verifying that when $\mathbf{v}$ is on a border of $\overline{Q}$, then $\mathbf{v} \pm \mathbf{e}_j$ is also on the same number of borders of $\overline{Q}$ for $j = \{1, 2\}$.

Let $\mathbf{J} = \mathbf{J}_1$. We first study the case where an arbitrary $\mathbf{v}$ whose second component has a modulus of $\frac{1}{2}$, placing it on the horizontal border of $\overline{Q}$. Then $\mathbf{v}, \mathbf{v} \pm \mathbf{e}_2 \in \overline{Q}$ and correspondingly $\mathbf{h}, \mathbf{h} \pm \mathbf{M}^{\mathrm{T}}\mathbf{e}_2 \in \mathcal{K}(\mathbf{M}^{\mathrm{T}})$. By evaluating $r_{\mathbf{N}}(\mathbf{h})$ and $r_{\mathbf{N}}(\mathbf{h} \pm \mathbf{M}^{\mathrm{T}}\mathbf{e}_2)$, we obtain

$$\begin{aligned} \mathbf{h}^{\mathrm{T}}\mathbf{N}^{-1}\mathbf{e}_j = \mathbf{v}^{\mathrm{T}}\mathbf{M}\mathbf{N}^{-1}\mathbf{e}_j = \mathbf{v}^{\mathrm{T}}\mathbf{J}\mathbf{e}_j \\ (\mathbf{h} \pm \mathbf{M}^{\mathrm{T}}\mathbf{e}_2)^{\mathrm{T}}\mathbf{N}^{-1}\mathbf{e}_j = \mathbf{v}^{\mathrm{T}}\mathbf{J}\mathbf{e}_j \pm \mathbf{e}_2^{\mathrm{T}}\mathbf{J}\mathbf{e}_j, \end{aligned}$$

For the last term, we have

$$\mathbf{e}_2^{\mathrm{T}}\mathbf{J}\mathbf{e}_j = \begin{cases} 0 & \text{if } j = 1, \\ 1 & \text{if } j = 2, \end{cases}$$

Thus, both $\mathbf{h}, \mathbf{h}+\mathbf{M}^{\mathrm{T}}\mathbf{e}_2 \in \mathcal{K}(\mathbf{M}^{\mathrm{T}})$, implying that $r_{\mathbf{N}}(\mathbf{h}) = r_{\mathbf{N}}(\mathbf{h} \pm \mathbf{M}^{\mathrm{T}}\mathbf{e}_2)$. This is illustrated in Figure 4.3a, where the green point represents $\mathbf{v}$ and the dashed arrow indicates the unit step $\mathbf{e}_2$. We observe that after taking a single step $\mathbf{e}_2$, we remain on the border of $\mathcal{K}(\mathbf{N}^{\mathrm{T}})$ and arrive at the other green point, $\mathbf{v} + \mathbf{e}_2$. We conclude that $r_{\mathbf{N}}(\mathbf{h}) = r_{\mathbf{N}}(\mathbf{h}+\mathbf{M}^{\mathrm{T}}\mathbf{z}) = 1$. In the scenario where the first component of $\mathbf{v}$ has a modulus of $\frac{1}{2}$, placing $\mathbf{v}$ on the vertical border of $\overline{Q}$, we have $\mathbf{M}^{\mathrm{T}}\mathbf{v} \notin \mathcal{K}(\mathbf{N}^{\mathrm{T}})$. This case is represented by the yellow point in the same figure. Consequently, $c_{\mathbf{h}+\mathbf{M}^{\mathrm{T}}\mathbf{z}}(D_{\mathbf{N}}^{\perp}) = 0$ for all $\mathbf{z} \in \mathbb{Z}^d$. This completes the proof for $\mathbf{J}_1$.

Considering $\mathbf{J} = \mathbf{J}_2$ we argue in the same way, only with $\mathbf{e}_1$ and $\mathbf{e}_2$ changing roles.

For $\mathbf{J} = \mathbf{J}_3$, we only need to consider the corners of the rotated scaled square $\mathbf{J}^{-\mathrm{T}}\overline{Q}$. These corners are the only points that reside on the border of $\overline{Q}$, as depicted in Figure 4.3b. The considered elements are characterized by one component

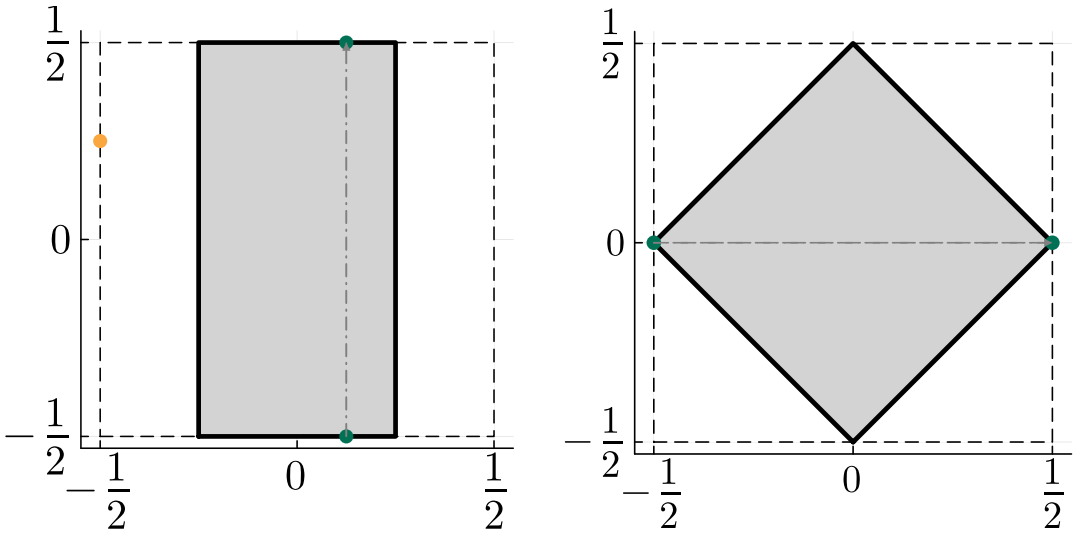

(a) $\mathbf{J} = \mathbf{J}_1$. (b) $\mathbf{J} = \mathbf{J}_3$.

Figure 4.3: Dashed square is $[-\frac{1}{2}, \frac{1}{2}]^2$, while the grey rectangle is $\mathbf{J}^{-\mathrm{T}}[-\frac{1}{2}, \frac{1}{2}]^2$. The green points represent an arbitrary $\mathbf{v}$ and $\mathbf{v} \pm \mathbf{e}_j$ for the case when it's on the boundary. The yellow point represents an arbitrary $\mathbf{v}$ on the vertical border of $\overline{Q}$.

having a modulus of $\frac{1}{2}$ and the other component being 0. By performing the same calculations as before, while considering the additional property

$$\mathbf{e}_k^{\mathrm{T}} \mathbf{J} \mathbf{e}_j = \begin{cases} 1 & \text{if } k = j \\ 0 & \text{if } k \neq j, \end{cases}$$

the equality $r_{\mathbf{N}}(\mathbf{h}) = r_{\mathbf{N}}(\mathbf{h} + \mathbf{M}^{\mathrm{T}}\mathbf{z})$ is validated for $\mathbf{J}_3$.

In the case where $\mathbf{v}$ is on no boundary of $\mathcal{K}(\mathbf{N}^{\mathrm{T}})$ for any of the given matrices $\mathbf{J}$, one unit step $\mathbf{e}_j$ for $j \in \{1, 2\}$ will place the element outside of $\overline{Q}$. Thus, $c_{\mathbf{h}}(D_{\mathbf{N}}^{\perp})$ is zero for the corresponding $\mathbf{h} + \mathbf{M}^{\mathrm{T}}\mathbf{e}_j$, by definition.

Consequently, we can find a matrix $\hat{\mathbf{a}} = (\hat{a}_{\mathbf{h}})_{\mathbf{h} \in \mathcal{G}(\mathbf{M}^{\mathrm{T}})}$ relating the coefficients of $D_{\mathbf{N}}^{\perp}$ and $D_{\mathbf{M}}^{\perp}$ as stated in Theorem 4.5. By rearranging the equality, we arrive at

$$\hat{a}_{\mathbf{h}} = \begin{cases} \sqrt{\frac{m}{n}} 2^{(r_{\mathbf{M}}(\mathbf{h}) - r_{\mathbf{N}}(\mathbf{h}))/2} & \text{if } \mathbf{h} \in \mathcal{K}(\mathbf{N}^{\mathrm{T}}) \cap \mathcal{G}(\mathbf{M}^{\mathrm{T}}), \\ 0 & \text{otherwise.} \end{cases}$$

□

Remark 4.14. For the matrices in Equation (3.20b) the inclusion $D_{\mathbf{N}}^{\perp} \in V_{\mathbf{N}}^{D_{\mathbf{M}}^{\perp}}$ fails. This is exemplified in Figure 4.4a, where we see that the periodicity $r_{\mathbf{N}}(\mathbf{h}) = r_{\mathbf{N}}(\mathbf{h} + \mathbf{M}^{\mathrm{T}}\mathbf{z})$ does not hold for all $\mathbf{v} = \mathbf{N}^{-\mathbf{T}}\mathbf{h}$, with $\mathbf{h} \in \mathcal{K}(\mathbf{N}^{\mathrm{T}})$ and $\mathbf{J} = \mathbf{J}_4$.

We adapt the function $D_{\mathbf{N}}^{\perp}$ to $\tilde{D}_{\mathbf{N}}^{\perp}$ such that $c_{\mathbf{h}}(\tilde{D}_{\mathbf{N}}^{\perp}) = c_{\mathbf{h}+\mathbf{M}^{\mathrm{T}}\mathbf{z}}(\tilde{D}_{\mathbf{N}}^{\perp})$ is obtained for all $\mathbf{h} \in \mathcal{K}(\mathbf{N}^{\mathrm{T}})$. This allows us to use $\tilde{D}_{\mathbf{N}}^{\perp}$ as a function to generate one of the decomposed spaces of $V_{\mathbf{M}}^{D_{\mathbf{M}}^{\perp}}$ in Theorem 4.11, as $\tilde{D}_{\mathbf{N}}^{\perp} \in V_{\mathbf{M}}^{D_{\mathbf{M}}^{\perp}}$. A visualization of this adaption is given in Figure 4.4b, where the yellow lines represent the extension of the orthonormal Dirichlet kernel, taking the same value as its black neighbor line. Note that these adapted functions are not proper Dirichlet kernels, as they do not fulfill the definition in (4.5).

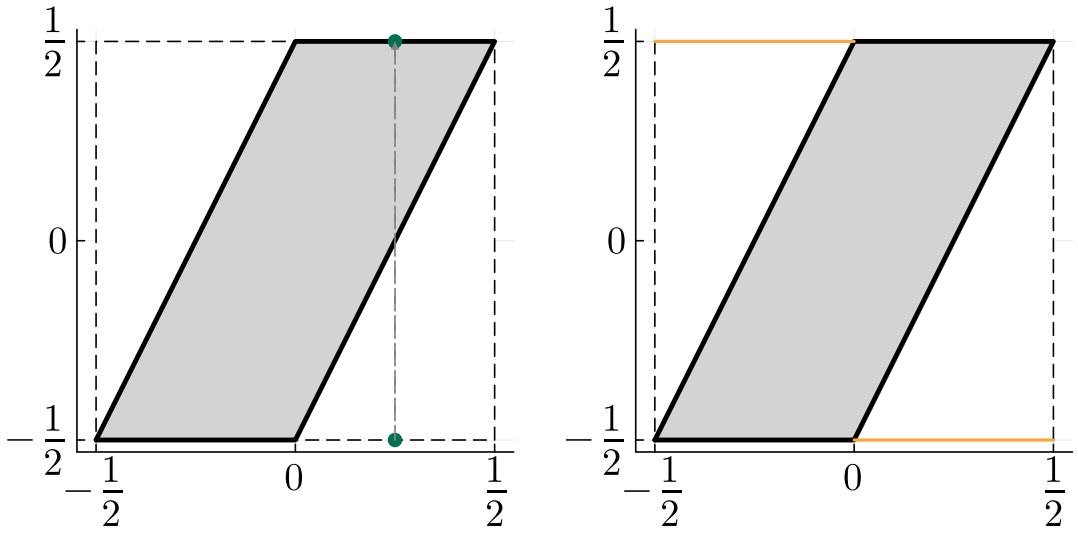

(a) $\mathbf{J} = \mathbf{J}_4$ (b) Adaption when using $\mathbf{J}_4$

Figure 4.4: Dashed square is $[-\frac{1}{2}, \frac{1}{2}]^2$, while the grey rectangle is $\mathbf{J}^{-\mathrm{T}}[-\frac{1}{2}, \frac{1}{2}]^2$. The green points represent an arbitrary $\mathbf{v}$ and $\mathbf{v} \pm \mathbf{e}_j$. The yellow lines represent the extension of the orthonormal Dirichlet kernel $D^{\perp}_{\mathbf{N}}$ to the adapted function $\tilde{D}^{\perp}_{\mathbf{N}}$.

While the Theorem 4.11 proves the existence of an orthogonal decomposition of $V^{\varphi}_{\mathbf{M}}$, the subsequent theorem presents a condition to verify whether a space $V^{\psi}_{\mathbf{N}}$ serves as the orthogonal complement of $V^{\xi}_{\mathbf{N}}$ in $V^{\varphi}_{\mathbf{M}}$, specifically when $|\det \mathbf{J}| = 2$.

Theorem 4.15 (Condition for orthogonal decomposition, [18, Theorem 4.3])**.** Let the matrices $\mathbf{M}, \mathbf{N}, \mathbf{J} \in \mathbb{Z}^{d\times d}$ be regular, such that $\mathbf{M} = \mathbf{J}\mathbf{N}$, with $|\det \mathbf{M}| = m$, $|\det \mathbf{N}| = n$ and $m = 2n$. Let the functions $\varphi, \xi \in L^2(\mathbb{T}^d)$ generate the m-dimensional $\mathbf{M}$-invariant space $V^{\varphi}_{\mathbf{M}}$ and the n-dimensional $\mathbf{N}$-invariant space $V^{\xi}_{\mathbf{N}}$, respectively. Further, let $\xi \in V^{\varphi}_{\mathbf{M}}$ with $(\hat{a}_{\mathbf{h}})_{\mathbf{h}\in\mathcal{G}(\mathbf{M}^{\mathrm{T}})}$ such that $c_{\mathbf{h}+\mathbf{M}^{\mathrm{T}}\mathbf{k}}(\xi) = \hat{a}_{\mathbf{h}} c_{\mathbf{h}+\mathbf{M}^{\mathrm{T}}\mathbf{k}}(\varphi)$ for all $\mathbf{h} \in \mathcal{G}(\mathbf{M}^{\mathrm{T}})$, $\mathbf{k} \in \mathbb{Z}^d$. Then the space $V^{\eta}_{\mathbf{N}}$ is orthogonal complement of $V^{\xi}_{\mathbf{N}}$ in $V^{\varphi}_{\mathbf{M}}$, i.e., $V^{\varphi}_{\mathbf{M}} = V^{\xi}_{\mathbf{N}} \oplus V^{\eta}_{\mathbf{N}}$, if and only if there exist numbers $\sigma_{\mathbf{h}} \in \mathbb{C}\backslash\{0\}$ for $\mathbf{h} \in \mathcal{G}(\mathbf{M}^{\mathrm{T}})$ with

$$\sigma_{\mathbf{h}} = -\sigma_{\mathbf{h}+\mathbf{N}^{\mathrm{T}}\mathbf{g}}, \qquad \text{for all } \mathbf{g} \in \mathcal{G}(\mathbf{J}^{\mathrm{T}})\backslash\{\mathbf{0}\}, \tag{4.9}$$

satisfying

$$c_{\mathbf{k}}(\eta) = \frac{\sigma_{\mathbf{k} \bmod \mathbf{M}^{\mathrm{T}}}\ \bar{\hat{a}}_{\mathbf{k}+\mathbf{N}^{\mathrm{T}}\mathbf{g} \bmod \mathbf{M}^{\mathrm{T}}}}{\sum_{\mathbf{l}\in\mathbb{Z}^d} |c_{\mathbf{k}+\mathbf{M}^{\mathrm{T}}\mathbf{l}}(\varphi)|^2} c_{\mathbf{k}}(\varphi), \qquad \text{for all } \mathbf{k} \in \mathbb{Z}^d. \tag{4.10}$$

Proof. First, assume $V^{\eta}_{\mathbf{N}}$ is orthogonal complement of $V^{\xi}_{\mathbf{N}}$ in $V^{\varphi}_{\mathbf{M}}$which implies $V^{\varphi}_{\mathbf{M}} = V^{\eta}_{\mathbf{N}} \oplus V^{\xi}_{\mathbf{N}}$. Theorem 4.5 guarantees the existence of a vector $(\hat{b}_{\mathbf{h}})_{\mathbf{h}\in\mathcal{G}(\mathbf{M}^{\mathrm{T}})}$ such that $c_{\mathbf{h}+\mathbf{M}^{\mathrm{T}}\mathbf{k}}(\eta) = \hat{b}_{\mathbf{h}} c_{\mathbf{h}+\mathbf{M}^{\mathrm{T}}\mathbf{k}}(\varphi)$ for all $\mathbf{h} \in \mathcal{G}(\mathbf{M}^{\mathrm{T}})$. Further, we know that the translates $\{T(\mathbf{y})\eta : \mathbf{y} \in \mathcal{P}(\mathbf{N})\}$ are orthogonal to $V^{\xi}_{\mathbf{N}}$ by assumption. Thus, by Theorem 4.12(ii), we can write for every $\mathbf{h} \in \mathcal{G}(\mathbf{M}^{\mathrm{T}})$ that

$$\langle T(\mathbf{y})\eta, T(\mathbf{x})\xi\rangle = \sum_{\mathbf{g}\in\mathcal{G}(\mathbf{J}^{\mathrm{T}})} \hat{a}_{\mathbf{h}+\mathbf{N}^{\mathrm{T}}\mathbf{g}} \bar{\hat{b}}_{\mathbf{h}+\mathbf{N}^{\mathrm{T}}\mathbf{g}} \sum_{\mathbf{k}\in\mathbb{Z}^d} |c_{\mathbf{h}+\mathbf{N}^{\mathrm{T}}\mathbf{g}+\mathbf{M}^{\mathrm{T}}\mathbf{k}}(\varphi)|^2 = 0,$$

where $\mathbf{x}, \mathbf{y} \in \mathcal{P}(\mathbf{N})$. Utilizing the uniqueness of the element $\mathbf{g} \in \mathcal{G}(\mathbf{J}^{\mathrm{T}})\backslash\{\mathbf{0}\}$, because $|\det \mathbf{J}| = 2$, we can express the above equation as follows

$$\hat{a}_{\mathbf{h}}\bar{\hat{b}}_{\mathbf{h}} \sum_{\mathbf{k}\in\mathbb{Z}^d} |c_{\mathbf{h}+\mathbf{M}^{\mathrm{T}}\mathbf{k}}(\varphi)|^2 + \hat{a}_{\mathbf{h}+\mathbf{N}^{\mathrm{T}}\mathbf{g}}\bar{\hat{b}}_{\mathbf{h}+\mathbf{N}^{\mathrm{T}}\mathbf{g}} \sum_{\mathbf{k}\in\mathbb{Z}^d} |c_{\mathbf{h}+\mathbf{N}^{\mathrm{T}}\mathbf{g}+\mathbf{M}^{\mathrm{T}}\mathbf{k}}(\varphi)|^2 = 0$$

holding for all $\mathbf{h} \in \mathcal{G}(\mathbf{N}^{\mathrm{T}})$. Complex conjugating the equation and rearranging it when $\hat{a}_{\mathbf{h}}, \hat{a}_{\mathbf{h}+\mathbf{N}^{\mathrm{T}}\mathbf{g}} \neq 0$, we arrive at

$$\frac{\hat{b}_{\mathbf{h}}}{\bar{\hat{a}}_{\mathbf{h}+\mathbf{N}^{\mathrm{T}}\mathbf{g}}} \sum_{\mathbf{k}\in\mathbb{Z}^d} |c_{\mathbf{h}+\mathbf{M}^{\mathrm{T}}\mathbf{k}}(\varphi)|^2 = -\frac{\hat{b}_{\mathbf{h}+\mathbf{N}^{\mathrm{T}}\mathbf{g}}}{\bar{\hat{a}}_{\mathbf{h}}} \sum_{\mathbf{k}\in\mathbb{Z}^d} |c_{\mathbf{h}+\mathbf{N}^{\mathrm{T}}\mathbf{g}+\mathbf{M}^{\mathrm{T}}\mathbf{k}}(\varphi)|^2.$$

Denoting the left-hand side by $\sigma_{\mathbf{h}}$ and the right-hand side as $\sigma_{\mathbf{h}+\mathbf{N}^{\mathrm{T}}\mathbf{g}}$ the required condition in (4.9) is fulfilled with

$$\sigma_{\mathbf{h}} = \frac{\hat{b}_{\mathbf{h}}}{\bar{\hat{a}}_{\mathbf{h}+\mathbf{N}^{\mathrm{T}}\mathbf{g}}} \sum_{\mathbf{k}\in\mathbb{Z}^d} |c_{\mathbf{h}+\mathbf{M}^{\mathrm{T}}\mathbf{k}}(\varphi)|^2 \quad \text{and} \quad \sigma_{\mathbf{h}+\mathbf{N}^{\mathrm{T}}\mathbf{g}} = \frac{\hat{b}_{\mathbf{h}+\mathbf{N}^{\mathrm{T}}\mathbf{g}}}{\bar{\hat{a}}_{\mathbf{h}}} \sum_{\mathbf{k}\in\mathbb{Z}^d} |c_{\mathbf{h}+\mathbf{N}^{\mathrm{T}}\mathbf{g}+\mathbf{M}^{\mathrm{T}}\mathbf{k}}(\varphi)|^2.$$

For the case where either $\hat{a}_{\mathbf{h}}$ or $\hat{a}_{\mathbf{h}+\mathbf{N}^{\mathrm{T}}\mathbf{g}}$ is zero, the σ that is well defined is used to determine $\sigma_{\mathbf{h}}$ or $\sigma_{\mathbf{h}+\mathbf{N}^{\mathrm{T}}\mathbf{g}}$ using the condition in Equation (4.9). Both $\hat{a}_{\mathbf{h}}$ and $\hat{a}_{\mathbf{h}+\mathbf{N}^{\mathrm{T}}\mathbf{g}}$ does not vanish simultaneously, which is ensured by the full rank of $V_{\mathbf{N}}^{\xi}$. This guarantees that either $\sigma_{\mathbf{h}}$ or $\sigma_{\mathbf{h}+\mathbf{N}^{\mathrm{T}}\mathbf{g}}$ is well defined when condition in Equation (4.10) is fulfilled.

Conversely, we assume that there exists numbers $\sigma_{\mathbf{h}}$ satisfying (4.9) and preform the reverse steps. □

The preceding theorem lets us determine the coefficients of $c_{\mathbf{k}}(\eta)$ with respect to the basis of $V_{\mathbf{M}}^{\varphi}$, when $c_{\mathbf{k}}(\xi)$ is fixed.

Corollary 4.16 ([18, Corollary 4.4])**.** Let $\mathbf{M}, \mathbf{J}, \mathbf{N} \in Z^{d\times d}$ be regular matrices with $\mathbf{M} = \mathbf{JN}$ and $|\det \mathbf{J}| = 2$. The orthogonal complement of $V_{\mathbf{N}}^{\xi}$ in $V_{\mathbf{M}}^{\varphi}$ is an $\mathbf{N}$-shift invariant space. Further, there is a function $\psi \in L^2(\mathbb{T}^d)$, the translates of which form a basis of $V_{\mathbf{M}}^{\varphi} \ominus V_{\mathbf{N}}^{\xi}$.

Proof. If we choose

$$\sigma_{\mathbf{h}} = 1 \quad \mathbf{h} \in \mathcal{G}(\mathbf{N}^{\mathrm{T}}) \quad \text{and} \quad \sigma_{\mathbf{h}+\mathbf{N}^{\mathrm{T}}\mathbf{g}} = -1 \quad \mathbf{h} \in \mathcal{G}(\mathbf{N}^{\mathrm{T}}) + \mathbf{N}^{\mathrm{T}}\mathbf{g}$$

with $\mathbf{g} \in \mathcal{G}(\mathbf{J}^{\mathrm{T}})\backslash\{\mathbf{0}\}$, the statement holds true by Theorem 4.15. □

To construct a so called wavelet $\psi \in V_{\mathbf{N}}^{\eta}$ we are free to choose the values $\sigma_{\mathbf{h}}$ with $\mathbf{h} \in \mathcal{G}(\mathbf{N}^{\mathrm{T}})$ as long as (4.9) is fulfilled, yielding the rest of the coefficients. By applying the following theorem, we can construct a wavelet η who's translates are orthonormal.

Theorem 4.17 ([3, Theorem 1.34])**.** Let $\mathbf{M}, \mathbf{J}, \mathbf{N} \in \mathbb{Z}^{d\times d}$ be regular matrices with $\mathbf{M} = \mathbf{JN}$ and $|\det \mathbf{J}|$. Let φ, ξ, η be related as in Theorem 4.15 with $V_{\mathbf{M}}^{\varphi} = V_{\mathbf{N}}^{\xi} \oplus V_{\mathbf{N}}^{\eta}$. Let $\sigma_{\mathbf{h}}$ for $\mathbf{h} \in \mathcal{G}(\mathbf{M}^{\mathrm{T}})$ satisfy the condition in Equation (4.9). Further, let the translates $\{T(\mathbf{x})\varphi : \mathbf{x} \in \mathcal{P}(\mathbf{M})\}$ and $\{T(\mathbf{x})\xi : \mathbf{y} \in \mathcal{P}(\mathbf{N})\}$ be orthonormal bases for $V_{\mathbf{M}}^{\varphi}$ and $V_{\mathbf{N}}^{\xi}$ respectively. Then the translates of $\{T(\mathbf{y})\eta : \mathbf{y} \in \mathcal{P}(\mathbf{M})\}$ are orthonormal if and only if

$$|\sigma_{\mathbf{h}}| = \frac{1}{m}, \quad \text{for all } \mathbf{h} \in \mathcal{G}(\mathbf{M}^{\mathrm{T}}).$$

Proof. Applying $c_{\mathbf{h}+\mathbf{M}^{\mathrm{T}}\mathbf{z}}(\eta) = \hat{b}_{\mathbf{h}} c_{\mathbf{h}+\mathbf{M}^{\mathrm{T}}\mathbf{z}}(\varphi)$ and the equivalent assertion of orthonormality of translates stated in Theorem 4.9, to Equation (4.10), we get

$$\hat{b}_{\mathbf{h}} = \frac{\sigma_{\mathbf{h}}\,\overline{\hat{a}}_{\mathbf{h}+\mathbf{N}^{\mathrm{T}}\mathbf{g}}}{\sum_{\mathbf{k}\in\mathbb{Z}^d} |c_{\mathbf{h}+\mathbf{M}^{\mathrm{T}}\mathbf{z}}(\varphi)|^2} = m\sigma_{\mathbf{h}}\overline{\hat{a}}_{\mathbf{h}+\mathbf{N}^{\mathrm{T}}\mathbf{g}}, \quad \mathbf{h}\in\mathcal{G}(\mathbf{M}^{\mathrm{T}}).$$

Now, let $\mathbf{g}\in\mathcal{G}(\mathbf{J}^{\mathrm{T}})\backslash\{\mathbf{0}\}$. By Lemma 4.12(iii) the set of translates $\{T(\mathbf{x})\eta : \mathbf{x}\in\mathcal{P}(\mathbf{M})\}$ are orthonormal if and only if for all $\mathbf{h}\in\mathcal{G}(\mathbf{N}^{\mathrm{T}})$ it holds that

$$\begin{aligned} 2 = |\det \mathbf{J}| &= \sum_{\mathbf{g}\in\mathcal{G}(\mathbf{J}^{\mathrm{T}})} |\hat{b}_{j,\mathbf{h}+\mathbf{N}^{\mathrm{T}}\mathbf{g}}|^2 = |\hat{b}_{\mathbf{h}}|^2 + |\hat{b}_{\mathbf{h}+\mathbf{N}^{\mathrm{T}}\mathbf{g}}|^2 \\ &= m^2|\sigma_{\mathbf{h}}|^2(|\hat{a}_{\mathbf{h}+\mathbf{N}^{\mathrm{T}}\mathbf{g}}|^2 + |\hat{a}_{\mathbf{h}}|^2) = 2m^2|\sigma_{\mathbf{h}}|^2, \end{aligned}$$

which completes the proof. □

Proposition 4.18 ([18, Theorem 6.6])**.** Let $\varphi = D^{\perp}_{\mathbf{M}}$ and $\xi = D^{\perp}_{\mathbf{N}}$ or $\tilde{D}^{\perp}_{\mathbf{N}}$ with coefficients $(a_{\mathbf{y}})_{\mathbf{y}\in\mathcal{P}(\mathbf{M})}$ with respect to $D^{\perp}_{\mathbf{M}}$ and use the setup from Theorem 4.15. Further, choose

$$\sigma_{\mathbf{h}} = \frac{\mathrm{e}^{-2\pi\mathrm{i}\mathbf{h}^{\mathrm{T}}\mathbf{N}^{-1}\mathbf{y}}}{m} \quad \text{and} \quad \sigma_{\mathbf{h}+\mathbf{N}^{\mathrm{T}}\mathbf{g}} = \frac{\mathrm{e}^{-2\pi\mathrm{i}(\mathbf{h}+\mathbf{N}^{\mathrm{T}}\mathbf{g})^{\mathrm{T}}\mathbf{N}^{-1}\mathbf{y}}}{m}$$

for $\mathbf{h}\in\mathcal{G}(\mathbf{M}^{\mathrm{T}})$, $\mathbf{g}\in\mathcal{G}(\mathbf{J}^{\mathrm{T}})\backslash\{\mathbf{0}\}$ and $\mathbf{y}\in\mathcal{P}(\mathbf{J})\backslash\{\mathbf{0}\}$. Then a wavelet ψ with orthonormal translates is generated, whose Fourier coefficients are given as

$$c_{\mathbf{k}}(\psi) = \begin{cases} \hat{a}_{\mathbf{k}+\mathbf{N}^{\mathrm{T}}\mathbf{g} \bmod \mathbf{M}^{\mathrm{T}}} \mathrm{e}^{-2\pi\mathrm{i}\mathbf{k}^{\mathrm{T}}\mathbf{N}^{-1}\mathbf{y}} c_{\mathbf{k}}(D^{\perp}_{\mathbf{M}}) & \text{for } \mathbf{k}\in\mathcal{K}(\mathbf{M}^{\mathrm{T}}), \\ 0 & \text{otherwise.} \end{cases}$$

Proof. We show that the chosen $\sigma_{\mathbf{h}}$ satisfy the condition in (4.9) for all $\mathbf{h}\in\mathcal{G}(\mathbf{M}^{\mathrm{T}})$.

$$\begin{aligned} m\sigma_{\mathbf{h}+\mathbf{N}^{\mathrm{T}}\mathbf{g}} &= \mathrm{e}^{-2\pi\mathrm{i}(\mathbf{h}+\mathbf{N}^{\mathrm{T}}\mathbf{g})^{\mathrm{T}}\mathbf{N}^{-1}\mathbf{y}} = \mathrm{e}^{-2\pi\mathrm{i}\mathbf{h}^{\mathrm{T}}\mathbf{N}^{-1}\mathbf{y}}\mathrm{e}^{-2\pi\mathrm{i}\mathbf{g}^{\mathrm{T}}\mathbf{N}\mathbf{N}^{-1}\mathbf{y}} \\ &= \mathrm{e}^{-2\pi\mathrm{i}\mathbf{h}^{\mathrm{T}}\mathbf{N}^{-1}\mathbf{y}} \cdot (-1) = -m\sigma_{\mathbf{h}} \end{aligned}$$

The translates of $D^{\perp}_{\mathbf{M}}$ and $D^{\perp}_{\mathbf{N}}$ are known by Proposition 4.10 to be orthonormal, and thus the orthonormality of the translates of ψ follows directly from Theorem 4.17. □

For the two functions $D^{\perp}_{\mathbf{N}}$ and ψ to be orthonormal translates the following must hold true

$$\begin{aligned} 0 = \langle c_{\mathbf{k}}(D^{\perp}_{\mathbf{N}}), c_{\mathbf{k}}(\psi)\rangle &= \sum_{\mathbf{k}\in\mathbb{Z}^d} c_{\mathbf{k}}(D^{\perp}_{\mathbf{N}})\overline{c_{\mathbf{k}}(\psi)} \\ &= \sum_{\mathbf{h}\in\mathcal{G}(\mathbf{M}^{\mathrm{T}})} \hat{a}_{\mathbf{h}}\overline{\hat{b}_{\mathbf{h}}} \sum_{\mathbf{z}\in\mathbb{Z}^d} |c_{\mathbf{h}+\mathbf{M}^{\mathrm{T}}\mathbf{z}}(D^{\perp}_{\mathbf{M}})|^2 \\ &= \sum_{\mathbf{h}\in\mathcal{G}(\mathbf{M}^{\mathrm{T}})} \hat{a}_{\mathbf{h}}\overline{\hat{b}_{\mathbf{h}}}. \end{aligned}$$

Note that there are several ways of choosing the $\sigma_{\mathbf{h}}$ such that the condition in (4.9) is satisfied and thus making the foregoing equation hold true, i.e., the constructed wavelet ψ in the foregoing proposition is not unique.

Example 4.19. We use the matrices $\mathbf{M} = \mathbf{A}_3$, $\mathbf{J} = \mathbf{J}_2$ and $\mathbf{N} = \left[\begin{smallmatrix} 8 & 2 \\ 0 & 16 \end{smallmatrix}\right]$. From the notation of Theorem 4.15, let $\varphi = D^{\perp}_{\mathbf{M}}$, $\xi = D^{\perp}_{\mathbf{N}}$ and $\eta = \psi$ from Proposition 4.18. We have the relation

$$\begin{aligned} c_{\mathbf{h}+\mathbf{M}^{\mathrm{T}}\mathbf{z}}(D^{\perp}_{\mathbf{N}}) &= \hat{a}_{\mathbf{h}} c_{\mathbf{h}+\mathbf{M}^{\mathrm{T}}\mathbf{z}}(D^{\perp}_{\mathbf{M}}), \\ c_{\mathbf{h}+\mathbf{M}^{\mathrm{T}}\mathbf{z}}(\psi) &= \hat{b}_{\mathbf{h}} c_{\mathbf{h}+\mathbf{M}^{\mathrm{T}}\mathbf{z}}(D^{\perp}_{\mathbf{M}}), \end{aligned} \qquad \mathbf{h} \in \mathcal{G}(\mathbf{M}^{\mathrm{T}}),\ \mathbf{z} \in \mathbb{Z}^d.$$

In Figure 4.5 we see $c_{\mathbf{k}}(D^{\perp}_{\mathbf{N}})$ and real and imaginary parts of the wavelet $c_{\mathbf{k}}(\psi)$ for $\mathbf{k} \in \mathbb{Z}^d$. For the indices $\mathbf{k} \in \mathbb{Z}^d$ which are not on the vertical border of $\mathcal{K}(\mathbf{N}^{\mathrm{T}})$, the product of the coefficients $c_{\mathbf{k}}(D^{\perp}_{\mathbf{N}})$ and $c_{\mathbf{k}}(\psi)$ is zero as one of the coefficients is zero. Considering the indices $\mathbf{k}$ on the vertical border of $\mathcal{K}(\mathbf{N}^{\mathrm{T}})$, the corresponding product of coefficients of the indices $\mathbf{k}$ and $\mathbf{k} + \mathbf{N}^{\mathrm{T}}\mathbf{g}$ for $\mathbf{g} \in \mathcal{G}(\mathbf{J}^{\mathrm{T}})\backslash\{\mathbf{0}\}$, have opposite signs, i. e.

$$c_{\mathbf{k}}(D^{\perp}_{\mathbf{N}}) c_{\mathbf{k}}(\psi) = -\big(c_{\mathbf{k}+\mathbf{N}^{\mathrm{T}}\mathbf{g}}(D^{\perp}_{\mathbf{N}}) c_{\mathbf{k}+\mathbf{N}^{\mathrm{T}}\mathbf{g}}(\psi)\big).$$

This property is gained by construction of the wavelet ψ in Proposition 4.18, as it then fulfills the condition in (4.9). We study one pair of indices on the border of $\mathcal{K}(\mathbf{N}^{\mathrm{T}})$, and have that $\mathbf{g} = (0,1)^{\mathbf{T}}$ which yields

$$\begin{aligned} \mathbf{k} &= (4,-6)^{\mathbf{T}} & c_{\mathbf{k}}(D^{\perp}_{\mathbf{N}}) c_{\mathbf{k}}(\psi) &\approx 0.001495 - 0.003609\mathrm{im} \\ \mathbf{k} + \mathbf{N}^{\mathrm{T}}\mathbf{g} &= (-4,-8)^{\mathbf{T}} & c_{\mathbf{k}+\mathbf{N}^{\mathrm{T}}\mathbf{g}}(D^{\perp}_{\mathbf{N}}) c_{\mathbf{k}+\mathbf{N}^{\mathrm{T}}\mathbf{g}}(\psi) &\approx -0.001495 + 0.003609\mathrm{im}, \end{aligned}$$

and we see that the sum of the two products is zero. This holds for every such pair of indices $\mathbf{k}$ and $\mathbf{k} + \mathbf{N}^{\mathrm{T}}\mathbf{g}$, and thus

$$\sum_{\mathbf{k} \in \mathbb{Z}^d} c_{\mathbf{k}}(D^{\perp}_{\mathbf{N}}) c_{\mathbf{k}}(\psi) = 0,$$

i.e., the space generated by the wavelet ψ is orthogonal to the space generated by $D^{\perp}_{\mathbf{N}}$.

4.3 Properties of Multivariate Scaling

In this paragraph, we examine how we can characterize the subpattern $\mathcal{P}(\mathbf{N})$ when we know $\mathcal{P}(\mathbf{M})$, additionally how we can extend a subpattern $\mathcal{P}(\mathbf{N})$ to $\mathcal{P}(\mathbf{M})$, with $\mathbf{M} = \mathbf{JN}$. Throughout the section the bases of the patterns $\mathcal{P}(\mathbf{M})$, $\mathcal{P}(\mathbf{N})$ and $\mathcal{P}(\mathbf{J})$ will be referred to as $\{\mathbf{x}_{\mathbf{e}_1}, \ldots, \mathbf{x}_{\mathbf{e}_{d_{\mathbf{M}}}}\}$, $\{\mathbf{y}_{\mathbf{e}_1}, \ldots, \mathbf{y}_{\mathbf{e}_{d_{\mathbf{N}}}}\}$ and $\{\mathbf{z}_{\mathbf{e}_1}, \ldots, \mathbf{z}_{\mathbf{e}_{d_{\mathbf{J}}}}\}$, respectively and are known by (3.6).

Lemma 4.20 (Projection, [4, Lemma 2])**.** Let $\mathbf{M}, \mathbf{J}, \mathbf{N} \in \mathbb{Z}^{d\times d}$ be regular matrices such that $\mathbf{M} = \mathbf{JN}$. Then there exists a matrix $\mathbf{P} \in \mathbb{N}_0^{d_{\mathbf{M}} \times d_{\mathbf{N}}}$ such that for any $\mathbf{w} \in \mathcal{P}(\mathbf{N})$ there exists $\boldsymbol{\mu} \in \mathbb{E}_{\mathbf{N}}$ and $\boldsymbol{\lambda} \in \mathbb{E}_{\mathbf{M}}$ such that

$$\mathbf{w} = \sum_{k=1}^{d_{\mathbf{N}}} \mu_k \mathbf{y}_{\mathbf{e}_k} = \sum_{l=1}^{d_{\mathbf{M}}} \lambda_l \mathbf{x}_{\mathbf{e}_l}, \qquad \text{with } \boldsymbol{\lambda} = \mathbf{P}\boldsymbol{\mu}.$$

Proof. Let $\mathbf{M} = \mathbf{JN}$. Then $\mathcal{P}(\mathbf{N}) \subset \mathcal{P}(\mathbf{M})$ implies that an element of $\mathcal{P}(\mathbf{N})$ also is an element of $\mathcal{P}(\mathbf{M})$. By (3.7) we have that for an arbitrary $\mathbf{w} \in \mathcal{P}(\mathbf{N})$ can be written as a linear combination of the basis vectors of $\mathcal{P}(\mathbf{N})$, i.e.,

$$\mathbf{w} = \sum_{k=1}^{d_{\mathbf{N}}} \mu_k \mathbf{y}_{\mathbf{e}_k},$$

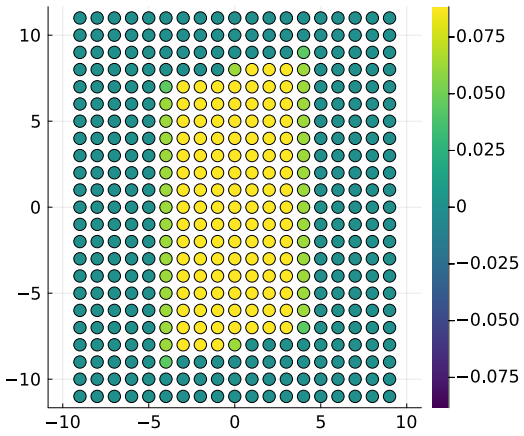

(a) $(c_{\mathbf{k}}(D^{\perp}_{\mathbf{N}}))_{\mathbf{k}\in\mathbb{Z}^d}$.

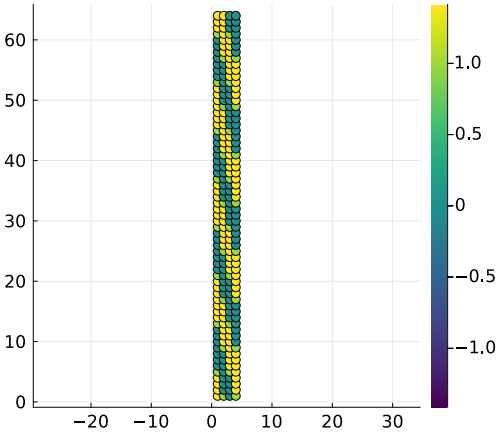

(b) $(\hat{a}_{\mathbf{h}})_{\mathbf{h}\in\mathcal{G}(\mathbf{N}^{\mathrm{T}})}$.

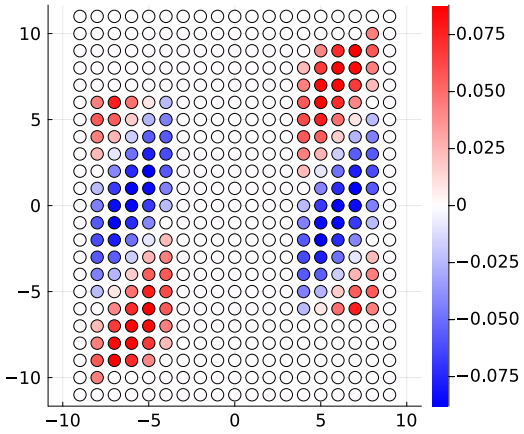

(c) $\mathrm{Re}\big((c_{\mathbf{k}}(\psi))_{\mathbf{k}\in\mathbb{Z}^d}\big)$.

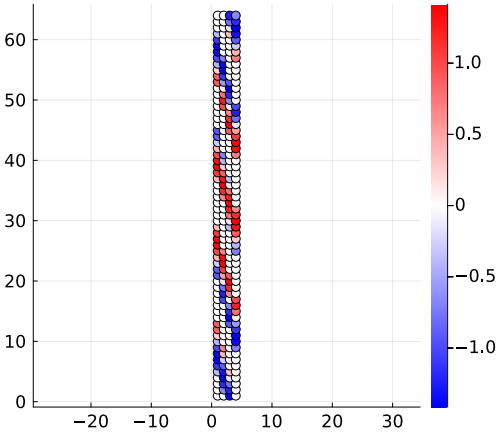

(d) $\mathrm{Re}\big((\hat{b}_{\mathbf{h}})_{\mathbf{h}\in\mathcal{G}(\mathbf{N}^{\mathrm{T}})}\big)$.

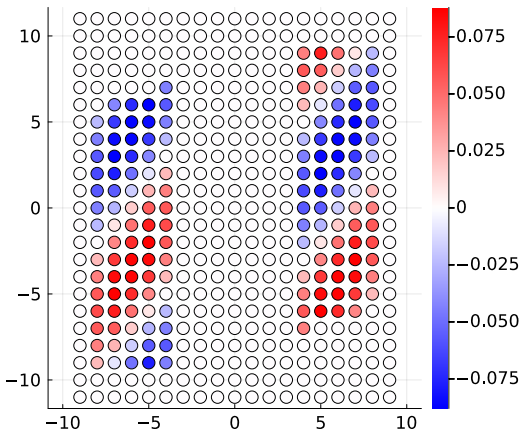

(e) $\mathrm{Im}\big((c_{\mathbf{k}}(\psi))_{\mathbf{k}\in\mathbb{Z}^d}\big)$.

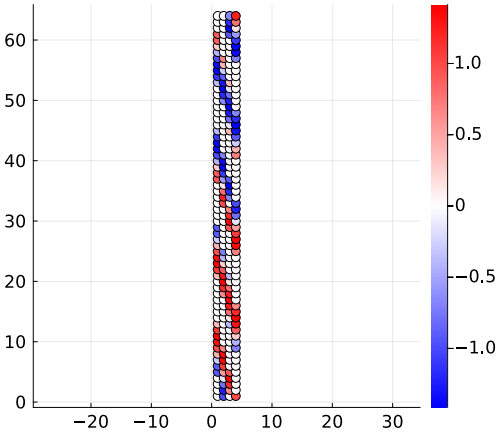

(f) $\mathrm{Im}((\hat{b}_{\mathbf{h}})_{\mathbf{h}\in\mathcal{G}(\mathbf{M}^{\mathrm{T}})})$.

Figure 4.5: To the left are the Fourier coefficients of $D^{\perp}_{\mathbf{N}}$ and ψ. To the right are the coefficients of $D^{\perp}_{\mathbf{N}}$ and $\psi_{\mathbf{N}}$ with respect to $D^{\perp}_{\mathbf{M}}$, in Fourier domain.

for a unique vector of coefficients $\boldsymbol{\mu} \in \mathbb{E}_{\mathbf{N}}$ defined in (3.8). Since $\mathcal{P}(\mathbf{N}) \subset \mathcal{P}(\mathbf{M})$, every basis vector $\mathbf{y}_{\mathbf{e}_k}$ of $\mathcal{P}(\mathbf{N})$ can be expressed in terms of a basis vector $\mathbf{x}_{\mathbf{e}_k}$ of $\mathcal{P}(\mathbf{M})$, i.e., there exists

$$\mathbf{p}_k = (p_{l,k})_{l=1}^{d_{\mathbf{M}}} \in \mathbb{N}_0^{d_{\mathbf{M}}} \text{ such that } \mathbf{y}_{\mathbf{e}_k} = \sum_{l=1}^{d_{\mathbf{M}}} p_{l,k} \mathbf{x}_{\mathbf{e}_l}, \quad k = 1, \dots, d_{\mathbf{N}}.$$

Inserting this reformulation into the linear combination of $\mathbf{w}$ we get that

$$\mathbf{w} = \sum_{k=1}^{d_{\mathbf{N}}} \mu_k \mathbf{y}_{\mathbf{e}_k} = \sum_{k=1}^{d_{\mathbf{N}}} \mu_k \sum_{l=1}^{d_{\mathbf{M}}} p_{l,k} \mathbf{x}_{\mathbf{e}_l} = \sum_{l=1}^{d_{\mathbf{M}}} \sum_{k=1}^{d_{\mathbf{N}}} \mu_k p_{l,k} \mathbf{x}_{\mathbf{e}_l} \coloneqq \sum_{l=1}^{d_{\mathbf{M}}} \lambda_l \mathbf{x}_{\mathbf{e}_l}.$$

The last equality provides the relation that $\boldsymbol{\lambda} = \mathbf{P}\boldsymbol{\mu}$, where $\mathbf{P} = (p_{l,k})_{l=1,k=1}^{d_{\mathbf{M}},d_{\mathbf{N}}} \in \mathbb{N}_0^{d_{\mathbf{M}} \times d_{\mathbf{N}}}$. □

Theorem 4.21 (Multivariate scaling property, [4, Theorem 3])**.** Let $\mathbf{J}, \mathbf{N} \in \mathbb{Z}^{d \times d}$ with $\mathbf{M} = \mathbf{J}\mathbf{N}$ such that the dimension $d_{\mathbf{J}} = 1$. Further, let the elementary divisors of $\mathbf{M}, \mathbf{N}, \mathbf{J}$ be denoted as $\varepsilon_j^{\mathbf{M}}, \varepsilon_j^{\mathbf{N}}, \varepsilon_j^{\mathbf{J}}$, respectively for $j = 1, \dots, d$. Then it holds that

1) for $\mathbf{N}^{-1}\mathbf{z}_{\mathbf{e}_1} \notin \operatorname{span}\{\mathbf{y}_{\mathbf{e}_1}, \dots, \mathbf{y}_{\mathbf{e}_{d_{\mathbf{N}}}}\}$, that
   a) $d_{\mathbf{M}} = d_{\mathbf{N}} + 1$
   b) there exists a $\mathbf{x}_{\mathbf{e}_l} \in \{\mathbf{x}_{\mathbf{e}_1}, \dots, \mathbf{x}_{\mathbf{e}_{d_{\mathbf{M}}}}\}$ so that

$$\mathbf{N}^{-1}\mathbf{z}_{\mathbf{e}_1} = \lambda \mathbf{x}_{\mathbf{e}_l} \bmod \mathbf{I}, \quad \lambda \in \{1, \dots, \varepsilon_d^{\mathbf{J}} - 1\} \quad \text{and} \quad \varepsilon_l^{\mathbf{M}} = \varepsilon_d^{\mathbf{J}}.$$

2) for $\mathbf{N}^{-1}\mathbf{z}_{\mathbf{e}_1} \in \operatorname{span}\{\mathbf{y}_{\mathbf{e}_1}, \dots, \mathbf{y}_{\mathbf{e}_{d_{\mathbf{N}}}}\}$, that
   a) $d_{\mathbf{M}} = d_{\mathbf{N}}$
   b) there exits decompositions

$$\mathbf{N}^{-1}\mathbf{z}_{\mathbf{e}_1} = \sum_{l=1}^{d_{\mathbf{M}}} \lambda_l \mathbf{x}_{\mathbf{e}_l}, \quad \lambda \in \mathbb{E}_{\mathbf{M}} \quad \text{and} \quad \mathbf{N}^{-1}\mathbf{z}_{\mathbf{e}_1} = \sum_{k=1}^{d_{\mathbf{N}}} \mu_k \mathbf{y}_{\mathbf{e}_k}, \quad \mu \in \mathbb{Q}^d$$

   which fulfill

$$\lambda = \frac{1}{\varepsilon_d^{\mathbf{J}}} \mathbf{P}\mu, \quad \mathbf{P} \in \mathbb{N}_0^{d_{\mathbf{M}} \times d_{\mathbf{M}}}.$$

Proof. Since $d_{\mathbf{J}} = 1$, we know that $\mathcal{P}(\mathbf{J})$ is spanned by one vector $\mathbf{z}_{\mathbf{e}_1}$. $\mathbf{N}^{-1}\mathbf{z}_{\mathbf{e}_1} \in \mathcal{P}(\mathbf{M})$ since $\mathbf{J}\mathbf{z}_{\mathbf{e}_1} = \mathbf{M}\mathbf{N}^{-1}\mathbf{z}_{\mathbf{e}_1} \in \mathbb{Z}^d$.

1) Let $\mathbf{N}^{-1}\mathbf{z}_{\mathbf{e}_1} \notin \operatorname{span}\{\mathbf{y}_{\mathbf{e}_1}, \dots, \mathbf{y}_{\mathbf{e}_{d_{\mathbf{N}}}}\}$, i.e., we cannot write $\mathbf{N}^{-1}\mathbf{z}_{\mathbf{e}_1}$ as a linear combination of the $\mathbf{y}_{\mathbf{e}_j}$. Then the extension of the set

$$\operatorname{span}\{\mathbf{y}_{\mathbf{e}_1}, \dots, \mathbf{y}_{\mathbf{e}_{d_{\mathbf{N}}}}\} \subset \operatorname{span}\{\mathbf{y}_{\mathbf{e}_1}, \dots, \mathbf{y}_{\mathbf{e}_{d_{\mathbf{N}}}}, \mathbf{N}^{-1}\mathbf{z}_{\mathbf{e}_1}\},$$

   holds without an equality. Hence, the extended set is linearly independent and the dimension of the extension is $d_{\mathbf{M}} = d_{\mathbf{N}} + 1$.

This also applies when restricting the weighted sums to the prefactors from the set of indices $\mathbb{E}_{\mathbf{N}}$ and $\mathbb{E}_{\mathbf{N}} \times \mathbb{E}_{\mathbf{J}}$, respectively. Further, we can decompose an element $\mathbf{x} \in \mathcal{P}(\mathbf{M})$ by Lemma 3.7 and express it in terms of the basis vectors of $\mathcal{P}(\mathbf{N})$ and $\mathcal{P}(\mathbf{J})$ as follows

$$\mathbf{x} = \sum_{k=1}^{d_{\mathbf{N}}} \mu_k \mathbf{y}_{\mathbf{e}_k} + \beta \mathbf{N}^{-1} \mathbf{z}_{\mathbf{e}_1},$$

for a unique $\boldsymbol{\mu} \in \mathbb{E}_{\mathbf{N}}$ and $\beta \in \mathbb{E}_{\mathbf{J}}$. As a result of $d_{\mathbf{J}} = 1$, the second term is comprised of a single summand. The inclusion $\mathcal{P}(\mathbf{N}) \subseteq \mathcal{P}(\mathbf{M})$ implies that all cycles of $\mathcal{P}(\mathbf{N})$ also is a cycle in $\mathcal{P}(\mathbf{M})$. Hence, there exists exacly one basis vector $\mathbf{x}_l$ which spans this new cycle.

2) On the other hand, let $\mathbf{N}^{-1}\mathbf{z}_{\mathbf{e}_1} \in \operatorname{span}\{\mathbf{y}_{\mathbf{e}_1}, \dots, \mathbf{y}_{\mathbf{e}_{d_{\mathbf{N}}}}\}$. Then the element $\mathbf{N}^{-1}\mathbf{z}_{\mathbf{e}_1} \in \{\mathbf{x}_{\mathbf{e}_1}, \dots, \mathbf{x}_{\mathbf{e}_{d_{\mathbf{M}}}}\}$ can be written as

$$\mathbf{N}^{-1}\mathbf{z}_{\mathbf{e}_1} = \theta \sum_{k=1}^{d_{\mathbf{N}}} \mu_k \mathbf{y}_{\mathbf{e}_k},$$

for unique coefficient vectors $\boldsymbol{\mu} \in \mathbb{E}_{\mathbf{N}}$ and $\theta \in \mathbb{E}_{\mathbf{J}}$. This decomposition shows that $d_{\mathbf{M}} = d_{\mathbf{N}}$.

By definition of the basis vectors, (3.6), and the construction of $\mathbf{R}$ from the Smith normal from $\mathbf{M} = \mathbf{QER}$ in Equation (2.7), we have that $\varepsilon_d^{\mathbf{J}} \mathbf{z}_{\mathbf{e}_1} \in \mathbb{Z}^d$. Furthermore, we have the decomposition

$$\varepsilon_d^{\mathbf{J}} \mathbf{N}^{-1}\mathbf{z}_{\mathbf{e}_1} = \sum_{k=1}^{d_{\mathbf{N}}} \mu_k \mathbf{y}_{\mathbf{e}_k},$$

for a unique $\boldsymbol{\mu} \in \mathbb{E}_{\mathbf{N}}$. Combining the precieding two equations yields

$$\mathbf{N}^{-1}\mathbf{z}_{\mathbf{e}_1} = \sum_{l=1}^{d_{\mathbf{M}}} \lambda_l \mathbf{x}_{\mathbf{e}_l} = \frac{1}{\varepsilon_d^{\mathbf{J}}} \sum_{k=1}^{d_{\mathbf{N}}} \mu_k \mathbf{y}_{\mathbf{e}_k} = \frac{1}{\varepsilon_d^{\mathbf{J}}} \sum_{k=0}^{d_{\mathbf{N}}} \mu_k \sum_{l=1}^{d_{\mathbf{M}}} p_{l,k} \mathbf{x}_{\mathbf{e}_l},$$

for a unique $\boldsymbol{\lambda} \in \mathbb{E}_{\mathbf{M}}$. The last equation is exacly the expression in b) and completes the proof. □

The foregoing theorem provides insights into the extension of $\mathcal{P}(\mathbf{N})$ to $\mathcal{P}(\mathbf{M})$ in the scenario where $\mathbf{M} = \mathbf{JN}$ and $d_{\mathbf{J}} = 1$. In the case where $|\det \mathbf{J}| = 2$, a cycle of length 2 is either appended to the existing cycles or one of the existing cycles is doubled in length.

Example 4.22. We will now do an example for the two different cases of Theorem 4.21. Both scenarios are visualized in Figure 4.6.

1) $\mathbf{N}^{-1}\mathbf{z}_{\mathbf{e}_1} \notin \operatorname{span}\{\mathbf{y}_{\mathbf{e}_1}, \dots, \mathbf{y}_{\mathbf{e}_{d_{\mathbf{N}}}}\}$:

Such a case arises for the matrices

$$\mathbf{J}_1 = \begin{bmatrix} 2 & 0 \\ 0 & 1 \end{bmatrix}, \qquad \mathbf{N} = \begin{bmatrix} 1 & 0 \\ 0 & 16 \end{bmatrix}, \qquad \text{such that } \mathbf{M} = \mathbf{JN} = \begin{bmatrix} 2 & 0 \\ 0 & 16 \end{bmatrix}.$$

This case is visualized in Figure 4.6a.

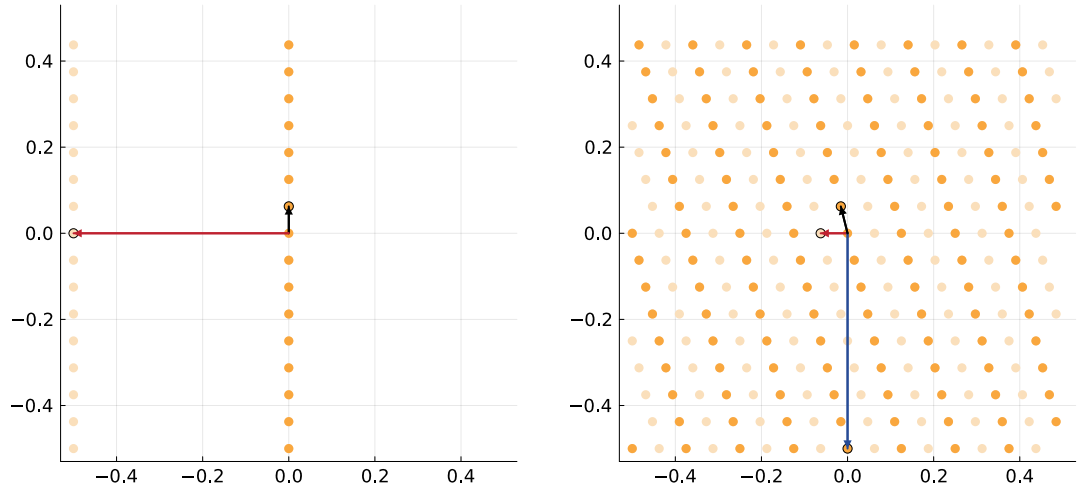

(a) $\mathbf{N}^{-1}\mathbf{z}_{\mathbf{e}_1} \notin \operatorname{span}\{\mathbf{y}_{\mathbf{e}_1}, \dots, \mathbf{y}_{\mathbf{e}_{d_\mathbf{N}}}\}$ (b) $\mathbf{N}^{-1}\mathbf{z}_{\mathbf{e}_1} \in \operatorname{span}\{\mathbf{y}_{\mathbf{e}_1}, \dots, \mathbf{y}_{\mathbf{e}_{d_\mathbf{N}}}\}$

Figure 4.6: Dark yellow is $\mathcal{P}(\mathbf{N})$. The light yellow and dark yellow is $\mathcal{P}(\mathbf{M})$. Red vectors are the vectors $\mathbf{N}^{-1}\mathbf{z}_{\mathbf{e}_1}$, the extended cycle. The black vectors represent the basis vector of $\mathcal{P}(\mathbf{N})$, as does the blue vector in the figure on the right-hand side.

a) We extend $\mathcal{P}(\mathbf{N})$ to $\mathcal{P}(\mathbf{M})$ using the vector $\mathbf{N}^{-1}\mathbf{z}_{\mathbf{e}_1}$ as a new basis vector, thus $d_\mathbf{M} = d_\mathbf{N} + 1$.
Figure 4.6a shows that the pattern of $\mathcal{P}(\mathbf{N})$ has the dimension $d_\mathbf{N} = 1$ spanned by one vector (black), i.e., every element lies on a line. The pattern $\mathcal{P}(\mathbf{M})$ is spanned by the additional vector $\mathbf{N}^{-1}\mathbf{z}_{\mathbf{e}_1}$ (red), making the pattern of $\mathcal{P}(\mathbf{M})$ having dimension $d_\mathbf{M} = 2$.

b) For this case we have that the $\mathcal{P}(\mathbf{M})$ is spanned by $\operatorname{span}\{\mathbf{x}_{\mathbf{e}_1}, \mathbf{x}_{\mathbf{e}_2}\} = \operatorname{span}\{\left[\frac{1}{2}, 0\right]^\mathrm{T}, \left[0, \frac{1}{16}\right]^\mathrm{T}\}$. For $l = 1$ it holds that

$$\mathbf{N}^{-1}\mathbf{z}_{\mathbf{e}_1} = \left[-\tfrac{1}{2}, 0\right]^\mathrm{T} = \lambda\left[\tfrac{1}{2}, 0\right]^\mathrm{T} \bmod \mathbf{I}, \qquad \text{for } \lambda = 1,$$

and we have $\varepsilon_1^\mathbf{M} = \varepsilon_2^\mathbf{J} = 2$. This adds a second cycle and extends $\mathcal{P}(\mathbf{N})$ to $\mathcal{P}(\mathbf{M})$.

2) $\mathbf{N}^{-1}\mathbf{z}_{\mathbf{e}_1} \in \operatorname{span}\{\mathbf{y}_{\mathbf{e}_1}, \dots, \mathbf{y}_{\mathbf{e}_{d_\mathbf{N}}}\}$:
The following situation occures for the matrices

$$\mathbf{J}_1 = \begin{bmatrix} 2 & 0 \\ 0 & 1 \end{bmatrix}, \qquad \mathbf{N}_1 = \begin{bmatrix} 8 & 2 \\ 0 & 16 \end{bmatrix}, \qquad \text{such that } \mathbf{M} = \mathbf{J}\mathbf{N} = \begin{bmatrix} 16 & 4 \\ 0 & 16 \end{bmatrix} = \mathbf{A}_3.$$

The basis vector of $\mathcal{P}(\mathbf{J})$ is $\mathbf{z}_{\mathbf{e}_1} = [-\frac{1}{2}, 0]^\mathrm{T}$, yielding $\mathbf{N}^{-1}\mathbf{z}_{\mathbf{e}_1} = \left[-\frac{1}{16}, 0\right]^\mathrm{T}$. The case is visualized in Figure 4.6b.

a) The dimension of $\mathcal{P}(\mathbf{M})$ is $d_\mathbf{M} = 2$, as it is spanned by two vectors (black and blue). Thus, the pattern of $\mathcal{P}(\mathbf{N})$ is not extended, as $d_\mathbf{N} = d_\mathbf{M}$ already.

b) We project the elements of $\mathcal{P}(\mathbf{N})$ onto $\mathcal{P}(\mathbf{M})$ by using Lemma 4.20. This tells us how to write elements of $\mathcal{P}(\mathbf{N})$ in terms of $\mathcal{P}(\mathbf{M})$. In

Figure 4.6b we observe that the pattern of $\mathcal{P}(\mathbf{N})$ is a subset of $\mathcal{P}(\mathbf{M})$, this scenario scales an already existing cycle, illustrated by the red vector.

4.4 The Fast Decomposition Algorithm

The matrix $\mathbf{B}_j$ in Lemma 4.12(iv) is a matrix representation of the fast decomposition algorithm. In the following section we will describe this algorithm in greater detail, as done in [4, Section 5.3].

Let $\mathbf{M}$ be a regular integer matrix with the given decomposition $\mathbf{M} = \mathbf{JN}$ and the functions $\varphi, \xi_1, \dots, \xi_{|\det \mathbf{J}|}$ such that

$$V_{\mathbf{M}}^{\varphi} = \bigoplus_{j=1}^{|\det \mathbf{J}|} V_{\mathbf{N}}^{\xi_j},$$
$$\xi_j = \sum_{\mathbf{y} \in \mathcal{P}(\mathbf{M})} b_{j,\mathbf{y}} T(\mathbf{y})\varphi \ \in V_{\mathbf{M}}^{\varphi}, \quad j = 1, \dots, |\det \mathbf{J}|.$$

Using any pair of bases $\{\mathbf{h}_{\mathbf{e}_1}, \dots, \mathbf{h}_{\mathbf{e}_{d_\mathbf{M}}}\}$ of $\mathcal{G}(\mathbf{M}^{\mathrm{T}})$ and $\{\mathbf{k}_{\mathbf{e}_1}, \dots, \mathbf{k}_{\mathbf{e}_{d_\mathbf{N}}}\}$ of $\mathcal{G}(\mathbf{N}^{\mathrm{T}})$, we can decompose any function

$$f = \sum_{\mathbf{y} \in \mathcal{P}(\mathbf{M})} a_{\mathbf{y}} T(\mathbf{y})\varphi \in V_{\mathbf{M}}^{\varphi}.$$

The decomposition consists of the following steps:

1) Calculate $\hat{\mathbf{a}} = \sqrt{m}\mathcal{F}(\mathbf{M})\mathbf{a}$ and $\hat{\mathbf{b}}_j = \sqrt{m}\mathcal{F}(\mathbf{M})\mathbf{b}_j$ for $j = 1, \dots, |\det \mathbf{J}|$.

2) Determine the matrix $\mathbf{P}$ relating the two sets of basis vectors $\{\mathbf{h}_{\mathbf{e}_1}, \dots, \mathbf{h}_{\mathbf{e}_{d_\mathbf{M}}}\}$ of $\mathcal{G}(\mathbf{M}^{\mathrm{T}})$ and $\{\mathbf{k}_{\mathbf{e}_1}, \dots, \mathbf{k}_{\mathbf{e}_{d_\mathbf{N}}}\}$ of $\mathcal{G}(\mathbf{N}^{\mathrm{T}})$ by using the projection of Lemma 4.20.

3) For each basis vector of the set $\{\mathbf{g}_{\mathbf{e}_1}, \dots, \mathbf{g}_{\mathbf{e}_{d_\mathbf{J}}}\}$ of $\mathcal{G}(\mathbf{J}^{\mathrm{T}})$, deduce the decomposition

$$\mathbf{N}^{\mathrm{T}}\mathbf{g}_{\mathbf{e}_l} = \sum_{i=1}^{d_\mathbf{M}} q_{i,l}\mathbf{h}_{\mathbf{e}_i} \Bigg|_{\mathcal{G}(\mathbf{M}^{\mathrm{T}})} \quad (q_{i,l})_{i=1}^{d_\mathbf{M}} \in \mathbb{E}_{\mathbf{M}}, \ l = 1, \dots, d_\mathbf{J}.$$

Now, address $\mathbf{N}^{\mathrm{T}}\mathbf{g} \in \mathcal{G}(\mathbf{M}^{\mathrm{T}})$, $\mathbf{g} \in \mathcal{G}(\mathbf{J}^{\mathrm{T}})$ using $\boldsymbol{\lambda}_\mathbf{g} \in \mathbb{E}_\mathbf{M}$.

4) Iterating through all $\boldsymbol{\mu} \in \mathbb{E}_\mathbf{N}$ and calculate $\boldsymbol{\lambda} = \mathbf{P}\boldsymbol{\mu}|_{\mathbb{E}_\mathbf{M}}$, with $\mathbf{P}$ from step 2, thus

$$\hat{d}_{j,\mathbf{h}} = \frac{1}{\sqrt{|\det \mathbf{J}|}} \sum_{\mathbf{g} \in \mathcal{G}(\mathbf{J}^{\mathrm{T}})} \overline{\hat{b}_{j,\mathbf{h}+\mathbf{N}^{\mathrm{T}}\mathbf{g}}} \hat{a}_{\mathbf{h}+\mathbf{N}^{\mathrm{T}}\mathbf{g}} \quad j = 1, \dots, |\det \mathbf{J}|, \ \mathbf{h} \in \mathcal{G}(\mathbf{N}^{\mathrm{T}}).$$

Use $\boldsymbol{\lambda} + \boldsymbol{\lambda}_\mathbf{g}|_{\mathbb{E}_\mathbf{M}}$ to address the indices of $\hat{\mathbf{a}}$ and $\hat{\mathbf{b}}$ and $\boldsymbol{\mu}$ to address the indices of $\hat{d}_{j,\mathbf{h}}$.

5) Lastly, for each $\hat{\mathbf{d}}_j$, perform the inverse Fourier transform, such that

$$f = \sum_{j=1}^{|\det \mathbf{J}|} \sum_{\mathbf{y} \in \mathcal{P}(\mathbf{N})} d_{j,\mathbf{y}} T(\mathbf{y}) \xi_j$$

and arrive at the decomposed functions of f.

When $|\det \mathbf{J}| = 2$ the two functions ξ_1 and ξ_2 serve to characterize low and high frequency components, respectively, i.e. a function $g_1 \in V_{\mathbf{N}}^{\xi_1}$ is the low frequency part of f, while $g_2 \in V_{\mathbf{N}}^{\xi_2}$ is the high frequency part of f. This algorithm represents a dyadic fast wavelet transform on a pattern. It is possbile to continue to further decompose the space $V_{\mathbf{N}}^{\xi_1}$, then only step 2-4 are necessary to compute on $\hat{\mathbf{b}}_1$. Analogously, the function g_1 can be further decomposed, using by using $\hat{\mathbf{d}}_1$. This process is called a multiresolusion analysis, and can be repeated until the desired level of decomposition is reached. Multiresolusion analysis is discussed in greater detail in Section 1.5 of [3].

Both the number of spaces $|\det \mathbf{J}|$ and the dimensionality of the problem d have an impact on the complexity of the algorithm, even though they remain constant with respect to $m = |\det \mathbf{M}|$. In the initial step, we execute $|\det \mathbf{J}| + 1$ Fourier transforms on a pattern of size m. In the concluding stage, we carry out $|\det \mathbf{J}|$ inverse Fourier transforms on a pattern of size $n = \frac{m}{|\det \mathbf{J}|}$. According to Section 3.3, the complexity of the Fourier transform on a pattern is given by $c_{\text{FFT}} m \log m$, where c_{FFT} is a constant dependent on the multiplication speed of the specific machine. Combining the required number of arithmetic operations for the Fourier transform in the first and last step yields a complexity of at most

$$(|\det \mathbf{J}| + 2) c_{\text{FFT}} m \log m.$$

Step 2 and 3 involve solving $d_{\mathbf{N}}$ and $d_{\mathbf{J}}$ linear systems of equations with up to d unknowns, respectively. The complexity of solving these linear systems is therefore $2c_1 d^4 = \mathcal{O}(d^4)$, where c_1 represents a constant the depends on the algorithm being used.

Finally, in step 4 we compute $|\det \mathbf{J}||\mathcal{G}(\mathbf{N}^{\mathrm{T}})| = m$ coefficients. Each coefficient is obtained by summing $|\det \mathbf{J}|$ values. This summation process combines the contributions from each of the $|\det \mathbf{J}|$ values to yield the final coefficient value. Considering the complexity of this step, it can be accomplished in $c_2 |\det \mathbf{J}| m = \mathcal{O}(m)$ compoutations.

Overall, the complexity of the algorithm of the fast wavelet transform is expressed as

$$(|\det \mathbf{J}| + 2) c_{\text{FFT}} m \log m + 2c_1 d^4 + c_2 |\det \mathbf{J}| m + \mathcal{O}(m) = \mathcal{O}(m \log m),$$

where c_1 and c_2 are constants that rely on the specific implementation. Notably, they are independent of m, $|\det \mathbf{J}|$, d, and n.

In the case where the input data already is in Fourier domain and the output is to be in Fourier domain, the first and last step of the algorithm is omitted. This again reduces the complexity of the wavelet transform to be carried out in $\mathcal{O}(m)$ calculation steps. To require the input and output to be in Fourier domain is advantageous when performing a multiresolution analysis on the Fourier domain, as this process also only requires repetition of step 2-4 [3, Section 3.3].

CHAPTER 5

Numerics

5.1 Interpolation

For a translation invariant space $V_{\mathbf{M}}^{\varphi}$, an interpolation problem arises when we aim to find a unique function $\gamma \in V_{\mathbf{M}}^{\varphi}$, satisfying the condition $f(2\pi\mathbf{y}) = \gamma(2\pi\mathbf{y})$ for all $\mathbf{y} \in \mathcal{P}(\mathbf{M})$. The function f must take function values at minimum for the elements on the pattern $\mathcal{P}(\mathbf{M})$, i.e., $f(2\pi\mathbf{y})$ must exist for all $\mathbf{y} \in \mathcal{P}(\mathbf{M})$. Determining the function γ is equivalent to finding the coefficients $(a_{\mathbf{y}})_{\mathbf{y}\in\mathcal{P}(\mathbf{M})}$, describing $\gamma \in V_{\mathbf{M}}^{\varphi}$, by solving a system of linear equations. Using the fundamental interpolant defined in [3, Definition 2.1] as

$$\mathrm{I}_{\mathbf{M}}(2\pi\mathbf{y}) = \begin{cases} 1, & \mathbf{y} = \mathbf{0}, \\ 0, & \mathbf{y} \in \mathcal{P}(\mathbf{M}) \setminus \{\mathbf{0}\}, \end{cases}$$

we can project the function f onto the space $V_{\mathbf{M}}^{\varphi}$. The projection yields a system of equations we can solve for the coefficients $(a_{\mathbf{y}})_{\mathbf{y}\in\mathcal{P}(\mathbf{M})}$.

We first look at when the fundamental interpolant $\mathrm{I}_{\mathbf{M}} \in V_{\mathbf{M}}^{\varphi}$ exists and is unique.

Lemma 5.1 ([3, Lemma 2.2])**.** Let $\mathbf{M} \in \mathbb{Z}^{d\times d}$ be a regular matrix, and $\varphi \in L^2(\mathbb{T}^d)$. Then the fundamental interpolant $\mathrm{I}_{\mathbf{M}} \in V_{\mathbf{M}}^{\varphi}$ exists and is unique if and only if

$$\sum_{\mathbf{z}\in\mathbb{Z}^d} c_{\mathbf{h}+\mathbf{M}^{\mathrm{T}}\mathbf{z}}(\varphi) \neq 0, \quad \text{for all } \mathbf{h} \in \mathcal{G}(\mathbf{M}^{\mathrm{T}}).$$

Proof. First, assume that the fundamental interpolant $\mathrm{I}_{\mathbf{M}} \in V_{\mathbf{M}}^{\varphi}$ exists. By Theorem 4.5 the functions $\mathrm{I}_{\mathbf{M}}$ and φ are related by

$$c_{\mathbf{h}+\mathbf{M}^{\mathrm{T}}\mathbf{z}}(\mathrm{I}_{\mathbf{M}}) = \hat{a}_{\mathbf{h}} c_{\mathbf{h}+\mathbf{M}^{\mathrm{T}}\mathbf{z}}(\varphi), \quad \mathbf{h} \in \mathcal{G}(\mathbf{M}^{\mathrm{T}}),\ \mathbf{z} \in \mathbb{Z}^d.$$

Further it holds that

$$\sum_{\mathbf{z}\in\mathbb{Z}^d} c_{\mathbf{h}+\mathbf{M}^{\mathrm{T}}\mathbf{z}}(\mathrm{I}_{\mathbf{M}}) = \hat{a}_{\mathbf{h}} \sum_{\mathbf{z}\in\mathbb{Z}^d} c_{\mathbf{h}+\mathbf{M}^{\mathrm{T}}\mathbf{z}}(\varphi).$$

Applying the discrete Fourier transform in (3.13) and the Aliasing formula stated in (3.15) to the definition of $\mathrm{I}_{\mathbf{M}}$ yields

$$\sum_{\mathbf{z}\in\mathbb{Z}^d} c_{\mathbf{h}+\mathbf{M}^{\mathrm{T}}\mathbf{z}}(\mathrm{I}_{\mathbf{M}}) = \frac{1}{m}. \tag{5.1}$$

Combining the last two equations we arrive at the assertion of the lemma.

Conversely, assume that $\sum_{\mathbf{z}\in\mathbb{Z}^d} c_{\mathbf{h}+\mathbf{M}^{\mathrm{T}}\mathbf{z}}(\varphi) \neq 0$, for all $\mathbf{h} \in \mathcal{G}(\mathbf{M}^{\mathrm{T}})$. Further, let the Fourier coefficients of a function g be given as

$$c_{\mathbf{k}}(g) = \frac{c_{\mathbf{k}}(\varphi)}{m \sum\limits_{\mathbf{z}\in\mathbb{Z}^d} c_{\mathbf{h}+\mathbf{M}^{\mathrm{T}}\mathbf{z}}(\varphi)}, \qquad \text{for all } \mathbf{k} \in \mathbb{Z}^d. \tag{5.2}$$

Then $g \in V_{\mathbf{M}}^{\varphi}$ if

$$\hat{a}_{\mathbf{h}} = \frac{1}{m \sum\limits_{\mathbf{z}\in\mathbb{Z}^d} c_{\mathbf{h}+\mathbf{M}^{\mathrm{T}}\mathbf{z}}(\varphi)}, \qquad \text{for all } \mathbf{h} \in \mathcal{G}(\mathbf{M}^{\mathrm{T}}). \tag{5.3}$$

Moreover, g is a fundamental interpolant $\mathrm{I}_{\mathbf{M}}$ to the pattern $\mathcal{P}(\mathbf{M})$ since it satisfies Equation (5.1), which (5.2) also states to be unique. □

Proposition 5.2. There exists a fundamental interpolant $\mathrm{I}_{\mathbf{M}} \in V_{\mathbf{M}}^{D_{\mathbf{M}}^{\perp}}$.

Proof. Using a similar approach as in the proof of Proposition 4.10, we have that for all $\mathbf{h} \in \mathcal{G}(\mathbf{M}^{\mathrm{T}})$

$$\begin{aligned}\sum_{\mathbf{z}\in\mathbb{Z}^d} c_{\mathbf{h}+\mathbf{M}^{\mathrm{T}}\mathbf{z}}(D_{\mathbf{M}}^{\perp}) &= \sum_{\mathbf{z}\in\mathbb{Z}^d} \frac{1}{\sqrt{m}} 2^{-r(\mathbf{h}+\mathbf{M}^{\mathrm{T}}\mathbf{z})/2} = \sum_{\mathbf{z}\in\mathbb{Z}^d} \frac{1}{\sqrt{m}} 2^{-r(\mathbf{h})/2} \\ &= 2^{r(\mathbf{h})/2} c_{\mathbf{h}}(D_{\mathbf{M}}^{\perp}) = \frac{1}{\sqrt{m}} \neq 0.\end{aligned}$$

By Theorem 5.1 we conclude that there exists a fundamental interpolant $\mathrm{I}_{\mathbf{M}} \in V_{\mathbf{M}}^{D_{\mathbf{M}}^{\perp}}$. □

When given a function f sampled on at least the pattern $\mathcal{P}(\mathbf{M})$, Theorem 5.1 provides the change of basis of f from using the translates of $\mathrm{I}_{\mathbf{M}}$ as a basis, to the translates of $D_{\mathbf{M}}^{\perp}$ as a basis. This is expressed as

$$g(\mathbf{x}) = \sum_{\mathbf{y}\in\mathcal{P}(\mathbf{M})} a_{\mathbf{y}} T(\mathbf{y}) \mathrm{I}_{\mathbf{M}}(\mathbf{x}) = \sum_{\mathbf{y}\in\mathcal{P}(\mathbf{M})} \tilde{a}_{\mathbf{y}} T(\mathbf{y}) D_{\mathbf{M}}^{\perp}(\mathbf{x}) \approx f(\mathbf{x}),$$

where $(\tilde{a}_{\mathbf{y}})_{\mathbf{y}\in\mathcal{P}(\mathbf{M})}$ contains the coefficients of f in terms of the translates of $D_{\mathbf{M}}^{\perp}$. These coefficients are calculated by Equation (5.3).

Under the assumption that the fundamental interpolant $\mathrm{I}_{\mathbf{M}} \in V_{\mathbf{M}}^{\varphi}$ exists, we can define the interpolation operator $L_{\mathbf{M}}$ as

$$L_{\mathbf{M}} f \coloneqq \sum_{\mathbf{y}\in\mathcal{P}(\mathbf{M})} f(2\pi\mathbf{y}) T(\mathbf{y}) \mathrm{I}_{\mathbf{M}},$$

which holds for any $f \in L^2(\mathbb{T}^d)$ when $f(2\pi\mathbf{y})$ exists for all $\mathbf{y} \in \mathcal{P}(\mathbf{M})$. Further, the Fourier coefficients of the $L_{\mathbf{M}} f$ are given by

$$c_{\mathbf{k}}(L_{\mathbf{M}} f) = m\Big(\sum_{\mathbf{z}\in\mathbb{Z}^d} c_{\mathbf{k}+\mathbf{M}^{\mathrm{T}}\mathbf{z}}(f)\Big) c_{\mathbf{k}}(\mathrm{I}_{\mathbf{M}}), \tag{5.4}$$

when using the same approach as in the previous lemma. For more on the interpolation and the interpolation error, see [3, Section 2.3].

5.2 Implementation

We present the implementation of functions needed to execute the algorithm described in Section 4.4 using the programming language `Julia, v1.8.1`, [6]. To ensure the efficiency of the code, we exploit existing packages. For the computation of the Smith normal form, (2.7), we employ the `IntegerSmithNormalForm.jl`[1] package, `v0.1.0`, while for the fast Fourier transform, we use FFTW.jl, `v1.6.0`, [13], and for offset arrays, we rely on OffsetArrays.jl, `v1.12.9`, [7]. Using these packages reduces the risk of errors and inefficiencies arising from the complexity of the underlying algorithms.

The code developed for this thesis built upon the foundation established during the earlier work of the specialization project [21]. Functions like `modM(x, M)`, `pattern(M)` and `generating_group(M)` were initially implemented during the specialization project and subsequently expanded upon in this thesis. This includes introducing functions such as `coefficients_in_space!(M, ahat, ck_phi, ck_xi)`, `generate_wavelet(N, J, ahat, ck_phi)` and `wavelet_decomposition(M, J, ahat, ck_f, ck_phi)` along with auxiliary functions and plotting functions, to enhance the functionality of the code. These functions are to be described in this section.

Prior to implementing the algorithm for the fast wavelet transform, we define some auxiliary functions and compute the Fourier coefficients of the function $D_{\mathbf{M}}^{\perp}$ from (4.4), whose translates span the translation invariant space $V_{\mathbf{M}}^{D_{\mathbf{M}}^{\perp}}$ from (4.1).

The function `modM(x, M)` computes an element of the generating group $\mathcal{G}(\mathbf{M})$ of $\mathbf{M}$. Given an input vector $\mathbf{x}$ belonging to the lattice $\Lambda(\mathbf{M})$ such that $\mathbf{x} = \mathbf{M}^{-1}\mathbf{k}$ for some $\mathbf{k} \in \mathbb{Z}^d$, we determine $\mathbf{y} = \mathbf{x} \mod \mathbf{1}$, which is in the pattern $\mathcal{P}(\mathbf{M})$ of $\mathbf{M}$, by definition. Finally, we compute $\mathbf{h} = \mathbf{M}\mathbf{y}$, an element of the generating group $\mathcal{G}(\mathbf{M})$ of $\mathbf{M}$. To ensure compatibility with the code implementation, we convert the components of $\mathbf{h}$ to integer values. This function, denoted by `modM(x, M)`, corresponds to the the modulo operation $+|_{\mathcal{G}(\mathbf{M})}$ described in (3.1).

The function `pattern(M)` computes each element in the pattern $\mathcal{P}(\mathbf{M})$ of $\mathbf{M}$, as described in (3.9). It returns a matrix containing all the elements in the pattern $\mathcal{P}(\mathbf{M})$ of $\mathbf{M}$, sorted in lexicographical order, that is, the returned matrix is of size $\varepsilon_1, \cdots, \varepsilon_d$ and each element of size d. Further, `generating_group(M)` elementwise computes `M * y for y in pattern(M)` and returns a matrix containing all the elements in the generating group $\mathcal{G}(\mathbf{M})$ of $\mathbf{M}$, sorted in lexicographical order, that is, the returned matrix is of the same form as `pattern(M)`.

We define a function `ck_Dirichlet_kernel(k, M)`, computing the values as specified in Equation (4.5). Additionally, we implement a function `ck_Dirichlet_kernel(M)`, which takes a regular integer matrix `M` as input. This function constructs a rectangular matrix `P`, whose size is determined by

$$\max \left\lceil \left| \mathbf{M}^{\mathrm{T}} \left[\pm \frac{1}{2}, \pm \frac{1}{2} \right] \mathbf{e}_j \right| \right\rceil + 1 \quad \text{for } j = \{1, 2\},$$

where $\lceil x \rceil$ denotes the ceiling function and 1 is added as a precaution. Moreover, we introduce the OffsetArray `OP`, which is derived from `P`. The OffsetArray changes the indexing of the matrix `P` such that the center of the matrix now has the index

[1] Code available at: https://github.com/dmerkert/IntegerSmithNormalForm.jl.git

`[0,0]`. This makes the indices of `ck_Dirichlet_kernel(M)` correspond to the notation in (4.5).

Next, we write a function called `coefficients_in_space!(M, ahat, ck_phi, ck_xi)` that computes the coefficients of `ck_xi` with respect to `ck_phi`, the Fourier coefficient of the function spanning $V_{\mathbf{M}}^{\varphi}$. The coefficients are computed in Fourier domain, using the formula from Theorem 4.5. The input parameter `ahat` is included to fix the size of the output matrix `a_hat`. We rearrange the formula from the theorem into the following

$$\hat{a}_{\mathbf{k} \bmod \mathbf{M}^{\mathrm{T}}} = \hat{a}_{\mathbf{h}} = \frac{c_{\mathbf{k}}(\xi)}{c_{\mathbf{k}}(\varphi)}, \quad \text{for } \mathbf{h} \in \mathcal{G}(\mathbf{M}^{\mathrm{T}}),$$

where $\mathbf{k} \bmod \mathbf{M}^{\mathrm{T}}$ is computed using the `modM(k,M')` function, where `M'` being the transpose of the matrix `M` in Julia. The coefficients are computed by iterating through each index `k` of the matrix `ck_Dirichlet_kernel(M)`. For each index, we determine the corresponding vector $\mathbf{h} = \mathbf{k} \bmod \mathbf{M}^{\mathrm{T}}$ and decompose $\mathbf{h}$ into its basis vector using the `decompose_into_basis(h, M')` function. This decomposition yields the coefficients μ_j described in (3.11). Finally, the Fourier coefficients $\hat{a}_{\mathbf{k} \bmod \mathbf{M}^{\mathrm{T}}}$ of ξ with respect to φ are computed and returned using the aforementioned formula.

In Remark 4.14 the matrices in (3.20b) were discussed, highlighting that they do not generate proper Dirichlet kernels $D_{\mathbf{N}}^{\perp}$ and thus are not contained in $V_{\mathbf{M}}^{D_{\mathbf{M}}^{\perp}}$. The behavior of `coefficients_in_space!(M, ahat, ck_phi, ck_xi)` can be modified in two ways if the chosen $\xi \notin V_{\mathbf{M}}^{\varphi}$. It can either be set to generate an adapted version $\tilde{\xi}$ of ξ, such that $\tilde{\xi} \in V_{\mathbf{M}}^{\varphi}$ holds true, or it can be set to raise an error.

It is worth noting that the implemented functions mentioned thus far can me applied to any function φ and ξ suitable for decomposition, as long as $\xi \in V_{\mathbf{M}}^{\varphi}$, or alternatively $\tilde{\xi} \in V_{\mathbf{M}}^{\varphi}$. However, when it comes to generating the wavelet, it depends on the specific choice of φ and ξ. Therefore, the implemented function `generate_wavelet(N, J, ahat, ck_phi)` is only applicable in the specific case where $\varphi = D_{\mathbf{M}}^{\perp}$ and $\xi = D_{\mathbf{N}}^{\perp}$ or $\tilde{D}_{\mathbf{N}}^{\perp}$, in accordance with Proposition 4.18.

Using the $\sigma_{\mathbf{h}}$ from Proposition 4.18 to generate the wavelet $\eta = \psi$, we compute the coefficients of ψ in Fourier domain in the function denoted as `generate_wavelet(N, J, ahat, ck_phi)`. Similar to the previous function, we iterate through the indices of the matrix `ck_Dirichlet_kernel(M)` and employ Equation (4.10) to compute the coefficients of ψ with respect to the basis for $V_{\mathbf{M}}^{D_{\mathbf{M}}^{\perp}}$ in Fourier domain.

To reconstruct the function f from its Fourier coefficients with respect to the translates of φ, we write a function denoted as `fourier_coeff_xi(M, ahat, ck_phi)`, where `ahat` is the coefficients of f with respect to the translates of `ck_phi`. The function performs the computations

$$c_{\mathbf{k}}(f) = \hat{a}_{\mathbf{k} \bmod \mathbf{M}^{\mathrm{T}}} c_{\mathbf{k}}(\varphi),$$

for all indices `k` of the matrix `ck_phi`, by Theorem 4.5. The index of `ahat` is computed by utilizing the functions `h = modM(k, M')` and `decompose_into_basis(h, M')`.

To implement the interpolation scheme described in Section 5.1, we sample a given function f on the pattern ensuring the existence of the function values $f(2\pi\mathbf{y})$ for $\mathbf{y} \in \mathcal{P}(\mathbf{M})$. We denote this sampling function `sample_on_pattern(M, f)`. Further, we perform the Fourier transform on these coefficients, naming the coefficients `ahat_f`. Subsequently, we determine $c_{\mathbf{k}}(f)$ using Equation (5.3), which yields the coefficients $\hat{\mathbf{a}}$ of f in the space $V_{\mathbf{M}}^{\varphi}$, in Fourier domain. Lastly, we multiply by m, according to (5.4) and get the correct scale. We refer to the coefficients with respect to the translates of φ as `ahat_f_DM`.

We now have the functions that are necessary to perform the decomposition of a function $f \in V_{\mathbf{M}}^{\varphi}$ into $g_1 \in V_{\mathbf{N}}^{\xi}$ and $g_2 \in V_{\mathbf{N}}^{\psi}$, when $\varphi = D_{\mathbf{M}}^{\perp}$ and $\xi = D_{\mathbf{N}}^{\perp}$. The function carrying out the fast wavelet transform of f is named `wavelet_decomposition(M, J, ahat, ck_xi, ck_phi)`. For a given function f, the function `coefficients_in_space!(M, ahat, ck_phi, ck_xi)` is applied to `ahat_f` with respect to the basis of $V_{\mathbf{M}}^{D_{\mathbf{M}}^{\perp}}$. We denote these coefficients as `b1hat`. The coefficients `b2hat` are determined by applying the function `generate_wavelet(N, J, b1hat, ck_phi)` with respect to the translates of ψ. These computations correspond to the first step of the algorithm. The subsequent three steps use the function `decompose_into_basis` to determine the basis vectors of $\mathcal{G}(\mathbf{N}^{\mathrm{T}})$ and $\mathcal{G}(\mathbf{M}^{\mathrm{T}})$, and also to determine the $\boldsymbol{\lambda}$ and $\boldsymbol{\lambda}_{\mathbf{g}}$ for $\mathbf{g} \in \mathcal{G}(\mathbf{J}^{\mathrm{T}})\backslash\{\mathbf{0}\}$. Lastly, we determine the $\hat{\mathbf{d}}_1$ and $\hat{\mathbf{d}}_2$ by using `b1hat` and `b2hat`, respectively, as described in step 4. These coefficients are denoted as `d1hat` and `d2hat`, respectively. The function `wavelet_decomposition(M, J, ahat, ck_xi, ck_phi)` returns the four coefficients `b1hat`, `b2hat`, `d1hat` and `d2hat`, respectively, in Fourier domain, such that `ck_xi = b1hat * ck_phi`, `ck_psi = b2hat * ck_phi`, `ck_g1 = d1hat * ck_xi` and `ck_g2 = d2hat * ck_psi`. The coefficients are returned in Fourier domain, enabling their direct utilization within a multi-level decomposition scheme, as elaborated in Section 4.4. With this output, we can construct the functions $g_1 \in V_{\mathbf{N}}^{D_{\mathbf{N}}^{\perp}}$ and $g_2 \in V_{\mathbf{N}}^{\psi}$.

Prior to performing step 5, i.e., the inverse Fourier transform, we zero pad the Fourier coefficients of functions g_1 and g_2. This process effectively increases the number of sampling points without altering the Fourier coefficients. The purpose of this technique is to achieve a higher resolution plot, providing more detailed visual representation. The implemented function `plot_f(ck_f, image_size)`, where the matrix `ck_f` contains the Fourier coefficients of a function f and `image_size` is the size to which the input matrix is padded to, incorporates the zero padding and the inverse Fourier transform.

In order to perform a multiresolution analysis, one update `ahat_f` to `b1hat`, the matrix `M` to `N` and `ck_Dirichlet_kernel(M)` to `ck_Dirichlet_kernel(N)` in the function `wavelet_decomposition`. An example of the implementation of both a first-level wavelet transform and a second-level wavelet transform is provided in Appendix A.

CHAPTER 6

Examples

Using the notation from Theorem 4.15 we set $\varphi = D^{\perp}_{\mathbf{M}}$ known by (4.4), $\xi = D^{\perp}_{\mathbf{N}}$ or $\tilde{D}^{\perp}_{\mathbf{N}}$ as discussed in Remark 4.14, and $\eta = \psi$ as stated in Proposition 4.18. For simplicity, we rename the spaces

$$V_{\mathbf{M}}^{D^{\perp}_{\mathbf{M}}} = V_{\mathbf{M}}, \qquad V_{\mathbf{N}_j}^{D^{\perp}_{\mathbf{N}_j}} = V^i_{\mathbf{N}_j}, \quad \text{and} \quad V^{\psi}_{\mathbf{N}_j} = W^i_{\mathbf{N}_j},$$

where j is the index of the corresponding matrix $\mathbf{J}$ with $\mathbf{M} = \mathbf{J}_j\mathbf{N}_j$, and i represents the level of decomposition, being 1 if not specified.

Further, we investigate different functions to exemplify how the fast wavelet transform from Section 4.4 is applied. First we look at how the shift invariant space $V_{\mathbf{M}}$ is affected by the matrix $\mathbf{M}$, and then how the decomposition is affected by the matrix $\mathbf{J}_j$ for three functions with various discontinuities by studying $g_2 \in W_{\mathbf{N}_j}$. Continuing, we perform a multi-level decomposition to narrow down the direction of the decomposition, and use this method to detect the direction of a rotated step function. For all the examples, we use the interpolation scheme described in Section 5.1 to interpolate the given function f on the pattern $\mathcal{P}(\mathbf{M})$.

To illustrate why we use $\mathbf{M} = 512\mathbf{I}$ to generate $D^{\perp}_{\mathbf{M}}$ whose translates span $V_{\mathbf{M}}$, we use matrices with a smaller determinant to see how the matrices affect the basis of the shift invariant space $V_{\mathbf{M}}$. We consider the matrices

$$\mathbf{A}_1 = \begin{bmatrix} 16 & 0 \\ 0 & 16 \end{bmatrix}, \quad \mathbf{A}_2 = \begin{bmatrix} 8 & 0 \\ 0 & 32 \end{bmatrix}, \quad \mathbf{A}_3 = \begin{bmatrix} 16 & 4 \\ 0 & 16 \end{bmatrix}, \quad \mathbf{A}_5 = \begin{bmatrix} 8 & 0 \\ 0 & 8 \end{bmatrix}.$$

Using these matrices with smaller determinants better reveal the variation of $D^{\perp}_{\mathbf{M}}$ when visualized, but the same principles hold for their multiples.

The functions $D^{\perp}_{\mathbf{A}_1}$ and $D^{\perp}_{\mathbf{A}_5}$ are sampled on uniform grids, leading to equal levels of details in both directions for each function. Since $D^{\perp}_{\mathbf{A}_1}$ is sampled on more points, it contains more detail than $D^{\perp}_{\mathbf{A}_5}$. Hence, the set of translates of $D^{\perp}_{\mathbf{A}_1}$ is a better basis to describe detailed functions compared to when using $D^{\perp}_{\mathbf{A}_5}$.

On the other hand, $\mathbf{A}_2$ makes $D^{\perp}_{\mathbf{A}_2}$ less detailed in y-direction, compared to $D^{\perp}_{\mathbf{A}_1}$. When studying $\mathbf{A}_2$, recall from Figure 3.1b that $\mathcal{G}(\mathbf{A}_2^{\mathrm{T}})$ has more samples in x-direction than y-direction. This makes $D^{\perp}_{\mathbf{A}_2}$ more detailed in x-direction than

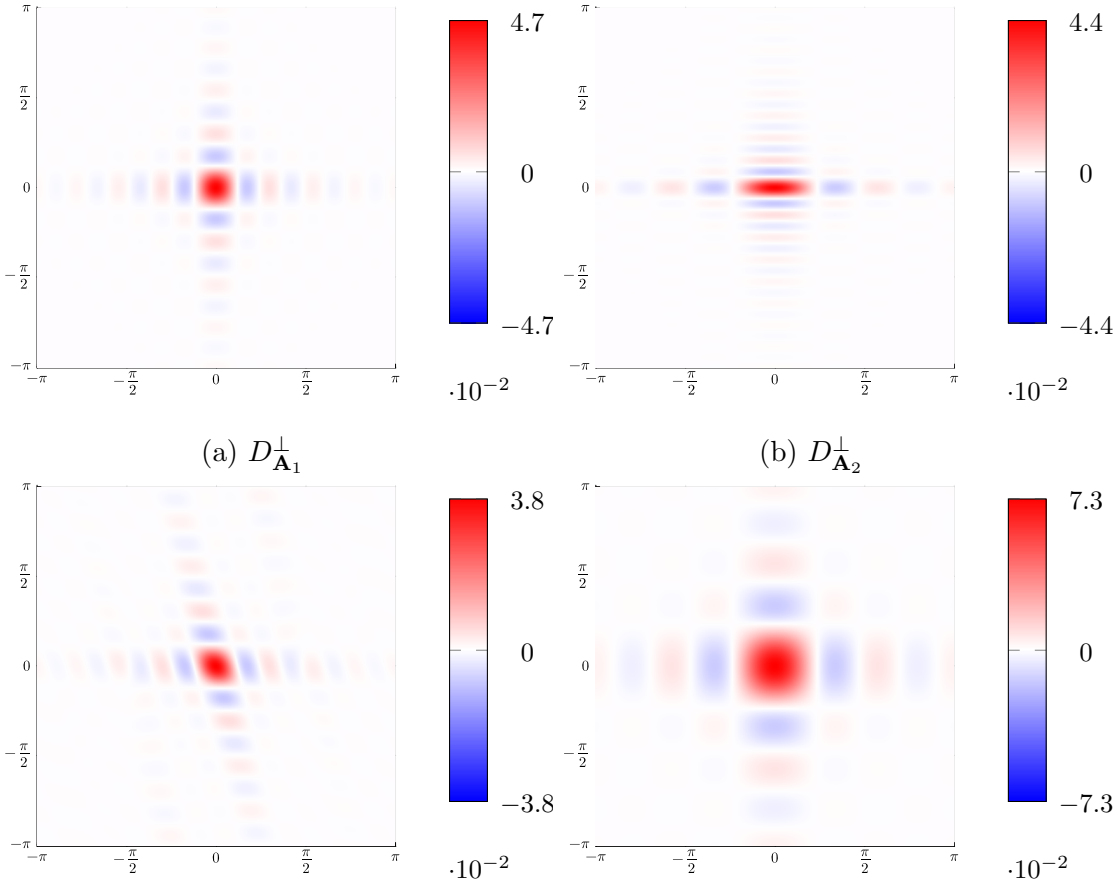

(a) $D^{\perp}_{\mathbf{A}_1}$ (b) $D^{\perp}_{\mathbf{A}_2}$

(c) $D^{\perp}_{\mathbf{A}_3}$ (d) $D^{\perp}_{\mathbf{A}_5}$

Figure 6.1: Visualization of the Dirichlet kernel $D^{\perp}_{\mathbf{A}_i}$ for $i = 1, 2, 3, 5$ showing the effect of the different choices of the matrices defining the kernel.

in y-direction. Lastly, $\mathbf{A}_3$ generates a sheared Dirichlet kernel $D^{\perp}_{\mathbf{A}_3}$. By choosing a matrix $\mathbf{M}$ being a multiple of the identity matrix $\mathbf{I}$, we get a Dirichlet kernel $D^{\perp}_{\mathbf{M}}$ which is not rotated and is equally detailed in both directions. Furthermore, $|\det \mathbf{M}| = m$ not only affects how much detail the space $V_{\mathbf{M}}$ is able to describe, but also the computational complexity of the fast wavelet transform, as discussed in the last part of Section 4.4. Therefore, the matrix $\mathbf{M}$ should be chosen such that it maintains a favorable trade-off between precision and computational cost. We choose the factor 512 such that $\mathbf{M} = 512\mathbf{I}$ and the translates of $D^{\perp}_{\mathbf{M}}$ provide sufficiently much possibility to describe detailed functions.

6.1 Functions With Discontinuities

The function

$$f_1(\mathbf{x}) = \begin{cases} 1 & \|\mathbf{x}\|_{\ell^2} \leq \frac{3\pi}{4}, \\ 0 & \text{else}, \end{cases} \quad \text{for } \mathbf{x} \in \mathbb{T}^d,$$

is a circled step function of radius $\frac{3\pi}{4}$ that is discontinuous in every direction. When representing the function as a Fourier series, and not using infinitely many terms, Gibbs's phenomenon will occur at the discontinuities, as discussed in Section 2.2.

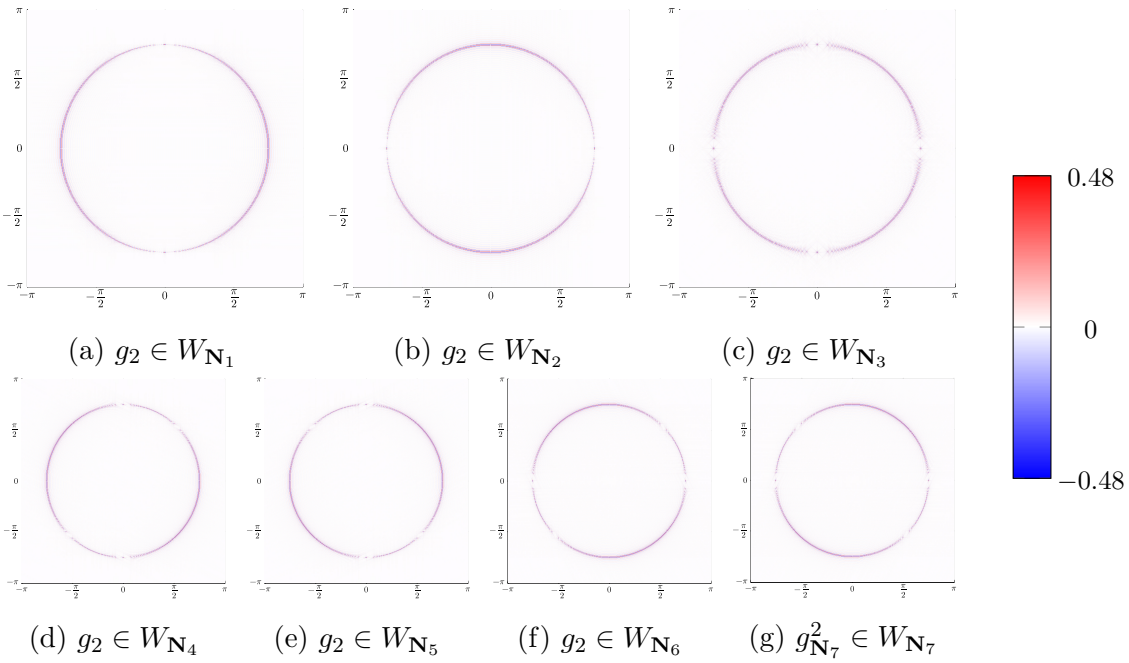

(a) $g_2 \in W_{\mathbf{N}_1}$ (b) $g_2 \in W_{\mathbf{N}_2}$ (c) $g_2 \in W_{\mathbf{N}_3}$

(d) $g_2 \in W_{\mathbf{N}_4}$ (e) $g_2 \in W_{\mathbf{N}_5}$ (f) $g_2 \in W_{\mathbf{N}_6}$ (g) $g_{\mathbf{N}_7}^2 \in W_{\mathbf{N}_7}$

Figure 6.2: Wavelets g_2 of $f_1(\mathbf{x})$ for all $\mathbf{J} \in \mathcal{J}$.

Further, the space $W_{\mathbf{N}}$ is spanned by a function representing high frequency, making the functions in $W_{\mathbf{N}}$ suitable for representing high-frequent functions. We decompose $f_1 \in V_{\mathbf{M}}$ into the functions $g_1 \in V_{\mathbf{N}_i}$ and $g_2 \in W_{\mathbf{N}_i}$ for the matrices $\mathbf{J}_i \in \mathcal{J}$ in Equation (3.20) for $\mathbf{M} = 512\mathbf{I} = \mathbf{J}_i\mathbf{N}_i$ using `wavelet_decomposition` described in Section 5.2, i.e., the fast wavelet transform described in Section 4.4. By doing so, the high frequent part of f_1 is represented by the wavelet g_2, makes us able to detect the location of the discontinuities of f_1 by studying the wavelet g_2. The wavelets are visualized in Figure 6.2 for the matrices $\mathbf{J} \in \mathcal{J}$. The scale of the wavelets is around 10^{-1}. For all of the matrices $\mathbf{J} \in \mathcal{J}$, the wavelet g_2 detects the discontinuities of f_1 around nearly the entire circle. Similarly as in Example 3.8, we see that the matrices $\mathbf{J}$ represent different directions, which becomes apparent by where there the wavelet g_2 is samples. Examining the wavelet of the decomposition using $\mathbf{J}_3$ in Figure 6.2c, to exemplify, we perceive that g_2 fluctuates closer to the axes. This is due to there being fewer samples present close to the axes, compared to those in closer proximity to the diagonal. A similar observation can be made in the context of the pattern $\mathcal{P}(\mathbf{M})$ and subpattern $\mathcal{P}(\mathbf{N})$, with $\mathbf{J}_3$ depicted in Figure 3.3c. The same behavior is also evident for the wavelets of the decomposition using $\mathbf{J}$ from Equation 3.20b at the bottom row of Figure 6.2.

Analyzing a function with a discontinuous first derivative, we define the function

$$f_2(\mathbf{x}) = \begin{cases} \cos\left(\frac{2}{3}\mathbf{x}\right) & \|\mathbf{x}\|_{\ell^2} \leq \frac{3\pi}{4}, \\ 0 & \text{else}, \end{cases} \quad \text{for } \mathbf{x} \in \mathbb{T}^d.$$

As the first derivative of f_2 is discontinuous, there is a sharp transition at $\|\mathbf{x}\|_{\ell^2} = \frac{3\pi}{4}$, illustrated in Figure 6.3a together with f_2 itself. Similarly as for the discontinuity of f_1, we therefore expect the wavelet to appear around $\mathbf{x} = \frac{3\pi}{4}$, by Gibbs' phenomenon. We decompose f_2 and visualize the wavelets in Figure 6.4 for all $\mathbf{J} \in \mathcal{J}$.

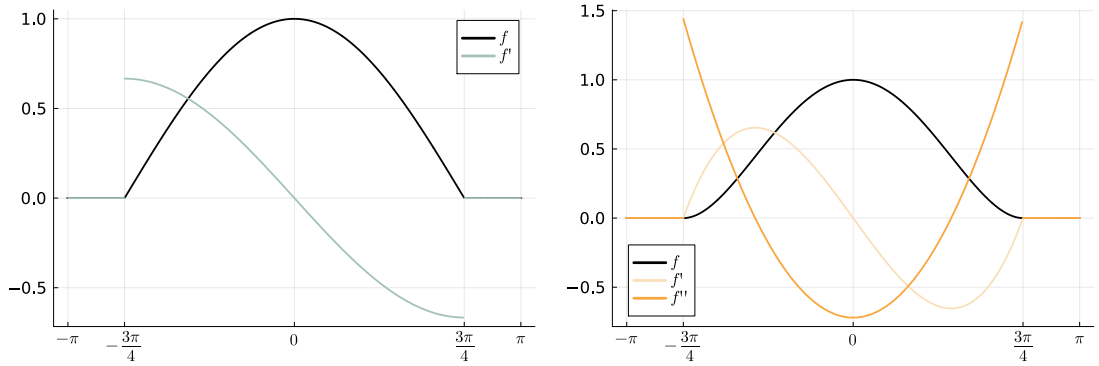

(a) f_2 and its derivative.

(b) f_3 and its derivatives.

Figure 6.3: Visualization of the function f_2 and its discontinuous first derivative, and f_3 and its discontinuous second derivative, both for $x \in \mathbb{T}^1$.

Note that the scale of f_2's wavelets is 10^{-3}, while the wavelets of f_1 had a scale of 10^{-1}. This difference in amplitude is expected as f_1 has a severe jump compared to the transition of f_2, which the partial Fourier sum more accurately approximates.

We investigate the function

$$f_3(\mathbf{x}) = \begin{cases} \left(\frac{4}{3\pi}\mathbf{x} - 1\right)^2 \left(\frac{4}{3\pi}\mathbf{x} + 1\right)^2 & \|\mathbf{x}\|_{\ell^2} \leq \frac{3\pi}{4}, \\ 0 & \text{else,} \end{cases} \quad \text{for } \mathbf{x} \in \mathbb{T}^d.$$

The function's derivatives are visualized in Figure 6.3b, where we see that the second derivative is discontinuous at $\frac{3\pi}{4}$. Again, $\|\mathbf{x}\|_{\ell^2} = \frac{3\pi}{4}$ is where we expect the wavelets to become evident. We decompose f_3 for $\mathbf{J} \in \mathcal{J}$ and present g_2 in Figure 6.5. The scale of these wavelets of f_3 is 10^{-6}, which is even smaller than for f_2. This is because the transition of f_2 is sharper than that of f_3.

6.2 Multiresolusion Analysis

In accordance with Section 4.4, we can continue do decompose the space $V_{\mathbf{N}_1}$, representing the low frequent part of $V_{\mathbf{M}}$. This procedure is exemplified by decomposing f_3, referred to as f henceforth, in five levels using the matrix $\mathbf{M} = 1024\mathbf{I} = \mathbf{J}_1\mathbf{J}_5\mathbf{J}_5\mathbf{J}_1\mathbf{J}_2\mathbf{N}$, where $\mathbf{N}$ is such that the equality holds. The first decomposition involves $\mathbf{M}$ and $\mathbf{N}_1 = \mathbf{J}_5\mathbf{J}_5\mathbf{J}_1\mathbf{J}_2\mathbf{N}$ and their orthonormal Dirichlet kernels, in the second decomposition we use $\mathbf{N}_1$ and $\mathbf{N}_2 = \mathbf{J}_5\mathbf{J}_1\mathbf{J}_2\mathbf{N}$, and so on. A representation of the five-level decomposition of the spaces looks like this

$$\begin{array}{ccccccccccc} V_{\mathbf{M}} & \longrightarrow & V^1_{\mathbf{N}_1} & \longrightarrow & V^2_{\mathbf{N}_2} & \longrightarrow & V^3_{\mathbf{N}_3} & \longrightarrow & V^4_{\mathbf{N}_4} & \longrightarrow & V^5_{\mathbf{N}} \\ & \searrow & & \searrow & & \searrow & & \searrow & & \searrow & \\ & & W^1_{\mathbf{N}_1} & & W^2_{\mathbf{N}_2} & & W^3_{\mathbf{N}_3} & & W^4_{\mathbf{N}_4} & & W^5_{\mathbf{N}} \end{array}$$

By employing the above-mentioned decompositions of the spaces, we are able to decompose the function f as follows

$$\begin{array}{ccccccccccc} f & \longrightarrow & g^1_1 & \longrightarrow & g^2_1 & \longrightarrow & g^3_1 & \longrightarrow & g^4_1 & \longrightarrow & g^5_1 \\ & \searrow & & \searrow & & \searrow & & \searrow & & \searrow & \\ & & g^1_2 & & g^2_2 & & g^3_2 & & g^4_2 & & g^5_2 \end{array}$$

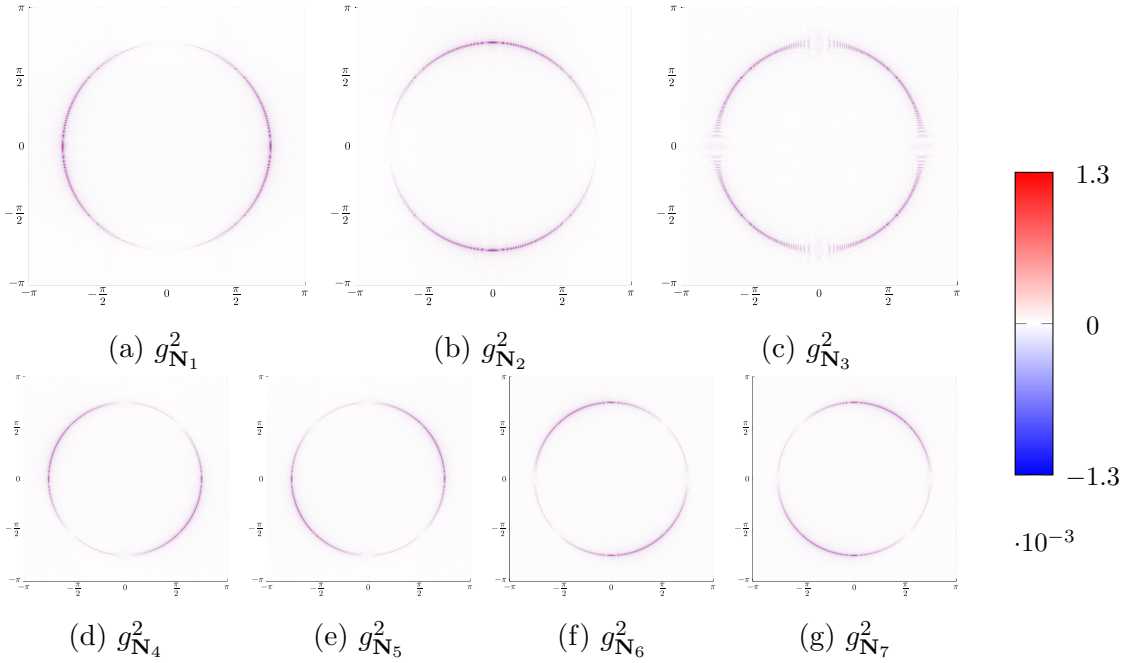

(a) $g^2_{\mathbf{N}_1}$ (b) $g^2_{\mathbf{N}_2}$ (c) $g^2_{\mathbf{N}_3}$

(d) $g^2_{\mathbf{N}_4}$ (e) $g^2_{\mathbf{N}_5}$ (f) $g^2_{\mathbf{N}_6}$ (g) $g^2_{\mathbf{N}_7}$

Figure 6.4: Wavelets g_2 of $f_2(\mathbf{x})$ for all $\mathbf{J} \in \mathcal{J}$, where red represents positive values and blue represents negative values.

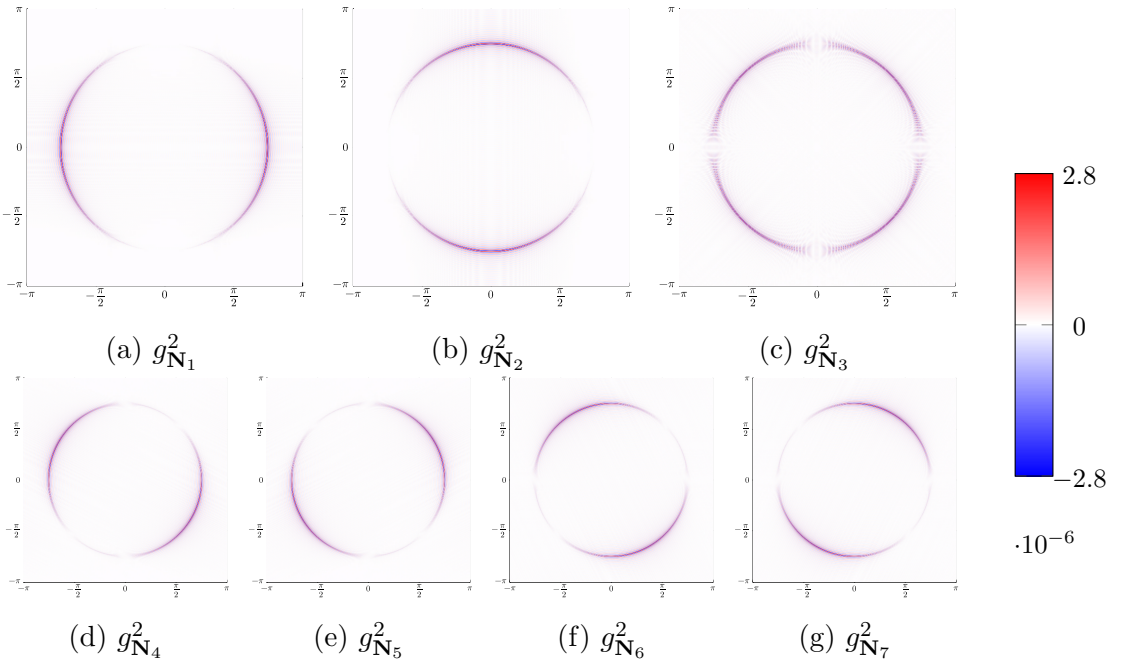

(a) $g^2_{\mathbf{N}_1}$ (b) $g^2_{\mathbf{N}_2}$ (c) $g^2_{\mathbf{N}_3}$

(d) $g^2_{\mathbf{N}_4}$ (e) $g^2_{\mathbf{N}_5}$ (f) $g^2_{\mathbf{N}_6}$ (g) $g^2_{\mathbf{N}_7}$

Figure 6.5: Wavelets g_2 of $f_3(\mathbf{x})$ for all $\mathbf{J} \in \mathcal{J}$, where red represents positive values and blue represents negative values.

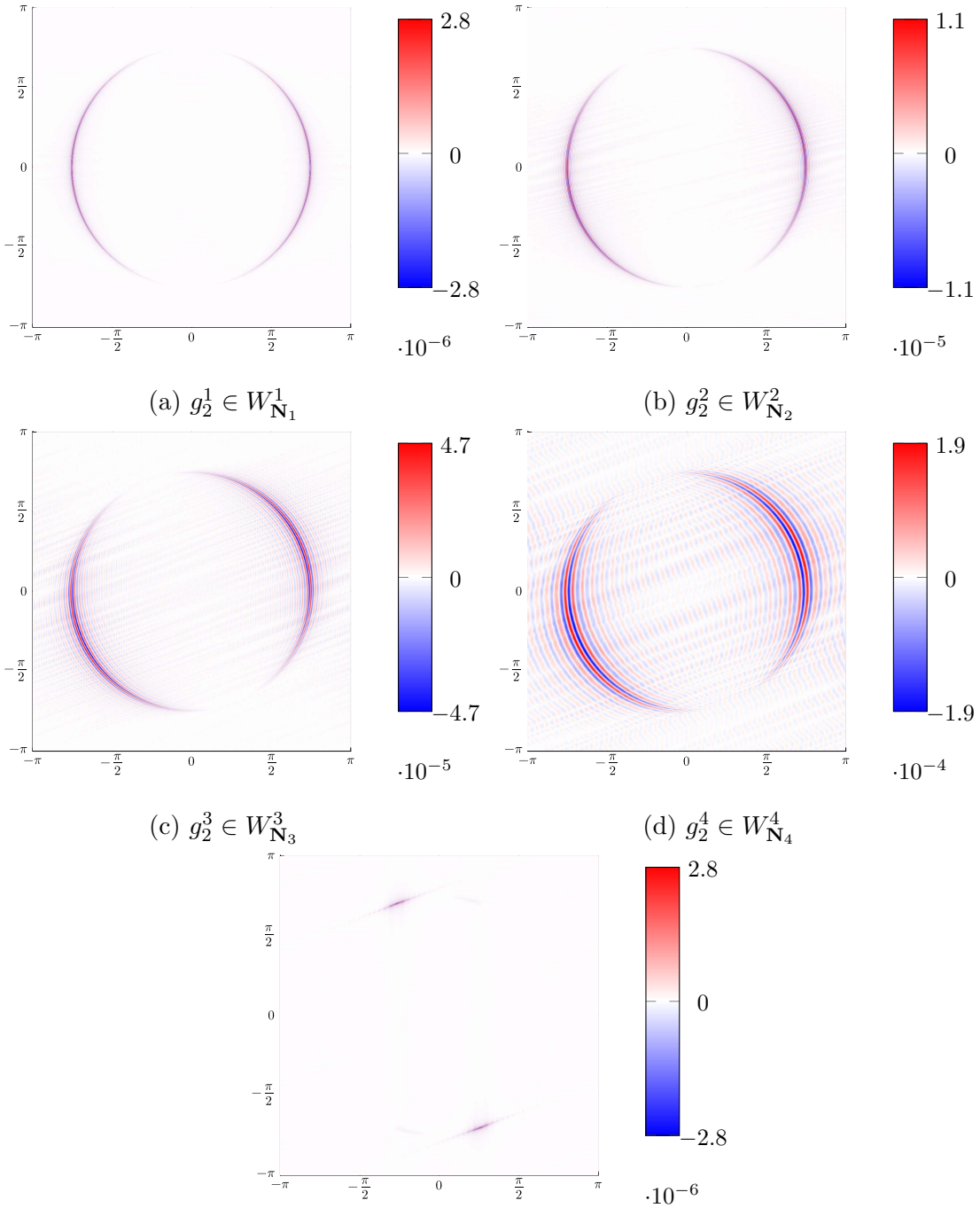

(a) $g_2^1 \in W_{\mathbf{N}_1}^1$

(b) $g_2^2 \in W_{\mathbf{N}_2}^2$

(c) $g_2^3 \in W_{\mathbf{N}_3}^3$

(d) $g_2^4 \in W_{\mathbf{N}_4}^4$

(e) $g_2^5 \in W_{\mathbf{N}}^5$

Figure 6.6: The wavelets g_2 for each 5 level of decomposition of f_3, when $\mathbf{M} = 1024\mathbf{I} = \mathbf{J}_1\mathbf{J}_5\mathbf{J}_5\mathbf{J}_1\mathbf{J}_2\mathbf{N}$.

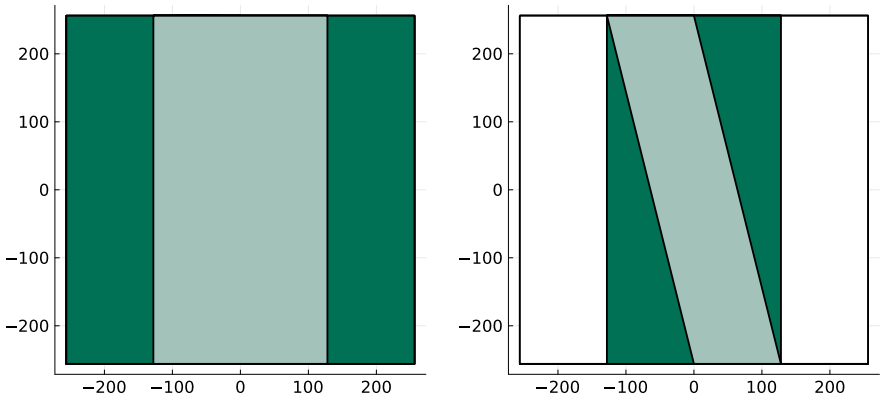

(a) First level decomposition.

(b) Second level decomposition.

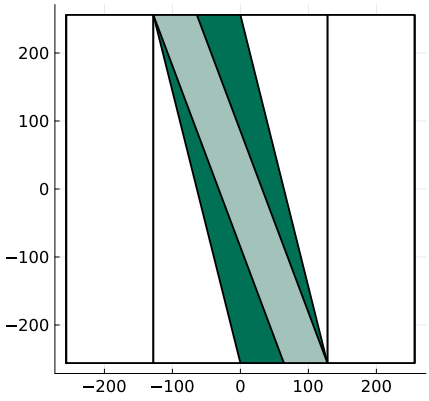

(c) Third level decomposition.

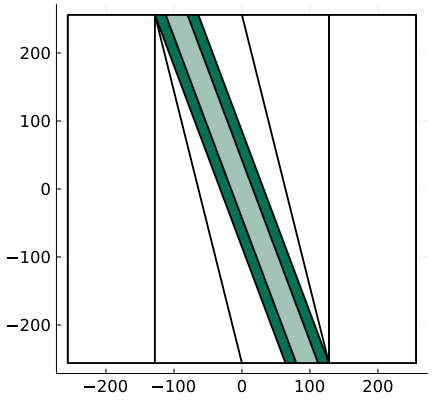

(d) Fourth level decomposition.

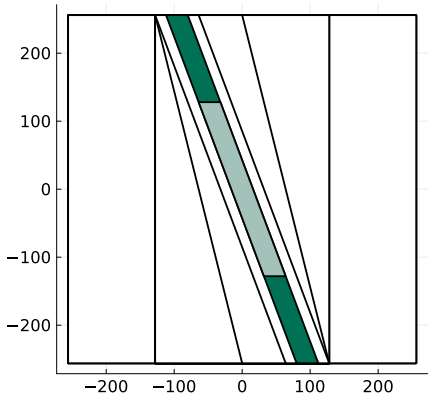

(e) Fifth level decomposition.

Figure 6.7: Scheme of the multi-level decomposition when $\mathbf{M} = 1024\mathbf{I} = \mathbf{J}_1\mathbf{J}_5\mathbf{J}_5\mathbf{J}_1\mathbf{J}_2\mathbf{N}$. The light green represents the spaces $V^i_{\mathbf{N}_j}$ where the low frequent part g^i_1 is, and the dark green represents $W^i_{\mathbf{N}_j}$ where the wavelet g^i_2 is present.

Here, $g_1^i \in V_{\mathbf{N}_i}^i$ and $g_2^i \in W_{\mathbf{N}_i}^i$, where i represents the level of decomposition.

Figure 6.6 showcases the wavelets g_2^i at all five levels, while Figure 6.7 provides schematic representations of the decomposition process at each level. The schematics visualize the cutting off of indices of $D_{\mathbf{M}}^{\perp}$ at each level of decomposition corresponds to. Figure 4.5 visualizes the same concept, but in terms of the Fourier coefficients of the functions. Finally, this narrowing represents a smaller and more specific range of directions compared to a 1-level decomposition.

In the first decomposition, where $\mathbf{J} = \mathbf{J}_1$, Figure 6.7a demonstrates the exclusion of information along the x-direction. In the second level of decomposition, employing $\mathbf{J} = \mathbf{J}_5$, Figure 6.7b shows the elimination of information in both the x- and y-directions, specifically in a counterclockwise sheared direction. This is also apparent in Figure 6.6b. Notably, the scales of the wavelet in Figure 6.6 increase in the first four levels and decrease in the last level. This is due to narrowing down the direction in a consistent manner for the initial four levels, resulting in larger wavelet amplitude. As information is eliminated in a specific direction, fewer Fourier coefficients are available to compute both g_1 and the wavelet g_2. Consequently, the wavelets become more spread out, particularly noticeable in level 4 as shown in Figure 6.6d. In the final level, we examine the highest frequencies of the direction of total decomposition, with a scale matching the first level. At this last level, we are able to observe the wavelet in the particular direction the total decomposition represents, as shown in Figure 6.6e. Through the implementation of a multi-level decomposition, we possess the capability to selectively scaling in various directions, thereby refining the specific direction under investigation.

6.3 Rotated Step Function

Knowing that we can use multiresolusion analysis to detect a more restricted direction of where an edge appears in an image, we now aim to use this method on a similar function as the one we worked with in the project [21]. We introduce the step function combined with a cosine as

$$\phi(\mathbf{x}) = \begin{cases} 0 & x_2 \leq 0, \\ \cos(2\pi \cdot x_2) & x_2 > 0. \end{cases}$$

Further, we rotate the function ϕ by 42° using the rotation matrix $R(\alpha)$ where α is the angle of clockwise rotation. For simplicity, we call

$$h(\mathbf{x}) = \phi(R(42)\mathbf{x})$$

and illustrate it in Figure 6.8.

To uncover the direction of the edge of h, our objective is to identify the matrix combination of $\mathbf{J}$s that corresponds to the direction orthogonal to the edge. In the orthogonal case the edge is steepest, thereby yielding the highest amplitude of the wavelet. Deviation from this specific direction will result in a lower amplitude of the wavelet. This enables us to discern whether the direction of the edge has been successfully identified, by studying the amplitude of the wavelets and compare it to its neighboring directions. The scenario where we see the smallest jump is when the direction of the decomposition is parallel to the direction of the edge.

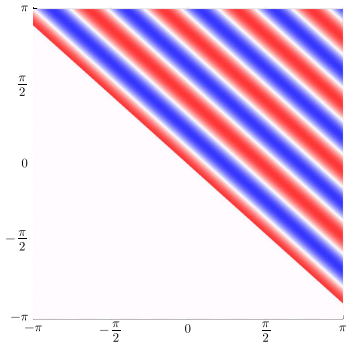

Figure 6.8: The step function $h(\mathbf{x})$ rotated at 42° clockwise from the x-axis.

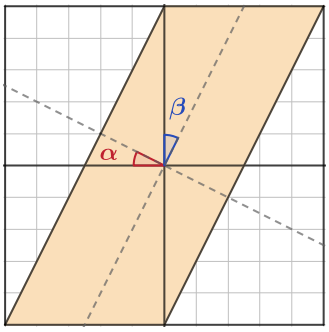

Figure 6.9: Explanation of how the angles are determined. The angle α is rotated clockwise from the x-axis. β is rotated clockwise from the y-axis.

The angle α in Figure 6.9 is rotated clockwise from the x-axis and represents the angle of the rotation of the function h. In the same figure, the angle β is rotated clockwise from the y-axis and represents the desired average angle of the decomposition. Our goal is to find the angle β, i.e., the angle corresponding to the direction orthogonal to the edge of h.

At first we performed a 5-level decomposition of the function h and use $\mathbf{M} = 1024\mathbf{I}$ to test different matrix combinations representing rotation and scaling in x-direction, comparing the amplitudes of the corresponding wavelets. We found that the matrix combination $\mathbf{M} = \mathbf{J}_4\mathbf{J}_4\mathbf{J}_4\mathbf{J}_1\mathbf{J}_2\mathbf{N}$ and $\mathbf{M} = \mathbf{J}_4\mathbf{J}_4\mathbf{J}_4\mathbf{J}_4\mathbf{J}_2\mathbf{N}$, denoted as 44412 and 44442, respectively, yield the highest amplitude of the wavelet $|g_2^5|$. Table 6.1 presents the maximum value of the wavelet $|g_2^5|$ and the related range of angles, corresponding to β in Figure 6.9, for the two matrix combinations. Note that the directions have a range of angles of approximately 4°. By performing yet another level of decomposition, we refine the angle further, honing it to a narrower range of possibilities. We anticipate that the direction aligned with the midpoint of these angle ranges will coincide with our overall intended direction.

Table 6.1: The maximum value of $|g_2^5|$ for different matrix combinations and the corresponding the angle β in Figure 6.9.

Matrix combination	**Maximum value of $\lvert g_2^5 \rvert$**	**Angle β**
44442	0.21160	$43.10 \pm 1.91°$
44412	0.22166	$41.12 \pm 2.03°$

Table 6.2: The maximum value of $|g_2^6|$ for different matrix combinations and the corresponding the angle β in Figure 6.9.

Matrix combination	**Maximum value of** $\|g_2^6\|$	**Angle** β
441412	0.03268	$39.08 \pm 1.08°$
441442	0.07235	$40.14 \pm 1.05°$
444112	0.21715	$41.17 \pm 1.01°$
444142	0.21138	$42.17 \pm 0.98°$
444412	0.18279	$43.14 \pm 0.96°$
444442	0.08181	$44.08 \pm 0.93°$

Table 6.3: The maximum value of $|g_2^6|$ for different matrix combinations and the corresponding the angle α in Figure 6.9.

Matrix combination	**Maximum value of** $\|g_2^6\|$	**Angle** α
772771	0.01315	$40.14 \pm 1.05°$
777221	0.01151	$41.17 \pm 1.01°$
777271	0.01561	$42.17 \pm 0.98°$
777721	0.01871	$43.14 \pm 0.96°$

We perform a 6-level decomposition of h, using $\mathbf{M} = 1024\mathbf{I}$. Table 6.2 presents the maximum value of the wavelet $|g_2^6|$ and the related range of angles, corresponding to β in Figure 6.9, for some interesting matrix combinations closely related to the direction of the 5-level decomposition. Among these combinations, $\mathbf{M} = \mathbf{J}_4\mathbf{J}_4\mathbf{J}_4\mathbf{J}_1\mathbf{J}_1\mathbf{J}_2\mathbf{N}$, yields the highest amplitude of $|g_2^6|$. This specific direction captures the high frequent part of h in the range of $41.19 \pm 1.01°$, with $42°$ being included within this range.

On the other hand, the matrix combination 444142 yields the direction where the average angle is closest to the angle being orthogonal to the edge of h. Despite this, the wavelet of this direction has a lower amplitude than the previously discussed direction. The wavelet g_2^6 for this particular decomposition is illustrated in Figure 6.10a, with the corresponding schematic in Figure 6.10b. The location of the wavelet of 444142 is compactly located close the edge of h. Also this matrix combination represents a direction range including the angle of $42°$ clockwise rotation from the y-axis.

The neighboring directions of 444112 and 444142 are 441442 counterclockwise and 444412 clockwise. When considering these neighboring directions 441442 and 444412, we observe a significant decrease in the amplitude of the wavelet compared to the aforementioned combinations 444112 and 444142. This suggests that the neighboring directions are slightly off, and that the direction orthogonal to the edge of h lies between these two directions. The angle ranges of 441442 and 444412 confirm this observation, in particular that the angle of $\beta = 42°$ falls slightly without the range captured by these decompositions.

The direction 777271 is the direction being the orthogonal to 444142. In Table 6.3, we see that the maximum value of $|g_2^6|$ is lower for the matrix combination 777271 than for the other matrix combinations being close to $\alpha = 42°$ clockwise rotation from the y-axis. This indicates that the direction of the decomposition

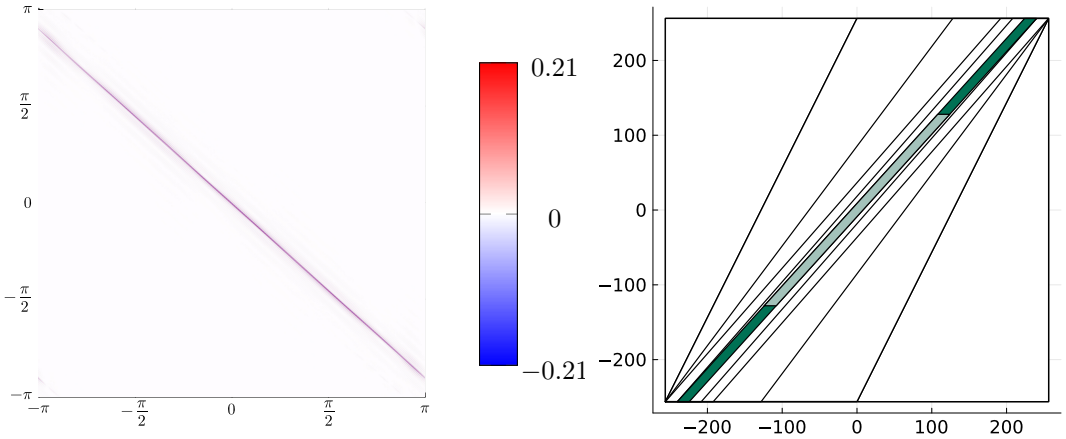

(a) $g_2^6 \in W_{\mathbf{N}}^6$ (b) Schematic of $W_{\mathbf{N}}^6$.

Figure 6.10: The sixth level wavelet $|g_2^6|$ of the function h and the schematic for the matrix combination $\mathbf{M} = 1024\mathbf{I} = \mathbf{J}_4\mathbf{J}_4\mathbf{J}_4\mathbf{J}_1\mathbf{J}_4\mathbf{J}_2\mathbf{N}$.

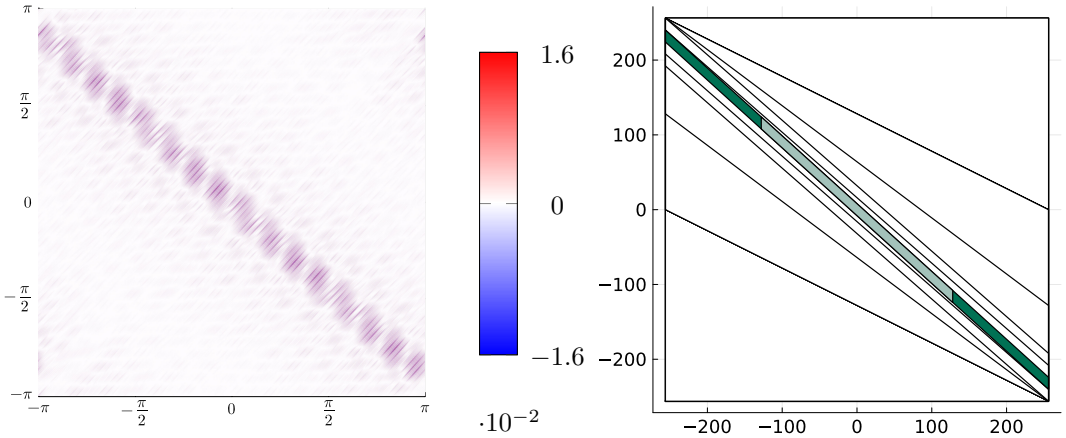

(a) $g_2^6 \in W_{\mathbf{N}}^6$ (b) Schematic of $W_{\mathbf{N}}^6$.

Figure 6.11: The sixth level wavelet $|g_2^6|$ of the function h and the schematic for the matrix combination $\mathbf{M} = 1024\mathbf{I} = \mathbf{J}_7\mathbf{J}_7\mathbf{J}_7\mathbf{J}_2\mathbf{J}_7\mathbf{J}_1\mathbf{N}$.

is parallel to the direction of the edge of h. The wavelet g_2^6 for this particular decomposition is portrayed in Figure 6.11a where we observe a widely dispersed wavelet. The corresponding schematic is depicted in Figure 6.10b. By studying the neighboring directions of 777271, we see a increase in amplitude of the wavelet. This again is in line with the parallel direction of the edge of h is the direction corresponding to 777271.

By increasing the level of decomposition beyond 6, the accuracy of the angle interval can be improved, leading to results with decreased uncertainty. However, this enhancement in precision is accompanied by an increase in computational complexity. The computational cost is affected by the determinant of the matrix $\mathbf{M}$ and subsequently influenced by the matrices $\mathbf{N}_i$ involved in the multi-level decomposition process. Therefore, higher levels of decomposition entail greater computational demands, which should be considered when deciding on the appropriate level for the analysis.

CHAPTER 7

Closing remarks

As exemplified in our experiments in Chapter 6, the framework of multivariate periodic wavelets can be used for edge detection in images. The fast wavelet transform separates the image into a low frequency part and a high frequency part. By Gibbs' phenomenon, the high frequency part is primarily concentrated around the edges present in the image. The method even enables detection of varying levels of discontinuities. Furthermore, we continued the exploration of the influence of the matrices $\mathbf{J} \in \mathcal{J}$ on the directionality of the decomposition process.

Through the utilization of multiresolution analysis, we showcased the ability to refine the direction of an edge within an image. This methodology was employed to ascertain the direction of a rotated edge at an angle of $42°$. Our investigation encompassed the exploration of different matrix combinations corresponding to various directions, both orthogonal and parallel to the edge of the rotated function. We compared the angle range of a 5-level decomposition to a 6-level decomposition, where a more constrained range of possible directions was observed for the latter case. With a 6-level decomposition, the interval of directions was narrowed down to approximately $2°$. Additionally, it is important to note that this increase in level of decomposition entails a rise in computational cost, necessitating a careful balance between accuracy and computational efficiency depending on the application at hand.

One of the goals for this thesis was to develop an readable code for the fast wavelet transform in Julia. Thus far, we have successfully written a functional code. However, it is not yet to be considered user-friendly and requires further refinement before publication. In order to achieve better usability, the functions should be given more self-explanatory names to better clarify their purpose. A review of the notation should be conducted to ensure consistency across functions. It could also be beneficial to include validations to the input parameters of the functions to ensure that the user is not able to input invalid parameters, such as a non-square or non-integer matrix $\mathbf{M}$ or matrix combinations $\mathbf{M} \neq \mathbf{JN}$. Additionally, the documentation for the functions can be enhanced by providing more details and greater precision. Moving forward, we plan to make the code available as a Julia package.

Bibliography

[1] Akram Aldroubi et al. “Invariance of a Shift-Invariant Space”. In: *Jurnal of Fourier Analysis and Applications* 16.1 (2010), pp. 60–75. DOI: 10.1007/s00041-009-9068-y (cit. on p. 24).

[2] Howard Anton and Chris Rorres. *Elementary linear algebra : Applications version*. Ed. by 11th edition. Wiley, 2014. ISBN: 9781118434413 (cit. on pp. 9, 25).

[3] R. Bergmann. “Translationsinvariante Räume multivariater anisotroper Funktionen auf dem Torus”. Dissertation. Universität zu Lübeck, 2013. ISBN: 978-3-8440-2266-7 (cit. on pp. 1, 14–16, 20, 21, 24, 27, 32, 40–42).

[4] Ronny Bergmann. “The fast Fourier transform and fast wavelet transform for patterns on the torus”. In: *Applied and Computational Harmonic Analysis* 35.1 (2013), pp. 39–51. DOI: 10.1016/j.acha.2012.07.007 (cit. on pp. 1, 7, 9–11, 14, 21, 34, 36, 39).

[5] Ronny Bergmann and Jürgen Prestin. “Multivariate Periodic Pavelets of de la Vallée Poussin Type”. In: *Journal of Fourier Analysis and Applications* 21.2 (2015), pp. 342–369. DOI: 10.1007/s00041-014-9372-z (cit. on pp. 1, 7, 19).

[6] J. Bezanson et al. “Julia: A Fresh Approach to Numerical Computing”. In: *SIAM review* 59.1 (2017), pp. 65–98. DOI: 10.1137/141000671 (cit. on pp. 1, 43).

[7] J. Bhattacharya, T. Holy, and other contributors. *OffsetArrays.jl*. Github. 2023. URL: https://github.com/JuliaArrays/OffsetArrays.jl (cit. on p. 43).

[8] Albert. Boggess and F. J. Narcowich. *A first course in wavelets with Fourier analysis*. 2nd ed. Hoboken, NJ.: Wiley, 2009. ISBN: 9780470431177 (cit. on pp. 5, 6).

[9] Peter J Cameron. *Introduction to Algebra*. Oxford: Oxford University Press, Incorporated, 2008. ISBN: 0198569130 (cit. on p. 6).

[10] Ingrid Daubechies. “Orthonormal bases of compactly supported wavelets”. In: *Communications on Pure and Applied Mathematics* 41.7 (1988), pp. 909–996. DOI: 10.1002/cpa.3160410705 (cit. on p. 1).

[11] C. de Boor, K. Höllig, and S. Riemenschneider. *The linear algebra of box spline spaces*. New York, NY: Springer New York, 1993, pp. 33–60. DOI: 10.1007/978-1-4757-2244-4_2 (cit. on p. 8).

[12] H Dym and H. P. McKean. *Fourier series and integrals*. 1st ed. Vol. 14. New York: Academic Press, 1972. ISBN: 0122264509 (cit. on p. 4).

[13] Matteo Frigo and Steven G. Johnson. "The Design and Implementation of FFTW3". In: *Proceedings of the IEEE* 93.2 (2005), pp. 216–231. DOI: 10.1109/JPROC.2004.840301 (cit. on p. 43).

[14] Say Song Goh, S.L. Lee, and K.M. Teo. "Multidimensional Periodic Multiwavelets". In: *Journal of Approximation Theory* 98.1 (1999), pp. 72–103. ISSN: 0021-9045. DOI: 10.1006/jath.1998.3279 (cit. on p. 1).

[15] A. Grossmann and J. Morlet. "Decomposition of Hardy Functions into Square Integrable Wavelets of Constant Shape". In: *SIAM Journal on Mathematical Analysis* 15.4 (1984), pp. 723–736. DOI: 10.1137/0515056 (cit. on p. 1).

[16] Christopher Heil. *Metrics, Norms, Inner Products, and Operator Theory*. Birkhäuser Boston, MA, 2009. DOI: 10.1007/978-3-319-65322-8 (cit. on pp. 3, 4).

[17] Rudolf Kochendörffer. *Introduction to Algebra*. Dordrecht: Springer Netherlands, 1972. DOI: 10.1007/978-94-009-8179-9 (cit. on p. 6).

[18] Dirk Langemann and Jürgen Prestin. "Multivariate periodic wavelet analysis". In: *Applied and Computational Harmonic Analysis* 28.1 (2010), pp. 46–66. DOI: 10.1016/j.acha.2009.07.001 (cit. on pp. 1, 8, 9, 14, 15, 19, 21, 23–26, 29, 31–33).

[19] Yves Meyer. *Wavelets and operators*. Vol. 37. Cambridge studies in advanced mathematics. Cambridge: Cambridge University Press, 1992. ISBN: 0521420008 (cit. on p. 1).

[20] G. Plonka et al. *Numerical Fourier Analysis*. Applied and Numerical Harmonic Analysis. Cham: Springer International Publishing AG, 2019. DOI: 10.1007/978-3-030-04306-3 (cit. on pp. 1, 3–5, 12, 13).

[21] Solvor Sevland. "Multivariate Fast Fourier Transform on the Pattern". TMA4500 Specialization Project, unpublished, Nowegian University of Science and Technology. 2023 (cit. on pp. 1, 43, 54).

[22] Elias M. Stein and Rami Shakarchi. *Fourier Analysis: An Introduction*. Vol. 1. Princeton, N.J: Princeton University Press, 2003. ISBN: 9780691113845 (cit. on p. 3).

[23] Terence Tao. *An introduction to measure theory*. Vol. vol. 126. Graduate studies in mathematics. Providence, R.I: American Mathematical Society, 2011. ISBN: 9780821869192 (cit. on p. 20).

APPENDIX A

Code for the Fast Wavelet Transform

```
using PeriodicWavelets      # Loads the implemented functions
using FFTW, LinearAlgebra

# Defining the matrices
first_J = [2 0; -1 1]; sec_J = [1 0; 0 2];
N1 = [256 0; 256 512]; N2 = [256 0; 128 256];
M = first_J * sec_J * N2;
m = abs(det(M));

# Defining the Dirichlet kernels
ckDM = PeriodicWavelets.ck_Dirichlet_kernel(M);
ckDN1 = PeriodicWavelets.ck_Dirichlet_kernel(N1);

# Defining the function to be decompose
f3(x) = x <= 3pi/4 ? (4x/(3pi) - 1)^2 * (4x/(3pi) + 1)^2 : 0;
f(x) = f3(norm(x));

# Sampling f on the pattern of M. Computing the coefficients of f
   w.r.t the ckDM
af = PeriodicWavelets.sample_on_pattern(M, f);
ahat_f = fft(af);
ahat_f_DM = PeriodicWavelets.coeff_Fourier2space(
    M, ahat_f, ckDM) .* m;

# Performing the wavelet transform of f
b1hat, b2hat, d1hat, d2hat =
    PeriodicWavelets.wavelet_decomposition(
        M, first_J, ahat_f_DM, ckDN1, ckDM);

# Constructing the functions generating the decomposed shift
   invariant spaces
ck_xi = PeriodicWavelets.fourier_coeff_xi(M, b1hat, ckDM);
ck_psi = PeriodicWavelets.fourier_coeff_xi(M, b2hat, ckDM);

# Constructing the decomposed functions of f
ck_g1 = PeriodicWavelets.fourier_coeff_xi(N1, d1hat, ck_xi);
ck_g2 = PeriodicWavelets.fourier_coeff_xi(N1, d2hat, ck_psi);
```

```
# Optional: Visualize the wavelet
plt_g2 = PeriodicWavelets.plot_f(ck_g2, (1024, 1024))

# If performing a multi-level decomposition, it is not necessary
   to compute ck_psi and ck_g2.

# ------------------------------
# Second level decomposition
# ------------------------------

# Dirichlet kernel for the second decomposition
ckDN2 = PeriodicWavelets.ck_Dirichlet_kernel(N2);

# Perform second the wavelet decomposition
sec_b1hat, sec_b2hat, sec_d1hat, sec_d2hat =
    PeriodicWavelets.wavelet_decomposition(
        N1, sec_J, d1hat, ckDN2, ck_xi);

# Construct the functions generating the second level decomposed
   shift invariant spaces
ck_xi_sec = PeriodicWavelets.fourier_coeff_xi(
    N1, sec_b1hat, ck_xi);
ck_psi_sec = PeriodicWavelets.fourier_coeff_xi(
    N1, sec_b2hat, ck_xi);

# Construct the second level decomposed functions
ck_g1_sec = PeriodicWavelets.fourier_coeff_xi(
    N2, sec_d1hat, ck_xi_sec);
ck_g2_sec = PeriodicWavelets.fourier_coeff_xi(
    N2, sec_d2hat, ck_psi_sec);
```

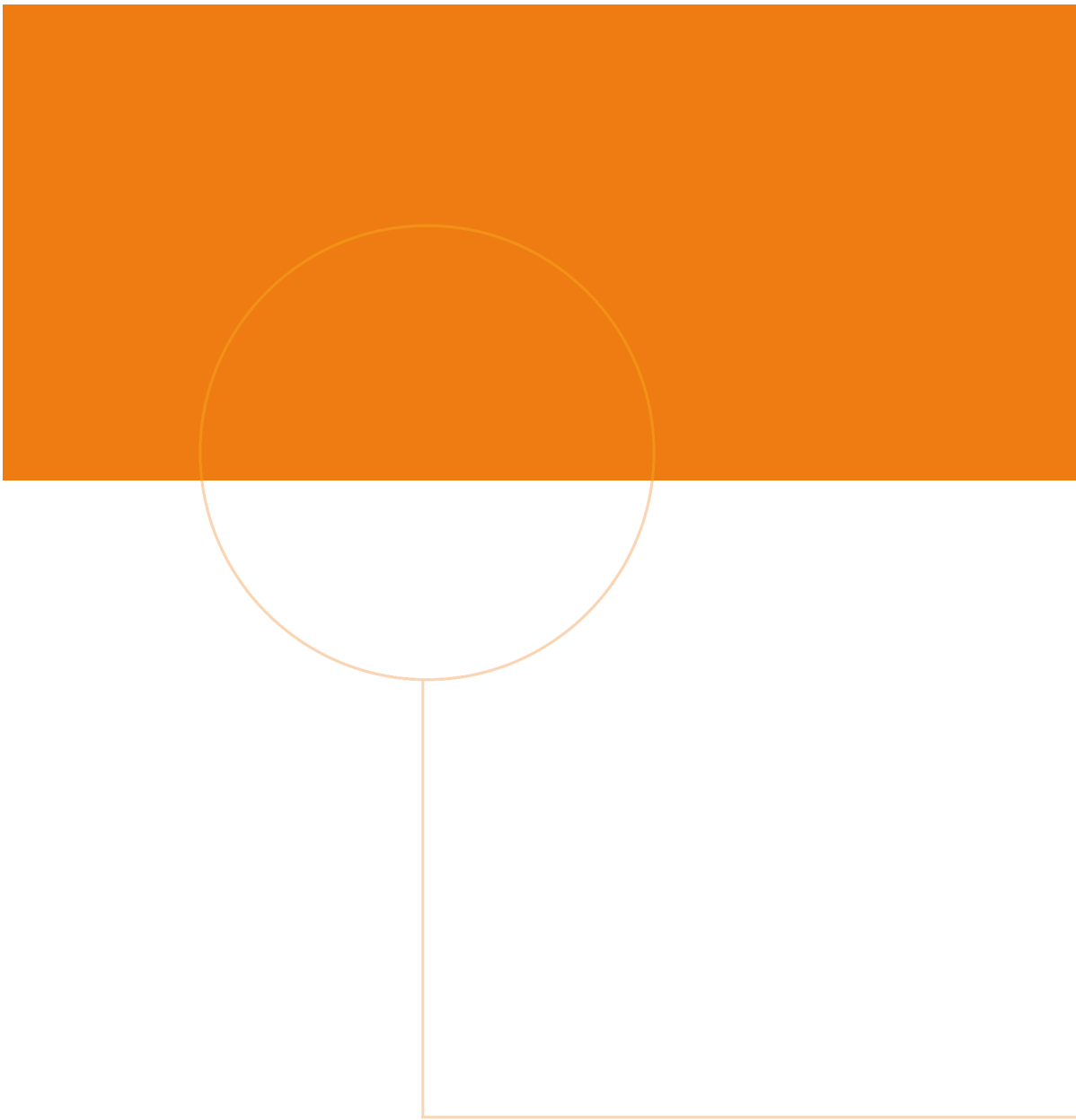

NTNU

Norwegian University of
Science and Technology